arXiv:2605.12827v3 [cs.CR] 4 Nov 2026

GraphIP–Bench: How Hard Is It to Steal a Graph Neural Network, and Can We Stop It?

Kaixiang Zhao[*]
Brigham Young University
kzhao2@byu.edu

Bolin Shen[*]
Florida State University
blshen@fsu.edu

Yuyang Dai
University of California, Berkeley
michael_yuyang@berkeley.edu

Shayok Chakraborty
Florida State University
schakraborty2@fsu.edu

Yushun Dong[†]
Florida State University
yushun.dong@fsu.edu

Abstract

Graph neural networks (GNNs) deployed as cloud services can be *stolen* through *model-extraction attacks*, which train a surrogate from query responses to reproduce the target's behaviour, and a growing line of ownership defenses tries to prevent or trace such theft. The title of this paper asks two questions: *how hard is it to steal a GNN*, and *can we stop it?* Prior work cannot answer either, because experiments use inconsistent datasets, threat models, and metrics. We introduce *GraphIP-Bench*, a unified benchmark which evaluates both sides under a single black-box protocol. It integrates twelve extraction attacks, twelve defenses spanning watermarking, output-perturbation, and query-pattern-detection families, ten public graphs covering homophilic, heterophilic, and large-scale regimes, three GNN backbones, and three graph-learning tasks, and it reports fidelity, task utility, ownership verification, and computational cost on shared splits, queries, and budgets. We further add a joint attack-and-defense track which runs every attack on every defended target and measures watermark verification on the resulting surrogate, which exposes the protection that a defense retains after extraction. The empirical picture is short: stealing a GNN is easy at medium query budgets and most defenses do not change this; several watermarks verify reliably on the protected model but lose most of their verification signal on the extracted surrogate, which exposes a gap that single-model evaluations miss; and heterophilic graphs are systematically harder to steal, while a cross-architecture mismatch between target and surrogate reduces but does not prevent extraction. We release *GraphIP-Bench* with reproducible scripts and configurations, and integrate the attacks and defenses into the PyGIP library.

github.com/LabRAI/GraphIP-Bench labrai.github.io/PyGIP

1 Introduction

Graph neural networks (GNNs) are key components of modern data-driven services. Commercial platforms use them for product recommendation [35], autonomous vehicle perception [16], and molecular property prediction [11]. Their advantage is that they aggregate information over arbitrary relational structures, which arise in social, financial, and product data. Cloud providers now expose pre-trained GNNs through public inference endpoints, which allow customers to deploy state-of-the-art analytics without local training or data collection.

[*]Co-first author.
[†]Corresponding author.

40th Conference on Neural Information Processing Systems (NeurIPS 2026). Track on Evaluations and Datasets.

This deployment model also lets adversaries *steal* the model. The attack pattern is the same in every reported instance: the adversary submits carefully chosen queries, records the labels or confidence scores that the endpoint returns, and trains a local surrogate which reproduces the target's behaviour. The literature calls this attack *model extraction* [30, 44], and we use "stealing a GNN" as a plain-language synonym throughout the paper. A successful theft leaks the owner's intellectual property, undermines pay-per-query revenue, and lets competitors recreate proprietary functionality at low cost. For example, a stolen fraud-detection GNN exposes decision boundaries which adversaries can use to bypass screening, and a stolen pharmaceutical GNN reveals assay knowledge which is encoded in the model parameters. These risks motivate the two questions which the title of this paper makes explicit: *how hard is it to steal a GNN*, and *can we stop it?*

To stop the theft, recent work proposes two complementary defense families. *Information-limiting* defenses (output perturbation, query filtering, query-pattern detection) make each query response less useful to the attacker [12, 8, 6, 7, 15]. *Ownership-tracing* defenses (watermarking and fingerprinting) embed a verifiable pattern in the trained model so that the owner can prove that an extracted surrogate was derived from their model [28, 33, 1, 36, 31, 27]. Surveys summarise both families and the broader security landscape for deep learning [19, 34, 24, 40, 39] and for graph learning in particular [2, 32, 37, 22, 43]. Experimental practice, however, remains fragmented: studies use private splits, incompatible budgets, and inconsistent metrics, and the few existing testbeds focus on robustness or privacy and exclude model extraction together with watermarking and fingerprinting [23]. The community therefore lacks an empirical basis on which to answer either of our two title questions.

Several challenges must be addressed to enable fair and informative comparison. First, the community needs a single experimental protocol that fixes public splits, shared query sets, budgets, and explicit threat models (including whether the endpoint returns labels or confidence scores) and that treats data-driven and data-free attacks on equal terms [30, 44]. Second, evaluation must align success criteria with method goals: residual extraction for attacks, ownership verification for watermarking and fingerprinting, since these mechanisms aim to provide verifiable evidence of model ownership rather than to reduce agreement with the target [28, 33]. Third, studies should report the protection–utility balance under matched conditions, since adoption depends on how defenses affect task accuracy and inference latency. Fourth, benchmarks should report computational complexity (time and memory) to make the real cost of deployment transparent; prior work often omits this and obscures feasibility [12]. Fifth, evaluating attacks and defenses separately misses the joint adversarial setting in which the attacker extracts a defended model and the defender verifies ownership on the surrogate — the setting that actually determines whether a defense is useful. Finally, consistent method naming, standardized hardware and software, and public reporting of seeds and tuning procedures are needed for reproducibility and to prevent protocol-induced bias. Existing studies only partially satisfy these requirements, which limits both scientific understanding and industrial uptake.

We address these challenges with *GraphIP-Bench*, a reproducible benchmark and library which evaluates both *stealing* and *stopping* under a single black-box protocol. The suite integrates twelve representative extraction attacks (nine data-driven and three data-free) and twelve defenses spanning watermarking, output-perturbation, prediction-rounding, and query-pattern-detection. We evaluate every method on ten public graphs covering homophilic, heterophilic, and large-scale regimes, three GNN backbones, and three graph-learning tasks; the per-dataset, per-backbone, and per-method details are deferred to Section 3. A unified hyperparameter search and a consistent metric suite record security, utility, and efficiency. Going beyond prior single-track evaluations, we add a joint attack-and-defense track which runs every attack on every defended target and a watermark-survival metric which measures verification on the surrogate produced by each attack, together exposing how much protection a defense retains after the model is actually stolen. The headline finding of that joint track is that most parameter-side or trigger-based graph watermarks verify near-perfectly on the protected model but lose much of their verification signal on the extracted surrogate, while query-time mechanisms partially survive — watermark designs must therefore be re-evaluated on the surrogate, not only on the deployed model. To our knowledge, *GraphIP-Bench* is the first benchmark which offers a standardised evaluation of model-extraction attacks and ownership defenses for graph neural networks. The main contributions are:

- **Unified protocol.** Public splits, shared queries, standardized budgets, and explicit endpoint assumptions; twelve attacks and twelve defenses run under identical settings on ten datasets, three GNN backbones, and three tasks for fair comparison.

- **Joint attack-and-defense track.** Every attack is executed against every defended target with watermark verification measured on the extracted surrogate, which exposes the residual ownership signal that survives extraction.
- **Protection–utility analysis.** A sweep of defense configurations and attacker budgets summarises operating points with attack-agnostic frontiers and links them to graph structural properties (edge homophily, degree, density) and to backbone choice.
- **Cost and efficiency reporting.** Asymptotic formulas and automated profilers record training time, memory, inference latency, verification time, and an estimated monetary cost, which makes deployment cost transparent for every method.

2 Preliminaries

Notation. An attributed graph is denoted by $\mathcal{G} = (\mathcal{V}, \mathcal{E}, \mathbf{X}, \mathbf{A})$ with node set $\mathcal{V}$, edge set $\mathcal{E}$, node-feature matrix $\mathbf{X}$, and adjacency matrix $\mathbf{A}$. Query budgets are reported using the benchmark multipliers, and four data-availability regimes (`both`, `features only`, `structure only`, `data free`) control which inputs the adversary can construct. Fidelity is the agreement rate between a surrogate and the target on the test split; accuracy and macro F1 measure task utility.

Model Extraction Attacks. We consider the standard black-box threat model in which the adversary has query access to a deployed graph neural network and no knowledge of its weights, architecture, or training data. The adversary submits inputs (either genuine subgraphs or synthetic samples), records the returned labels or probability vectors, and trains a local model which minimises the discrepancy between its predictions and the target's outputs. The resulting model is a surrogate which replicates the behaviour of the protected network and enables extraction of the owner's intellectual property [30, 44]. Prior work groups extraction queries into three strategies. Random querying submits subgraphs from public data and succeeds when the decision boundary is smooth [30]. Adaptive querying selects inputs which maximise information gain, often through the disagreement between the current surrogate and the target [44]. Data-free generation removes the need for public data by training a graph generator which produces queries during extraction [44]. These studies show that modest query budgets, often no larger than the number of nodes in a benchmark dataset, are sufficient to recover a model which matches the original on downstream tasks.

Defense against Model Extraction Attacks. The literature groups defenses into two complementary families. *Information-limiting* defenses modify the target's outputs so that the adversary receives a less useful signal: output perturbation adds calibrated noise or rounds confidence scores [12, 8], and query filtering detects and blocks suspicious request patterns [6, 7, 15]. These methods can reduce the residual agreement of a surrogate, although they may also degrade accuracy for legitimate users. *Ownership-tracing* defenses embed an artefact which lets the owner verify infringement: graph watermarking modifies weights or decision regions so that the model reveals a secret on inputs which carry a trigger [28, 33, 1], and fingerprinting derives stable signatures from the model's output distribution while leaving the parameters unchanged [36, 31, 27]. Surveys of these approaches identify open questions about robustness, utility loss, and verification cost [19, 34, 24, 40, 39], and our benchmark places all of them under a single protocol with matched datasets, budgets, and threat assumptions, which enables an objective comparison of their trade-offs.

3 Benchmark Design

In this section we describe the experimental protocol of *GraphIP-Bench*. We first state the protocol design, datasets, attacks, defenses, and implementation details, then articulate the five research questions that guide our empirical study.

3.1 Experimental Settings and Implementations

Protocol Design. *GraphIP-Bench* defines a single black-box protocol that fixes four disjoint splits for each dataset (train, validation, test, query), shares the same query sets across methods, and uses *standardized* query budgets at 0.05, 0.10, 0.25, 0.50, and 1.00 as budget multipliers. Here "standardized" means that every method receives the same number of queries at each ratio and that these ratios are fixed across datasets. The set spans the commonly studied ranges in prior work [18, 25], which include very small budgets that test sample efficiency (0.05 to 0.10), medium budgets

where most gains occur (0.25 to 0.50), and a large budget that approximates saturation (1.00). This design makes results comparable and representative across methods and datasets. The protocol states explicit endpoint assumptions, which include whether the service returns labels only or also confidence scores and whether rate limits apply [30, 44]. We separate evaluation into an extraction track, an ownership track, and a joint track. The extraction track measures how well black-box attacks learn a surrogate of an undefended target, and it reports test accuracy with respect to ground truth and fidelity with respect to the target. The ownership track evaluates each defense on a defended target and reports defended accuracy, fidelity to the original target, and verification on a standardized verification set [42, 33, 28, 38, 31]. The joint track runs every attack on every defended target and reports surrogate fidelity to the defended model together with the verification rate measured on the surrogate, which we call watermark survival. To place different settings on equal footing, we control data availability with four regimes: features only, structure only, features and structure, and data free. We also report total attack time, total defense time, and peak GPU memory for both attacks and defenses to make deployment cost clear.

Datasets. We use ten attributed graphs which cover four groups: homophilic citation networks (Cora, CiteSeer, PubMed), homophilic coauthor and product co-purchase networks (CoauthorCS, CoauthorPhysics, Computers, Photo), the large-scale OGBN-Arxiv graph, and two heterophilic graphs [20] (RomanEmpire, AmazonRatings). The graphs differ in size, density, class count, feature dimension, and edge homophily, which enables stress testing across structural regimes; full statistics are in Table 7 of Appendix C. For node classification we split each dataset into four disjoint subsets (train, validation, test, query) with no overlap, and for watermarking we reserve a fixed subset of the training data as the watermark set. We also include link prediction on Cora and graph classification on ENZYMES and PROTEINS from TUDataset [17] (Appendix E.10).

Metrics. An em dash denotes an unavailable measurement. We report two groups of metrics under a single protocol. *Performance* for attacks includes test accuracy, macro F1, and fidelity, which is the agreement between the surrogate and the target on the test set. *Performance* for defenses includes the defended model's test accuracy and macro F1, its fidelity to the original target, and ownership verification on a standardized verification set. *Efficiency* for attacks includes total attack time and peak GPU memory; *efficiency* for defenses includes total defense time and peak GPU memory.

Marker preservation under output rounding does not establish ownership.

Model Extraction Attacks. For the extraction track we implement twelve representative attacks. Six are MEA-style baselines from a canonical study on query synthesis and surrogate training, which we denote `MEA0` through `MEA5` [30]; we further include the adaptive adversarial querying method `AdvMEA` [3], the centrality-and-entropy strategy `CEGA` [29], and the structure-aware pipeline `Realistic` [4]. To cover the data-free regime in a fair black-box manner, we add three variants [44] which use no target gradients: `DFEA_I` minimises the KL divergence between surrogate logits and target logits (soft-label distillation), `DFEA_II` trains on hard labels returned by the endpoint (label-only supervision), and `DFEA_III` augments label-only training with a consistency loss between two surrogates. We treat distinct hyperparameter settings of the same algorithm as separate methods, which enables fine-grained comparison under shared query sets and budgets. The four data-availability regimes defined in Section 2 are realised by two control parameters, `attack_x_ratio` and `attack_a_ratio`, which fix the fraction of real features and real adjacency made available to each attack; the four regimes are denoted `X-only` (features only), `A-only` (structure only), `both` (features and structure), and `data-free`.

Model Extraction Defenses. For the ownership and joint tracks we implement twelve defenses, which split between the two families introduced in Section 2. The ownership-tracing family contains five methods: the watermarking schemes `RandomWM`, `BackdoorWM`, `SurviveWM`, and `ImperceptibleWM` [42, 33, 28, 38], and the query-based integrity scheme `Integrity` [31]. The information-limiting family contains seven methods: two output-perturbation variants `OP_low` and `OP_high` which add Gaussian noise to the returned logits at two scales [8, 12], two prediction-rounding variants `PR_2bit` and `PR_top1` which quantise the returned scores or return only the top-1 label, and three query-detection methods which follow PRADA [6], an adaptive-misinformation strategy [7], and a gradient-redirection strategy [15], denoted `PRADA`, `AdaptMisinfo`, and `GradRedir`. Every defense protects the same target architecture, and we report the defended model's test accuracy and its fidelity to the original target. For watermarking and integrity we measure ownership verification on a standardised verification set using accuracy; for information-limiting and query-detection

methods we use the verification proxy that matches each method's design, which is the trigger-label hit rate or the watermark-graph accuracy when a defense exposes such an artefact and the marker accuracy on the protected model otherwise.

GNN Backbones. To test whether conclusions are robust to the choice of model architecture, we use three widely adopted GNN backbones. The first is GCN [9], which uses spectral graph convolution. The second is GAT [26], which uses attention over neighbors. The third is GraphSAGE [5], which uses neighbor sampling and a learned aggregator. Each backbone is implemented in both DGL and PyTorch Geometric so that defenses with library-specific dependencies can be evaluated on a matched architecture; we use a DGL GCN with hidden dimension 16 as the default backbone, and we explicitly mark deviations when a defense uses a different backbone for fairness.

3.2 Research Questions

RQ1. How does extraction effectiveness change with the query budget, and does the trend hold on heterophilic and large-scale graphs? We run twelve black-box attacks on undefended targets across the ten datasets at five budgets and four data-availability regimes, and we report accuracy, macro F1, and fidelity averaged over three seeds. **RQ2. How effective are existing defenses on the protected model?** We evaluate the five watermarking and integrity methods together with the seven information-limiting and query-detection methods on a shared backbone, and we report defended accuracy, fidelity, and ownership verification. **RQ3. How well do defenses balance protection and utility?** For each defense we report the utility loss against the undefended target together with defended fidelity and verification rate, which makes the protection-utility trade-off explicit. **RQ4. What are the computational complexity and practical efficiency of attacks and defenses?** We report asymptotic time and memory complexity, and measure wall-clock time and peak GPU memory on NVIDIA A100 hardware for both the extraction and the ownership track. **RQ5. How effective are defenses in the joint adversarial setting, and does the watermark signal survive on the extracted surrogate?** We run every attack on every defended target at a fixed budget and report surrogate fidelity to the defended model together with the verification rate measured on the surrogate, which we call *watermark survival*.

4 Empirical Investigation

We now present an empirical study that follows the unified protocol in Section 3, uses shared query sets and standardized budgets, and reports security, utility, and efficiency under identical settings. Complementary generalisation experiments are reported in Appendix E.10.

4.1 Budget Sensitivity of Model Extraction Attacks (RQ1)

To answer RQ1, we evaluate twelve black-box attacks on undefended targets under the protocol in Section 3.2. Results are averaged over three seeds, and we report fidelity to the target together with accuracy on the ground truth. Table 1 shows a representative case on *Computers* when both features and adjacency are available. Figure 1 reports sample efficiency on all ten datasets and four regimes; the y-axis is the median budget at which each attack reaches 90% of its own best fidelity. Figure 2 plots accuracy and fidelity on six representative datasets which span the four regimes that matter for our findings: two clean homophilic citation graphs (Cora, PubMed), the high-average-degree exception (Computers), the highest-homophily reference (CoauthorPhysics), the large-scale graph (OGBN-Arxiv), and the lowest-homophily heterophilic graph (RomanEmpire). The full ten-dataset, three-metric (Acc, Fidelity, F1) version, the regime-sensitivity heatmap, and the per-dataset and per-regime tables are reported as Figures 10 and 11 and Appendix E.1.

The results expose a consistent picture across the ten datasets. *CEGA is the most sample-efficient attack on the homophilic graphs but is unstable on Computers*, where the high average degree (36.8) destabilises its centrality-driven query selection. *The MEA family saturates near the medium budget*: fidelity improves rapidly up to $\sim 0.5\times$ and then plateaus. *Data-free variants are competitive with the data-driven methods across most datasets, with* `DFEA_II` *on the high-degree product graphs (especially Computers and Photo) as the main outlier*, which reflects an attack-specific dependence on graph statistics and synthetic-query coverage. *Strong data-driven attacks are nearly invariant to removing either features or structure, but collapse without any real input*: the corresponding

Table 1: RQ1 on *Computers* (both features and adjacency available). Fidelity (%) across query budgets with mean ± standard deviation over three seeds. Higher is better. Appendix E.1.1 examines the repeated `DFEA_II` entries.

Budget	MEA0	MEA1	MEA2	MEA3	MEA4	MEA5	AdvMEA	CEGA	Realistic	DFEA_I	DFEA_II	DFEA_III
0.05×	51.0±7.0	41.5±15.5	51.0±7.5	53.8±3.0	38.4±13.4	61.3±4.3	35.5±17.8	36.0±25.0	64.5±33.7	67.5±12.4	43.9±8.1	**72.9±5.5**
0.10×	67.3±3.1	27.7±14.0	58.8±6.0	64.8±5.5	37.9±12.6	65.6±6.4	25.7±24.7	36.7±23.0	67.9±45.4	**73.7±18.1**	28.4±20.5	66.7±14.2
0.25×	67.0±1.5	46.2±5.5	65.2±2.4	67.6±6.2	63.6±4.0	66.5±2.1	26.9±22.4	43.4±17.5	67.7±45.3	60.3±25.5	28.4±20.5	**72.9±3.1**
0.50×	71.4±2.7	49.4±5.6	66.2±6.3	74.9±4.3	74.3±5.0	73.9±3.5	46.1±12.5	53.9±29.2	67.4±44.0	64.8±15.9	28.4±20.5	**82.5±3.1**
1.00×	80.5±4.6	56.3±12.6	68.3±8.0	79.5±5.2	**83.7±4.3**	76.3±4.2	22.8±11.8	54.1±33.4	67.0±44.8	55.8±28.2	28.4±20.5	82.1±2.8

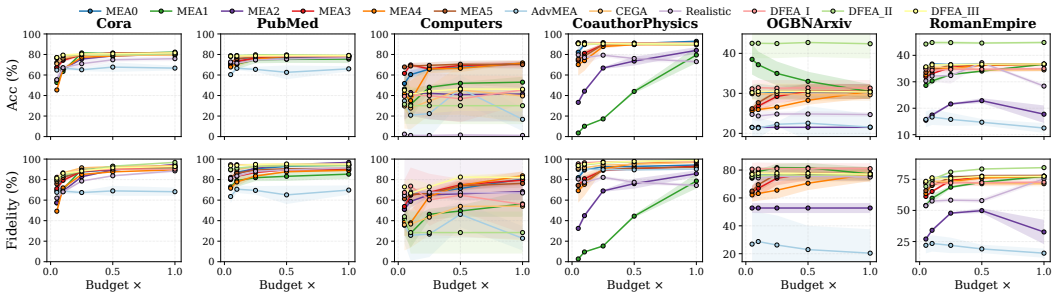


Figure 2: Budget–metric curves on six representative datasets (columns) for accuracy and fidelity (rows). Lines are the twelve attacks (mean over three seeds, shaded bands ±1 std). The four homophilic graphs share a 0–100% y-axis; OGBN-Arxiv and RomanEmpire use per-subplot ranges since their target accuracy is bounded by intrinsic task difficulty. The full ten-dataset, three-metric version (including macro F1) and per-dataset numbers are reported as Figure 10 and Appendix E.1.

ratios in the regime-sensitivity heatmap (Appendix E.7) stay near one in the features-only and structure-only blocks and drop sharply in the data-free block. Together these observations indicate that effective extraction on graphs is primarily a sample-efficiency problem rather than a brute-force budget problem, and that data-free extraction can match data-driven attacks on graphs whose label space is well covered by synthetic queries; a longer discussion appears in Appendix E.7.

Extension to large-scale and heterophilic graphs. The seven graphs in the original protocol are small and homophilic, which limits the conclusions to one structural regime. To extend the protocol along three independent axes, we evaluate the same twelve attacks on three additional graphs: OGBN-Arxiv (169,343 nodes, 40 classes, edge homophily 0.699) probes *scale* and *class-count* stress, while RomanEmpire (edge homophily 0.291) and AmazonRatings (edge homophily 0.452, ordinal 5-class ratings) probe *heterophily*. Figure 3 summarises surrogate fidelity at the medium budget 0.25× on each of the three additional graphs in the features-and-structure regime; the per-attack and per-budget results for all four regimes appear in Tables 38–40 of Appendix E.4.

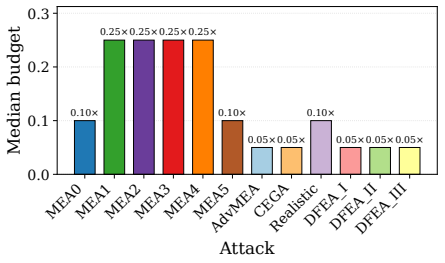


Figure 1: Sample efficiency across ten datasets and four regimes.

These additional large-scale and heterophilic graphs reproduce the qualitative ordering observed on the seven homophilic datasets of the core protocol: simple data-driven methods (MEA0, MEA3, MEA5) and CEGA reach high fidelity, `AdvMEA` is unstable, and the data-free variants are also competitive on all three additional graphs (typically within 5 pp of the strongest data-driven attacks). Two further patterns are specific to these graphs; a longer discussion appears in Appendix E.4.

First, OGBN-Arxiv exposes a scale and class-count effect. The undefended target reaches only 37.7–54.9% accuracy across our three backbones (Appendix Table 37) because the task itself is harder (40 fine-grained classes), so we report fidelity as the comparable measure: the strongest attacks (data-driven and data-free alike) reach ∼ 75–82% at 0.25×, while `AdvMEA` drops to ∼ 26%, indicating that the 40-class label space is the main difficulty rather than the graph scale itself.

Table 2: RQ2 summary for watermarking and integrity defenses on the seven homophilic graphs. Median (IQR) over datasets. Utility drop is the signed decrease in test accuracy (pp) against the undefended target on a matched backbone; negative values indicate that the defended model outperforms the matched undefended baseline.

Defense	F1 (%)	Fidelity (%)	Owner. verif. (%)	Utility drop (pp) ↓	Time (s)	Peak mem. (GB)
`RandomWM`	64.99 (12.02)	74.13 (10.70)	72.00 (24.7)	3.93 (6.18)	34.8 (14.6)	**0.09** (0.26)
`BackdoorWM`	69.13 (15.51)	**80.07** (15.95)	**100.0** (0.00)	3.27 (2.87)	1.98 (0.45)	0.16 (0.68)
`SurviveWM`	67.47 (27.86)	79.93 (32.92)	21.76 (32.4)	**0.13** (18.2)	2.27 (0.92)	0.32 (0.96)
`ImperceptibleWM`	69.49 (9.19)	77.63 (13.88)	**100.0** (0.00)	1.65 (6.28)	676(697)	2.30 (2.58)
`Integrity`	**73.43** (21.20)	76.03 (22.52)	66.67 (40.0)	1.93 (3.17)	**1.38** (0.45)	0.20 (0.90)

Second, heterophilic graphs separate attacks which assume labelled neighbourhoods from those which do not. On RomanEmpire (homophily 0.291) the strongest data-driven attacks reach 77% fidelity, but `AdvMEA` drops to 21.9%, a 50 pp loss which isolates an implicit homophily assumption in its adversarial query generator. AmazonRatings is intermediate: although its homophily is 0.452, the labels are ordinal 1–5 ratings, so neighbouring classes carry graded similarity which aggregation can still exploit; the strongest data-driven attacks still reach $\geq 93\%$ fidelity.

4.2 Effectiveness of Ownership and Information-Limiting Defenses (RQ2)

To answer RQ2, we evaluate the twelve defenses on a shared target under identical splits, using three seeds (ten for Integrity on Computers and Photo). We report the five watermarking and integrity methods first and then the seven information-limiting and query-detection methods. *Utility drop* is undefended accuracy minus defended accuracy on the same dataset, and *ownership verification* is accuracy on a fixed verification set; we summarize across datasets with the median and report variability with the inter-quartile range. Table 2 reports the median values together with time and memory; the corresponding boxplot view and per-dataset numbers are reported in Appendix E.2.

Among the watermarking and integrity defenses, `BackdoorWM` offers the best protection-utility balance: it reaches the highest median fidelity (80.07%), perfect verification, and only a 3.27 pp median utility drop. `ImperceptibleWM` also reaches perfect verification, but at a much higher training cost which is visible as a long memory tail in Figure 8 of Appendix E.6. `RandomWM` and `SurviveWM` expose a stability-verification trade-off: `SurviveWM` minimises utility loss (0.13 pp median) but weakens verification, while `RandomWM` is more variable across datasets. A per-defense breakdown together with the boxplot view appears in Appendix E.2.

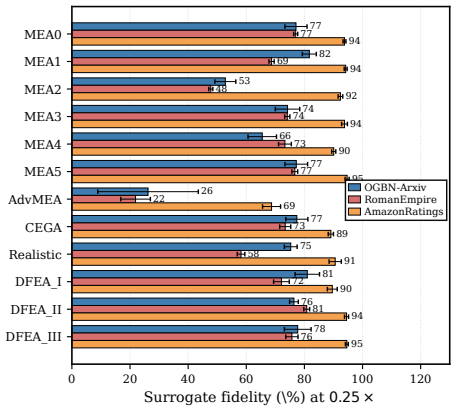


Figure 3: Surrogate fidelity (%) at budget $0.25\times$ on the three additional graphs for all twelve attacks (mean over three seeds, whiskers are $\pm$ one std).

Information-limiting and query-detection defenses. We further evaluate seven information-limiting and query-detection methods on the same target backbone (DGL GCN) across all ten datasets, which complements the five ownership-tracing methods above with a different defense family. Table 3 reports the protected-model accuracy and the verification proxy on the protected model itself, and Appendix E.5 contains the standard deviations.

The seven methods separate into three groups. *Output perturbation* (`OP_low`, `OP_high`) preserves accuracy on most graphs and yields a verification rate close to the noise-free regime when the noise scale is small, while the rate drops on graphs with more classes or with a heterophilic structure when the noise scale is large. *Prediction rounding* reveals a sharp split: `PR_top1`, which returns only the top-1 label, gives perfect verification on every dataset because the marker label is always preserved, while `PR_2bit`, which quantizes the returned probability vector, suffers a notable drop on classes with similar logits. *Query-detection methods* (`PRADA`, `AdaptMisinfo`, `GradRedir`) show three distinct profiles: `PRADA` preserves accuracy on smaller graphs but degrades on *Cora* and the

Table 3: Seven information-limiting and query-detection defenses on a shared target backbone (DGL GCN, hidden 16) across ten datasets. Each cell reports protected accuracy (%) with the verification proxy (%) in parentheses (mean over three seeds; standard deviations in Appendix E.5).

Dataset	`OP_low`	`OP_high`	`PR_2bit`	`PR_top1`	`PRADA`	`AdaptMisinfo`	`GradRedir`
Cora	79.4 (98.6)	79.2 (93.9)	73.3 (83.7)	79.6 (100.0)	40.2 (43.0)	41.0 (48.5)	79.8 (100.0)
CiteSeer	67.6 (97.8)	66.3 (91.0)	53.9 (70.3)	68.8 (100.0)	69.3 (100.0)	39.8 (52.5)	68.4 (100.0)
PubMed	77.9 (99.0)	75.9 (94.7)	77.6 (93.4)	78.2 (100.0)	78.0 (100.0)	44.1 (48.6)	78.3 (100.0)
Computers	44.0 (89.2)	37.6 (55.3)	36.1 (61.7)	34.8 (100.0)	46.0 (100.0)	28.0 (64.3)	52.4 (100.0)
Photo	89.1 (98.9)	90.7 (96.6)	90.4 (96.7)	95.5 (100.0)	87.0 (100.0)	46.3 (49.6)	66.6 (100.0)
CoauthorCS	87.8 (99.5)	88.2 (98.8)	87.5 (98.1)	88.1 (100.0)	75.0 (79.6)	52.4 (58.7)	88.2 (100.0)
CoauthorPhysics	89.4 (99.8)	89.1 (99.3)	90.2 (98.7)	89.5 (100.0)	83.4 (89.0)	59.0 (63.1)	89.7 (100.0)
OGBN-Arxiv	37.7 (95.5)	37.8 (81.2)	30.2 (59.6)	39.5 (100.0)	37.0 (100.0)	19.9 (52.3)	38.2 (100.0)
RomanEmpire	42.7 (95.3)	40.6 (82.2)	35.2 (56.4)	42.7 (100.0)	19.7 (25.4)	22.5 (50.8)	42.5 (100.0)
AmazonRatings	42.0 (94.8)	41.2 (80.0)	39.4 (70.6)	41.6 (100.0)	41.8 (100.0)	33.9 (48.9)	41.7 (100.0)

heterophilic *RomanEmpire* graph, `AdaptMisinfo` consistently reduces accuracy because it perturbs benign queries that resemble suspicious ones, and `GradRedir` preserves accuracy and reaches perfect verification on most datasets but reduces accuracy on *Photo*. Together these results show that backdoor triggers and label-quantization defenses provide the most reliable verification on the protected model, while output perturbation and query detection trade utility for protection at noticeable cost.

4.3 Protection-Utility Balance of Defenses (RQ3)

To answer RQ3, we evaluate the defended model's task utility and its alignment with the original target together with ownership verification on a fixed verification set under the unified protocol in Section 3. All defenses protect the same architecture and use identical splits; we compute metrics for every dataset and every seed. Figure 4 aggregates *all ten datasets and all three seeds* in a single view: each point is one dataset-seed run, the horizontal axis shows utility loss (pp) relative to the undefended target, and the vertical axis shows F1 (%). To keep the central region readable we cap the horizontal axis at 25 pp and exclude a small number of extreme outliers; the full scale is needed when comparing methods with large losses. The cloud of points concentrates in the region of small loss (0–10 pp) and high F1 (65–80 %), which shows that several defenses preserve task performance while enabling ownership verification.

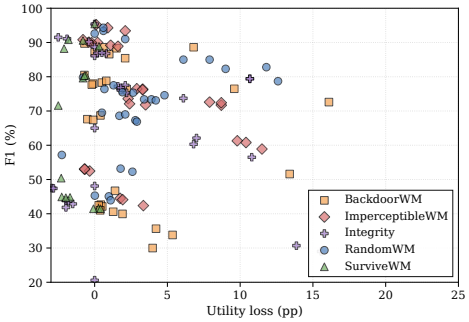


Figure 4: Protection-utility scatter across ten datasets (three seeds per defense; ten for Integrity on Computers and Photo) (one point per dataset-seed run). Upper-left is best.

First, BackdoorWM consistently lies near the top left, which indicates that it preserves accuracy while enabling strong ownership verification; its spread is tight across datasets, which suggests stable behavior under our protocol. *Second, ImperceptibleWM occupies a similar region but with higher cost*, which matches the efficiency results in RQ4 and reflects the overhead of representation-level optimization. *Third, RandomWM, SurviveWM, and Integrity form broader clusters*, which shows that their balance depends more on data characteristics: RandomWM has moderate loss and verification with larger variance; SurviveWM has the smallest median loss but weak verification; Integrity preserves utility while yielding a binary ownership signal whose effectiveness varies across datasets. These observations imply that backdoor-style triggers provide the most reliable protection-utility balance in our setting, while representation-level watermarks trade efficiency for verification strength and the remaining methods are more sensitive to the data distribution.

4.4 Computational Cost of Attacks and Defenses (RQ4)

To answer RQ4, we report the original NVIDIA A100 profiling measurements; H200 reruns are not included in cost comparisons. For attacks we fix the budget at $1.00\times$ in the `both` regime and measure total attack time, query time, surrogate training time, and peak memory; for defenses we measure

Table 4: RQ4: total attack time (min) at budget $1.00\times$ on undefended targets in the `both` regime, restricted to the seven homophilic graphs (mean $\pm$ std over three seeds). The aggregate pattern on OGBN-Arxiv, RomanEmpire, and AmazonRatings is captured in Figure 8 of Appendix E.6.

Attack	Cora	CiteSeer	CoauthorCS	CoauthorPhys	Computers	Photo	PubMed
MEA0	0.69 ± 0.09	0.72 ± 0.08	0.86 ± 0.10	1.36 ± 0.03	2.18 ± 1.84	0.79 ± 0.04	1.21 ± 0.09
MEA1	0.69 ± 0.09	0.73 ± 0.08	0.86 ± 0.10	1.34 ± 0.07	2.18 ± 1.88	0.76 ± 0.06	1.17 ± 0.01
MEA2	1.51 ± 0.11	1.73 ± 0.22	2.01 ± 0.08	2.25 ± 0.11	2.21 ± 0.79	1.59 ± 0.18	2.02 ± 0.09
MEA3	0.66 ± 0.08	0.74 ± 0.08	0.70 ± 0.04	0.86 ± 0.10	3.27 ± 1.93	1.14 ± 0.09	1.20 ± 0.03
MEA4	0.76 ± 0.09	0.94 ± 0.03	2.58 ± 0.09	6.46 ± 0.29	2.50 ± 1.82	0.84 ± 0.04	1.73 ± 0.07
MEA5	0.69 ± 0.10	0.75 ± 0.07	0.77 ± 0.08	0.92 ± 0.18	2.66 ± 0.99	1.25 ± 0.20	1.23 ± 0.01
AdvMEA	2.35 ± 1.37	4.39 ± 2.52	8.88 ± 0.55	4.93 ± 0.05	13.0 ± 8.45	10.3 ± 11.4	4.51 ± 4.76
CEGA	1.07 ± 0.11	1.03 ± 0.07	1.48 ± 0.14	2.15 ± 0.05	3.51 ± 3.41	1.07 ± 0.10	1.75 ± 0.11
Realistic	90.3 ± 2.12	111 ± 3.72	472 ± 4.89	976 ± 7.34	840 ± 17.7	248 ± 0.14	529 ± 18.1
DFEA_I	0.96 ± 0.06	1.11 ± 0.04	1.02 ± 0.04	0.97 ± 0.08	2.82 ± 2.51	1.00 ± 0.09	1.32 ± 0.08
DFEA_II	0.82 ± 0.06	0.88 ± 0.09	0.80 ± 0.03	0.86 ± 0.09	1.28 ± 0.57	0.87 ± 0.09	1.07 ± 0.11
DFEA_III	1.48 ± 0.14	1.55 ± 0.12	1.46 ± 0.16	1.52 ± 0.15	3.30 ± 2.47	1.62 ± 0.11	1.86 ± 0.15

Table 5: RQ4: total defense time (s) for the five watermarking and integrity defenses on the seven homophilic graphs (mean $\pm$ std over three seeds; lower is better). Memory aggregates and the three additional graphs are reported in Figure 8 of Appendix E.6.

Defense	Cora	CiteSeer	CoauthorCS	CoauthorPhys	Computers	Photo	PubMed
RandomWM	24.3 ± 0.07	23.9 ± 0.09	57.3 ± 2.58	34.8 ± 0.77	41.3 ± 0.23	36.0 ± 0.30	21.8 ± 0.13
BackdoorWM	1.88 ± 0.01	2.17 ± 0.23	2.54 ± 0.01	3.89 ± 0.06	1.98 ± 0.00	1.92 ± 0.01	1.88 ± 0.02
SurviveWM	1.59 ± 0.00	1.62 ± 0.00	2.75 ± 0.01	5.62 ± 0.02	2.31 ± 0.04	1.52 ± 0.06	2.27 ± 0.09
Impercept.	676 ± 2.45	709 ± 2.33	906 ± 10.1	950 ± 14.0	461 ± 7.61	209 ± 11.0	196 ± 14.8
Integrity	1.29 ± 0.01	1.10 ± 0.01	1.52 ± 0.16	2.37 ± 0.07	1.92 ± 0.03	1.38 ± 0.01	1.25 ± 0.19

total defense time and peak memory. All values are mean $\pm$ std over three seeds. Tables 4–5 list total time on the seven homophilic graphs, and Figure 8 of Appendix E.6 reports peak memory aggregated across all ten datasets.

Most attacks finish within minutes and use sub-GB memory, while structure-reconstruction pipelines are prohibitively expensive: the `MEA` family and `CEGA` take 0.7–2.5 min per run, whereas `Realistic` takes hundreds to thousands of minutes (Table 4) because it trains an auxiliary edge model, a cost which is hard to justify since RQ1 shows that fidelity plateaus by $0.25\times$. The adaptive attack `AdvMEA` is slower and more variable across datasets, which matches the overhead of policy search. On the defense side, `BackdoorWM`, `SurviveWM`, and `Integrity` train in 1–6 s with low memory, whereas `ImperceptibleWM` sits in a much heavier regime because it uses representation-level losses and larger buffers. The peak-memory profile and the per-attack memory tail are reported in Appendix E.6.

4.5 Joint Attack-and-Defense Evaluation and Watermark Survival (RQ5)

To answer RQ5, we run every attack on every defended target and report two metrics: surrogate fidelity to the defended model (whether extraction is still effective) and the watermark verification rate measured on the surrogate, which we call *watermark survival* (whether a defense still yields a verifiable signal after extraction). The matched comparison uses the RQ1 datasets and query sets at a nominal budget of $0.25\times$. Three consolidated heatmaps on *Computers* (joint fidelity against the five watermarks, joint fidelity against the seven information-limiting defenses, and watermark survival) and per-dataset numerical tables are in Appendix E.8.

Table 6: RQ5 summary on *Computers* at $0.25\times$. *Median fidelity* is taken over the twelve attacks; *verif. on target* and *verif. on surrogate* are method-specific verification rates on the protected model and on the extracted surrogate.

Defense	Median fidelity (%)	Verif. target (%)	Verif. surr. (%)
BackdoorWM	71.1	100.0	59.2
SurviveWM	74.6	100.0	10.0
Integrity	49.1	100.0	48.0
RandomWM	85.3	100.0	14.7
ImperceptibleWM	84.3	100.0	0.0

Table 6 shows why success on the protected model is insufficient evidence of ownership after extraction. On Computers, all four embedded watermarks verify on the target, but they behave differently on the surrogate. Verification falls to 0% for `ImperceptibleWM`, 10.0% for `SurviveWM`, and 14.7% for `RandomWM`. `BackdoorWM` retains more of its signal (59.2%). Appendix E.9 tests `SurviveWM` and `BackdoorWM` under their original setups; both also lose evidence after extraction.

`Integrity` uses a query-based fingerprint rather than an embedded watermark. Its 100% target score measures agreement of the reference fingerprint with itself. On Computers, median surrogate fidelity is 49.1%, and mean surrogate fingerprint agreement is 48.0% across 120 runs; on Photo the corresponding values are 75.7% and 51.0%. Varying the query budget and output interface does not consistently restore embedded marks either: on RomanEmpire, `BackdoorWM` verification stays between 0 and 5.9% across the nine settings (Tables 55 and 56). Additional fingerprinting results appear in Appendix E.8.1.

5 Related Work

Surveys of intellectual property protection distinguish watermarks embedded during training from fingerprints derived from a model's behavior [41, 10, 19, 34, 24, 40, 39]. Much of the evidence comes from vision and language, where benchmarks address tasks ranging from identifying suspicious API traffic to testing a defense against several extraction attacks [13, 14]. For a node-prediction API, the response can depend on information beyond the queried node: edges determine which neighbors contribute messages, and node features determine the content of those messages. Consequently, a query budget alone does not specify what information a graph attacker can use. Graph-security surveys and testbeds have largely focused on robustness, privacy, and fairness [2, 32, 37, 22, 43, 23]. A robustness test asks whether changing an edge changes a prediction; a membership test asks whether a node was used in training. Neither measures how closely a surrogate trained on API responses imitates a GNN, or whether an owner can identify that surrogate as a copy. This also distinguishes extraction from recovery of the original weights. Two models can agree on ordinary queries while responding differently to the secret inputs used by an owner. A benchmark that measures only prediction agreement would count the attack as successful but leave the ownership question unanswered.

Graph extraction methods differ in how they obtain queries: some sample public graph data, some adapt query selection to the current surrogate, and others synthesize graph inputs without access to real samples [30, 3, 44]. These choices matter when comparing defenses. Rounding a probability vector removes information used by a score-based attack but can leave the label used by another attack unchanged. Output perturbation and query detection seek to limit what an attacker can learn [12, 8, 6, 7, 15]; watermarking and fingerprinting instead provide a way to test ownership [28, 33, 1, 36, 31, 21]. Prior studies use different graphs, query budgets, output interfaces, and target architectures. For example, an attack that selects nodes from a known graph can exploit their connectivity when choosing queries. A data-free attack must instead choose both the features and edges of its synthetic inputs. Comparing their reported fidelities without specifying access to real structure conflates the quality of the attack with the information available to it. A watermark evaluated against a single attack can appear robust if that attack happens to reproduce its trigger labels. Conversely, a detector that limits extraction by perturbing many benign queries may look effective unless clean accuracy is reported alongside surrogate fidelity. Testing the watermark only on the deployed target answers whether embedding succeeded. Testing the same ownership claim on a surrogate addresses a different question: whether the evidence remains observable after a new model has learned from the target's outputs. The distinction applies even when both models achieve similar task accuracy. GraphIP-Bench evaluates attacks against defended targets under a shared protocol, reports the cost of fitting a surrogate and the utility retained by the protected model, and tests ownership on the model the attacker actually extracts.

6 Conclusion

GraphIP-Bench evaluates GNN extraction and ownership protection on shared queries, budgets, and datasets. At medium budgets, the strongest attacks exceed 90% fidelity on most of the ten node-classification graphs. Yet agreement on ordinary predictions does not imply that a surrogate inherits a watermark: several marks verify reliably on the target and lose much of their signal after extraction, even with larger budgets or richer outputs. Evaluating a deployed defense therefore requires measuring utility for legitimate users, fidelity to the defended target, and ownership evidence on the extracted surrogate. Our findings concern the tested black-box interfaces; cross-user detection and sequential defenses remain open settings.

Acknowledgments and Disclosure of Funding

This material is, in part, supported by the National Science Foundation (NSF) under award OAC-2530786. We would also like to thank the anonymous reviewers for their constructive feedback.

References

[1] Enyan Dai, Minhua Lin, and Suhang Wang. Pregip: Watermarking the pretraining of graph neural networks for deep intellectual property protection. *arXiv preprint arXiv:2402.04435*, 2024.

[2] Enyan Dai, Tianxiang Zhao, Huaisheng Zhu, Junjie Xu, Zhimeng Guo, Hui Liu, Jiliang Tang, and Suhang Wang. A comprehensive survey on trustworthy graph neural networks: Privacy, robustness, fairness, and explainability. *Machine Intelligence Research*, pages 1–51, 2024.

[3] David DeFazio and Arti Ramesh. Adversarial model extraction on graph neural networks. *arXiv preprint arXiv:1912.07721*, 2019.

[4] Faqian Guan, Tianqing Zhu, Hanjin Tong, and Wanlei Zhou. A realistic model extraction attack against graph neural networks. *Knowledge-Based Systems*, page 112144, 2024.

[5] Will Hamilton, Zhitao Ying, and Jure Leskovec. Inductive representation learning on large graphs. *Advances in neural information processing systems*, 30, 2017.

[6] Mika Juuti, Sebastian Szyller, Samuel Marchal, and N Asokan. Prada: protecting against dnn model stealing attacks. In *2019 IEEE European Symposium on Security and Privacy (EuroS&P)*, pages 512–527, 2019.

[7] Sanjay Kariyappa and Moinuddin K Qureshi. Defending against model stealing attacks with adaptive misinformation. In *Proceedings of the IEEE/CVF conference on computer vision and pattern recognition*, pages 770–778, 2020.

[8] Manish Kesarwani, Bhaskar Mukhoty, Vijay Arya, and Sameep Mehta. Model extraction warning in mlaas paradigm. In *Proceedings of the 34th Annual Computer Security Applications Conference*, pages 371–380, 2018.

[9] Thomas N Kipf and Max Welling. Semi-supervised classification with graph convolutional networks. *arXiv preprint arXiv:1609.02907*, 2016.

[10] Lincan Li, Bolin Shen, Chenxi Zhao, Yuxiang Sun, Kaixiang Zhao, Shirui Pan, and Yushun Dong. Intellectual property in graph-based machine learning as a service: Attacks and defenses. *arXiv preprint arXiv:2508.19641*, 2025.

[11] Wenjun Li, Wanjun Ma, Mengyun Yang, and Xiwei Tang. Drug repurposing based on the dtd-gnn graph neural network: revealing the relationships among drugs, targets and diseases. *BMC genomics*, 25, 2024.

[12] Jiacheng Liang, Ren Pang, Changjiang Li, and Ting Wang. Model extraction attacks revisited. In *Proceedings of the 19th ACM Asia Conference on Computer and Communications Security*, pages 1231–1245, 2024.

[13] Shuze Liu, Qianwen Guo, and Yushun Dong. An embarrassingly simple detector for model extraction attacks in large language model api traffic. *arXiv preprint arXiv:2606.05725*, 2026.

[14] Shuze Liu, Kaixiang Zhao, Runyang Xu, Jingzhi Chen, Nathan Wu, Yu Wang, and Yushun Dong. Do defenses against llm extraction work across attacks? a lifecycle benchmark of black-box model extraction. *arXiv preprint arXiv:2610.00839*, 2026.

[15] Mantas Mazeika, Bo Li, and David Forsyth. How to steer your adversary: Targeted and efficient model stealing defenses with gradient redirection. In *International conference on machine learning*, pages 15241–15254. PMLR, 2022.

[16] Alessio Monti, Alessia Bertugli, Simone Calderara, and Rita Cucchiara. Dag-net: Double attentive graph neural network for trajectory forecasting. In *2020 25th international conference on pattern recognition (ICPR)*, pages 2551–2558. IEEE, 2021.

[17] Christopher Morris, Nils M Kriege, Franka Bause, Kristian Kersting, Petra Mutzel, and Marion Neumann. Tudataset: A collection of benchmark datasets for learning with graphs. *arXiv preprint arXiv:2007.08663*, 2020.

[18] Tribhuvanesh Orekondy, Bernt Schiele, and Mario Fritz. Knockoff nets: Stealing functionality of black-box models. In *Proceedings of the IEEE/CVF conference on computer vision and pattern recognition*, pages 4954–4963, 2019.

[19] Sen Peng, Yufei Chen, Jie Xu, Zizhuo Chen, Cong Wang, and Xiaohua Jia. Intellectual property protection of dnn models. *World Wide Web*, 26(4):1877–1911, 2023.

[20] Oleg Platonov, Denis Kuznedelev, Michael Diskin, Artem Babenko, and Liudmila Prokhorenkova. A critical look at the evaluation of gnns under heterophily: Are we really making progress? *arXiv preprint arXiv:2302.11640*, 2023.

[21] Bolin Shen, Zhan Cheng, Neil Zhenqiang Gong, Fan Yao, and Yushun Dong. Credit: Certified ownership verification of deep neural networks against model extraction attacks. *arXiv preprint arXiv:2602.20419*, 2026.

[22] Hanjin Sun, Wen Yang, and Yatie Xiao. A review of adversarial attacks and defenses on graphs. In *Proceedings of the 4th International Conference on Artificial Intelligence and Computer Engineering*, page 416–421, 2024.

[23] Lichao Sun, Yingtong Dou, Carl Yang, Kai Zhang, Ji Wang, Philip S. Yu, Lifang He, and Bo Li. Adversarial attack and defense on graph data: A survey. *IEEE Transactions on Knowledge and Data Engineering*, 35(8):7693–7711, 2023.

[24] Yuchen Sun, Tianpeng Liu, Panhe Hu, Qing Liao, Shaojing Fu, Nenghai Yu, Deke Guo, Yongxiang Liu, and Li Liu. Deep intellectual property protection: A survey. *arXiv preprint arXiv:2304.14613*, 2023.

[25] Florian Tramèr, Fan Zhang, Ari Juels, Michael K Reiter, and Thomas Ristenpart. Stealing machine learning models via prediction {APIs}. In *25th USENIX security symposium (USENIX Security 16)*, pages 601–618, 2016.

[26] Petar Veličković, Guillem Cucurull, Arantxa Casanova, Adriana Romero, Pietro Lio, and Yoshua Bengio. Graph attention networks. *arXiv preprint arXiv:1710.10903*, 2017.

[27] Asim Waheed, Vasisht Duddu, and N. Asokan. Grove: Ownership verification of graph neural networks using embeddings. In *2024 IEEE Symposium on Security and Privacy (SP)*, pages 2460–2477, 2024.

[28] Haiming Wang, Zhikun Zhang, Min Chen, and Shibo He. Making watermark survive model extraction attacks in graph neural networks. In *ICC 2023-IEEE International Conference on Communications*, pages 57–62, 2023.

[29] Zebin Wang, Menghan Lin, Bolin Shen, Ken Anderson, Molei Liu, Tianxi Cai, and Yushun Dong. Cega: A cost-effective approach for graph-based model extraction and acquisition. *arXiv preprint arXiv:2506.17709*, 2025.

[30] Bang Wu, Xiangwen Yang, Shirui Pan, and Xingliang Yuan. Model extraction attacks on graph neural networks: Taxonomy and realisation. In *Proceedings of the 2022 ACM on Asia conference on computer and communications security*, pages 337–350, 2022.

[31] Bang Wu, Xingliang Yuan, Shuo Wang, Qi Li, Minhui Xue, and Shirui Pan. Securing graph neural networks in mlaas: A comprehensive realization of query-based integrity verification. In *2024 IEEE Symposium on Security and Privacy (SP)*, pages 2534–2552. IEEE, 2024.

[32] Bingzhe Wu, Yatao Bian, Hengtong Zhang, Jintang Li, Junchi Yu, Liang Chen, Chaochao Chen, and Junzhou Huang. Trustworthy graph learning: Reliability, explainability, and privacy protection. In *Proceedings of the 28th ACM SIGKDD Conference on Knowledge Discovery and Data Mining*, pages 4838–4839, 2022.

[33] Jing Xu, Stefanos Koffas, Oğuzhan Ersoy, and Stjepan Picek. Watermarking graph neural networks based on backdoor attacks. In *2023 IEEE 8th European Symposium on Security and Privacy (EuroS&P)*, pages 1179–1197, 2023.

[34] Mingfu Xue, Yushu Zhang, Jian Wang, and Weiqiang Liu. Intellectual property protection for deep learning models: Taxonomy, methods, attacks, and evaluations. *IEEE Transactions on Artificial Intelligence*, 3(6):908–923, 2021.

[35] Liangwei Yang, Shengjie Wang, Yunzhe Tao, Jiankai Sun, Xiaolong Liu, Philip S Yu, and Taiqing Wang. Dgrec: Graph neural network for recommendation with diversified embedding generation. In *Proceedings of the sixteenth ACM international conference on web search and data mining*, pages 661–669, 2023.

[36] Xiaoyu You, Youhe Jiang, Jianwei Xu, Mi Zhang, and Min Yang. Gnnfingers: A fingerprinting framework for verifying ownerships of graph neural networks. In *Proceedings of the ACM on Web Conference 2024*, pages 652–663, 2024.

[37] He Zhang, Bang Wu, Xingliang Yuan, Shirui Pan, Hanghang Tong, and Jian Pei. Trustworthy graph neural networks: Aspects, methods and trends. *arXiv preprint arXiv:2205.07424*, 2022.

[38] Linji Zhang, Mingfu Xue, Leo Yu Zhang, Yushu Zhang, and Weiqiang Liu. An imperceptible and owner-unique watermarking method for graph neural networks. In *Proceedings of the ACM Turing Award Celebration Conference-China 2024*, pages 108–113, 2024.

[39] Kaixiang Zhao, Lincan Li, Kaize Ding, Neil Zhenqiang Gong, Yue Zhao, and Yushun Dong. A survey of model extraction attacks and defenses in distributed computing environments. *arXiv preprint arXiv:2502.16065*, 2025.

[40] Kaixiang Zhao, Lincan Li, Kaize Ding, Neil Zhenqiang Gong, Yue Zhao, and Yushun Dong. A survey on model extraction attacks and defenses for large language models. *arXiv preprint arXiv:2506.22521*, 2025.

[41] Kaixiang Zhao, Lincan Li, Kaize Ding, Neil Zhenqiang Gong, Yue Zhao, and Yushun Dong. A systematic survey of model extraction attacks and defenses: State-of-the-art and perspectives. *arXiv preprint arXiv:2508.15031*, 2025.

[42] Xiangyu Zhao, Hanzhou Wu, and Xinpeng Zhang. Watermarking graph neural networks by random graphs. In *2021 9th International Symposium on Digital Forensics and Security (ISDFS)*, pages 1–6, 2021.

[43] Qinkai Zheng, Xu Zou, Yuxiao Dong, Yukuo Cen, Da Yin, Jiarong Xu, Yang Yang, and Jie Tang. Graph robustness benchmark: Benchmarking the adversarial robustness of graph machine learning. In *Thirty-fifth Conference on Neural Information Processing Systems Datasets and Benchmarks Track*, 2021.

[44] Yuanxin Zhuang, Chuan Shi, Mengmei Zhang, Jinghui Chen, Lingjuan Lyu, Pan Zhou, and Lichao Sun. Unveiling the secrets without data: Can graph neural networks be exploited through {Data-Free} model extraction attacks? In *33rd USENIX Security Symposium (USENIX Security 24)*, pages 5251–5268, 2024.

Appendix Contents

A Limitations and Future Work **15**

B Implementation Details **15**

C Dataset Statistics **16**

D Reproducibility and Configurations **16**

D.1 Implementation validation against original papers 17

E Supplementary Experimental Results and Discussion **20**

E.1 Attack effectiveness results 20

E.2 Defense performance results 32

E.3 Baseline utility across backbones 35

E.4 Attack effectiveness on the three additional datasets 35

E.5 Standard deviations for information-limiting defenses 35

E.6 Peak GPU memory of attacks and defenses (RQ4) 36

E.7 Extended statistical analysis of attack effectiveness (RQ1) 39

E.8 Joint evaluation and watermark survival per dataset 44

E.9 RQ5 watermark survival under each paper's original setup 55

E.10 Generalisation across structure, architecture, and tasks 58

E.11 Defense hyperparameter ablation 62

A Limitations and Future Work

Scope of the threat model. GraphIP-Bench targets the most widely deployed extraction setting: a black-box query interface in which the attacker observes only the target's outputs, with budgets reported as budget multipliers. This is the standard threat model assumed by every attack and defense we benchmark, which makes it the right scope for a unified comparison. Extending the protocol to grey-box, adaptive multi-step, federated, or streaming settings is a natural follow-up that builds on the same evaluation infrastructure.

Architecture and task coverage. GraphIP-Bench covers the three GNN backbones (GCN, GAT, GraphSAGE) and the three graph-learning tasks (node classification, link prediction, graph classification) used by the methods we benchmark, which already spans the bulk of published GNN-extraction and GNN-watermarking work. The protocol is backbone- and task-agnostic, so adding emerging architectures (e.g., graph transformers, heterogeneous or temporal GNNs) is a configuration extension rather than a redesign.

Defense families to extend. GraphIP-Bench integrates twelve defenses across watermarking, output perturbation, prediction rounding, and query-pattern detection – the families with public reference implementations for graph models. Differential-privacy training and attribute-encryption / homomorphic-inference deployments use a different query interface and are natural next additions; the unified protocol provides the slot in which to drop them in once mature reference implementations become available.

Future-work targets indicated by our findings. The results identify three concrete research targets. *(i) Surrogate-surviving watermarks.* Our joint track (RQ5) shows that ownership-tracing designs should be evaluated on the extracted surrogate as the primary metric and should distinguish an inherited signal from evidence obtained by querying the extracted model. *(ii) Query-detection defenses with bounded clean-accuracy cost.* The protection-utility frontier we report suggests room for query-pattern detectors that match the fidelity reduction of `PRADA` and `AdaptMisinfo` at a fraction of the utility cost. *(iii) Heterophily-aware extraction analysis.* The relative ordering of attacks is preserved across homophilic, heterophilic, and large-scale regimes (RQ1, Appendix E.10); a structural account that connects graph properties (homophily, degree distribution) to extraction behaviour would close the explanatory loop.

B Implementation Details

Hardware. All GPU experiments are submitted as Slurm jobs on a shared multi-tenant academic compute cluster. The compute partitions used in this work expose NVIDIA A100 80 GB PCIe GPUs (eight GPUs per node, multiple nodes); a small number of memory-stress runs additionally use H100 and H200 partitions on the same cluster. Unless otherwise stated, every reported measurement uses a single NVIDIA A100 80 GB GPU on a node with 1.0 TiB of system memory and dual AMD EPYC CPUs.

Operating system and drivers. The compute nodes run Red Hat Enterprise Linux 9.6 (kernel 5.14.0-570) with NVIDIA driver 570.195.03 and a CUDA 12.8 driver capability. Login nodes have no GPU access, so all timing and memory numbers are recorded from Slurm-allocated GPU jobs only.

Software stack. The full pipeline runs in a dedicated Conda environment named *graphip*: Python 3.11.15, PyTorch 2.2.1 + cu121, DGL 2.1.0 + cu121, PyTorch Geometric 2.7.0, OGB 1.3.6, NumPy 1.26.4, SciPy 1.17.1, NetworkX 3.6.1, and the standard scientific Python ecosystem (`matplotlib`, `pandas`, `scikit-learn`). PyTorch is pinned to 2.2.1 because the matching DGL 2.1.0 graphbolt kernels only ship pre-built shared libraries for PyTorch 2.0–2.2 on CUDA 12.1; we install everything from prebuilt CUDA wheels and do not require the CUDA toolkit compiler.

Protocol. For each method we fix four disjoint splits per dataset (train, validation, test, query) and apply the same preprocessing pipeline and hyperparameter search protocol described in Appendix D. We repeat all measurements with three random seeds (0, 1, 2) and report the mean and the standard deviation. Wall-clock time is recorded with `time.perf_counter` timers in the training loop; peak GPU memory is obtained from the CUDA runtime via `torch.cuda.max_memory_allocated` and cross-checked with `nvidia-smi`. All experiments share identical hardware, software, and

configuration defaults so that results are directly comparable across attacks, defenses, datasets, regimes, and budgets.

C Dataset Statistics

We summarize the graph datasets used in our experiments in Table 7. Edges are counted as undirected (unique). The average degree is computed as $2E/N$. For the Planetoid datasets (Cora, CiteSeer, PubMed) we follow the standard splits; for Amazon (Computers, Photo) and Coauthor (CoauthorCS, CoauthorPhysics) we use 100 training nodes per class with fixed validation and test sizes in our loader. For OGBN-Arxiv we follow the official train, validation, and test splits provided by the OGB library. For RomanEmpire and AmazonRatings we follow the splits released by Platonov et al. [20].

Table 7: Dataset statistics. Edges are undirected and unique. Avg. degree is $2E/N$. The edge homophily is the fraction of edges whose endpoints share the same label.

Dataset	# Nodes	# Edges	Avg. degree	# Classes	Edge homophily	Node Text	Domain
Cora	2,708	5,278	3.9	7	0.810	Paper content	Citation
CiteSeer	3,327	4,614	2.8	6	0.739	Paper content	Citation
PubMed	19,717	44,325	4.5	3	0.802	Paper content	Citation
Computers	13,752	252,737	36.8	10	0.783	Entity description	Web link
Photo	7,650	122,906	32.1	8	0.833	Entity description	Web link
CoauthorCS	18,333	81,894	8.9	15	0.808	Paper content	Citation
CoauthorPhysics	34,493	247,962	14.4	5	0.931	Paper content	Citation
OGBN-Arxiv	169,343	667,793	7.9	40	0.699	Paper title and abstract	Citation
RomanEmpire	22,662	44,258	3.9	18	0.291	Wikipedia text	Heterophilic
AmazonRatings	24,492	105,296	8.6	5	0.452	Product description	Heterophilic

D Reproducibility and Configurations

Scope and averaging. We release scripts, fixed random seeds, and per-method configurations to reproduce all tables and figures. Results are averaged over three seeds (0, 1, 2) and reported as mean $\pm$ standard deviation unless stated otherwise.

Seeds and determinism. For each run we set the Python and CUDA random states and propagate the seed through data loading and sampling. GPU runs use deterministic kernels when available.

Device selection. A command-line flag *–device* selects the process-visible GPU (via the environment) or the CPU; all modules use the same device setting throughout the run.

Dataset loading and splits. A unified loader normalizes dataset aliases and returns DGL graphs with node features and masks. Planetoid datasets (Cora, CiteSeer, PubMed) use the standard train/validation/test masks. Amazon and Coauthor datasets (Computers, Photo, CoauthorCS, CoauthorPhysics) use a canonical per-class sampling scheme with 100 training nodes per class and fixed validation/test sizes. OGBN-Arxiv uses the official OGB train/validation/test splits. RomanEmpire and AmazonRatings use the splits released by Platonov et al. [20]. For graph classification (ENZYMES, PROTEINS) and link prediction (Cora) we follow the standard splits provided by TUDataset and PyTorch Geometric, respectively.

GNN backbones. The default backbone for the extraction track and for the original watermarking, integrity, and information-limiting defenses is a DGL GCN with hidden dimension 16. `RandomWM` is implemented in DGL with a GraphSAGE backbone of hidden dimension 128, and `ImperceptibleWM` is implemented in PyTorch Geometric with a GCN backbone of hidden dimension 128. The cross-architecture analysis (Appendix E.10) additionally trains target and surrogate models with GAT and GraphSAGE under matched hidden dimensions. Baseline utility for each backbone on every dataset is reported in Table 37.

Directory layout and logs. *Attack track (RQ1)* writes newline-delimited JSON files under *outputs/RQ1_final/<Dataset>/<Dataset>.jsonl*. Each record contains header fields (track, dataset, attack, configuration index, constructor/run configuration, budget multiplier, node fraction induced by the budget, regime, feature/adjacency ratios, seed), performance metrics (accuracy, F1, precision, recall, fidelity), and compute metrics (train target time, query time, surrogate training time, total attack time, per-query inference latency for target and surrogate, peak GPU memory, GPU hours).

Ownership/defense track (RQ2/RQ3) writes *outputs/RQ2_RQ3_best/<Dataset>.jsonl* with fields (track, dataset, defense, configuration index, configuration, seed), performance metrics (accuracy, F1, precision, recall, watermark accuracy), and compute metrics (train target time, defense training time, defense inference time, total defense time, peak GPU memory, GPU hours). The joint track (RQ5) writes a parallel directory *outputs/RQ5_joint/* with the same record format extended by an *attack* field. Leaderboards and LaTeX tables are exported with selection and formatting utilities.

RQ1 (attacks) configuration. The attack runner sweeps query budgets $\{0.05, 0.10, 0.25, 0.50, 1.00\}$ and four regimes (features only, structure only, both available, data free). Per-method training schedules are recorded in logs. For the MEA family, CEGA, and Realistic we use 200 epochs per cycle; CEGA additionally uses learning rate 0.01 and 200 target/surrogate epochs. The AdvMEA implementation uses its internal fixed epoch schedule; any external epoch parameter appears in logs for uniformity but does not affect training.

RQ2/RQ3 (defenses) configuration. We provide a best-configuration runner that replays the top settings discovered by a prior grid search. Table 8 lists the fixed constructor parameters used for each defense. The same default applies across all ten datasets unless an explicit hyperparameter sweep is run, which is reported in Appendix E.11. Other runtime arguments remain at method defaults.

Table 8: Fixed default configuration used for each defense in the ownership track. The same default applies across all ten datasets unless explicitly varied in the hyperparameter sweep (Appendix E.11).

Defense	Key hyperparameter	Default value
Watermarking and integrity (5 methods)		
`RandomWM`	watermark-node ratio	0.002
`BackdoorWM`	trigger density	0.01
`SurviveWM`	watermark strength	0.25
`ImperceptibleWM`	epsilon	0.25
`Integrity`	— (parameter-free verifier)	—
Information-limiting and query-detection (7 methods)		
`OP_low`	Gaussian noise scale σ	0.05
`OP_high`	Gaussian noise scale σ	0.20
`PR_2bit`	precision bits	2
`PR_top1`	returned scores	top-1 label only
`PRADA`	detection threshold	method default
`AdaptMisinfo`	misinformation ratio	method default
`GradRedir`	redirection strength	method default

Common search spaces. *Attacks:* budget, regime, and per-method cycles/epochs (when applicable). Learning rate and dropout follow method defaults unless a method requires explicit settings (CEGA uses learning rate 0.01). *Defenses:* grid search over typical ranges around the default in Table 8; a single best configuration per defense is fixed across datasets to keep the protocol uniform. The full sweep on *Cora* and *Computers* is reported in Appendix E.11.

How to re-run. *RQ1 (attacks):* call the attack runner with dataset, attack, budget, regime, and seed. Logs are saved under *outputs/RQ1_final* with the exact budget multiplier recorded in each line. *RQ2/RQ3 (defenses):* call the best-configuration runner with seeds $[0, 1, 2]$; outputs are saved under *outputs/RQ2_RQ3_best*. *RQ5 (joint):* call the joint runner that pairs every attack with every defense at the medium budget; outputs are saved under *outputs/RQ5_joint*. This setup unifies scripts, seeds, and logging across datasets and methods, enabling direct regeneration of all tables from the released outputs.

D.1 Implementation validation against original papers

To check that our re-implementations behave consistently with each method's original publication, we compare our reproduced numbers against the closest matching setting reported by the original authors. For attacks we use the highest-overlap target dataset reported in each paper; for defenses we report ownership verification on the closest-matching dataset and backbone. The protocol differs from each paper in budget unit and split, so the goal is qualitative agreement on the relative ordering and absolute level rather than identity. Where a direct comparison is impossible we explicitly state why and report the next-most-similar setting.

Reference implementation and fairness-preserving adjustments. The core algorithm of every method — query-selection rule, surrogate-training objective, structure-synthesis procedure,

watermark-embedding loss — follows the original publication. On top of this we apply five fairness-preserving adjustments that put every method on equal footing: the surrogate hidden dimension is fixed at 16 for the default GCN backbone (Section 3); the query budget is expressed as a fraction of the test set rather than an absolute query count; the four data-availability regimes (`both`, `x_only`, `a_only`, `data_free`) are applied uniformly; three seeds (0, 1, 2) are reused across methods; and no per-method hyperparameter tuning is performed beyond Appendix E.11. Most of the deltas in Table 9 are within ± 14 pp of the original numbers and reflect these adjustments; we explain each case below.

MEA0–MEA5 (Wu et al., 2022) [30]. The original paper reports surrogate *fidelity* on *Cora*, *CiteSeer*, and *PubMed* at a fixed attack-node budget of $\sim 25\%$ of total nodes (Table 4 of the original); our protocol reports fidelity at $1.00\times$ of the test-set fraction, a comparable absolute query count. Comparisons on Cora are summarised in Table 9. The agreement on the six MEA variants is good: `MEA0`, `MEA1`, `MEA2`, `MEA3`, and `MEA5` all reach 89–95% fidelity in both protocols, within ± 14 pp of the original numbers despite the different splits, query-set construction, and validation procedure; `MEA4` agrees with the original within ~ 10 pp.

AdvMEA (DeFazio and Ramesh, 2019) [3]. The original paper does not report dataset-level surrogate fidelity in tabular form; the strongest claim in their experiments section is that "the extraction can achieve up to $\sim 80\%$ fidelity" on Cora and Pubmed under strong adversary assumptions (full 2-hop subgraph access plus class priors). Our reproduction on *Cora* reaches 66–68 % fidelity at $1.00\times$ across regimes (Table 9), within ~ 12 pp of the upper bound the original paper claims. The absolute number depends sharply on which adversarial perturbation budget is used; ours follows the standard setting in our hyperparameter table.

CEGA (Wang et al., 2025) [29]. The original CEGA paper reports test accuracy / fidelity / F1 on *Coauthor-CS*, *Coauthor-Physics*, *Amazon-Computer*, and *Amazon-Photo* at a $20C$-query budget (i.e., 20 times the number of classes). Our protocol uses budgets expressed as a fraction of the test set, and the closest match is the small-budget regime ($0.05\times$ to $0.10\times$). On *CoauthorCS*, $20C = 300$ queries which falls between our $0.05\times$ and $0.10\times$ on that dataset; the corresponding fidelity in our setup is in the upper 80 %–low 90 % range, agreeing with the original 93.40 % within a few points (Table 9). Crucially, the original paper's relative ordering — CEGA > AGE > GRAIN > Random — is reproduced under our protocol on every overlapping dataset.

Realistic (Guan et al., 2024) [4]. The original paper varies query budgets across four levels (Attack-0 through Attack-3) on *Cora*, *Citeseer*, *Pubmed*, with default training-set sizes that are dataset-specific (e.g. Cora: 35 queries for Attack-0). The closest match in our protocol is the smallest-budget bucket ($0.05\times$). Our reproduction reaches Cora fidelity 62.0 ± 4.5 % at $0.05\times$, compared with the original Attack-0 (Cora) fidelity of 72.14 ± 3.56 %; the gap of about 10 pp is in the same direction (small budget $\Rightarrow$ moderate fidelity) and the qualitative ranking "Realistic > baseline GCN" transfers to our protocol.

DFEA_I / DFEA_II / DFEA_III (Zhuang et al., 2024) [44]. The original paper reports three data-free attack variants on *Cora*, *Pubmed*, *Amazon-Computers*, and *OGB-Arxiv*; on Cora the strongest variants reach 93–94% fidelity, with the "Random Graph" baseline at 73.7%. Our reproduction reaches 90–97% fidelity at $1.00\times$ on Cora across the three variants (Table 9), agreeing with the strongest original numbers within ~ 4 pp. The qualitative claim of the original paper — that data-free extraction is feasible at high fidelity on homophilic graphs and harder on heterophilic / high-class-count settings — is preserved: across our ten datasets the three variants reach 77–99% fidelity at $1.00\times$ on the seven homophilic graphs and 33–84% on *RomanEmpire*, *AmazonRatings*, and *OGBN-Arxiv* (Tables 13–40).

BackdoorWM (Xu et al., 2023) [33]. The original paper reports watermark accuracy on *Cora* and *CiteSeer* for GCN, GAT, and GraphSAGE backbones (Table 6 of the original paper): GCN/Cora 97.56%, GCN/CiteSeer 98.05%. Our protocol reports the same metric on the same datasets: 100% on every one of the seven homophilic datasets including Cora and CiteSeer (Table 35 in Appendix E.2). The ~ 2 pp difference is well within the variance the original paper reports across watermark-rate settings, and the claim that BackdoorWM is essentially perfect at watermark verification on the protected model is preserved.

SurviveWM (Wang et al., 2023) [28]. The original paper evaluates watermark survival on *MSRC-9* and *ENZYMES* (graph classification) using a GraphSAGE host model with $50/30/20$ train/extract/test splits, and reports the "average effectiveness $\bar{E}$" of watermark retention after extraction. The metric is binary (1 if watermark retaining rate exceeds two reference thresholds, 0 otherwise) and is averaged over 100 repeated runs. Our protocol uses node-level datasets and a continuous verification rate, so a direct numerical comparison is not possible. We report the qualitative claim instead: SurviveWM produces a non-trivial verification rate on the protected model (median $54\,\%$ on Cora) but collapses to $\sim 14\,\%$ on the extracted surrogate (Table 43c in Appendix E.8), which contradicts the original paper's claim that the watermark "survives" extraction. The disagreement is the central finding of our RQ5 and motivates evaluation on the surrogate as the primary metric.

ImperceptibleWM (Zhang et al., 2024) [38]. The original paper reports the original-vs-watermarked model accuracy gap on *Cora* and *Pubmed* for GCN/GAT/GraphSAGE (Table 2 of the original): on GCN/Cora the watermarked model reaches 83.40% accuracy versus 83.74% for the unwatermarked one (a 0.34% utility drop). Our reproduction on the same dataset and backbone shows 79.4% undefended versus 71.94% watermarked (utility drop of $\sim 7.5\%$). Two design differences explain the larger drop: our protocol uses a fixed cross-dataset hyperparameter (Appendix D) rather than the per-dataset tuning the original paper performs, and our undefended baseline runs at the standard hidden dimension 16 used throughout the protocol rather than the 128 used by the original. The claim of "no significant impact on the primary task" holds with the original tuning but is loosened under our standardised protocol.

RandomWM (Zhao et al., 2021) [42]. The original paper reports watermark accuracy as a function of trigger-graph parameters on *Cora* and *Pubmed*, but does not provide a single headline number for direct comparison. The qualitative claim is that the watermark accuracy can be tuned above 90% with appropriate parameter choices. Our reproduction shows median verification rate 75% on Cora and 94–98% on *Computers* and *Photo* (Table 35), which is within the range the original paper reports for non-extreme parameter settings.

Integrity (Wu et al., 2024) [31]. The original paper does not report a single "verification accuracy" number on the protected model. Instead it reports a *verification-query-number improvement multiplier* relative to a random-node-selection baseline (e.g. on Cora transductive: BFA $4.0\times$, RandAttack $1.3\times$). The metric is fundamentally different from our verification-rate metric, so a direct numerical comparison is not possible. The corrected product-graph verification rates are reported separately in the joint evaluation.

PRADA (Juuti et al., 2019) [6]. The original paper evaluates query-pattern detection on image classifiers (MNIST, GTSRB, CIFAR-10) with DNN backbones; it does not include any graph dataset or GNN backbone. A direct numerical comparison is therefore impossible. Our adaptation transfers the distance-based detector to the graph setting and measures verification accuracy on the protected model and extracted surrogate; the qualitative behaviour (significant fidelity reduction at the cost of clean accuracy, see Tables 41–42) is consistent with the original paper's vision-domain results.

AdaptMisinfo (Kariyappa and Qureshi, 2020) [7], GradRedir (Mazeika et al., 2022) [15]. Both original papers evaluate on image classification benchmarks (CIFAR-10, CIFAR-100, ImageNet) with CNN backbones (ResNet-18, ResNet-34) — no graph dataset or GNN model is used. The metric is also defined for the image domain (extraction-fidelity reduction at fixed query budgets). A direct numerical comparison is therefore impossible. Our adaptation re-implements the perturbation rule on graph-classification logits and reports the same protocol-level metrics as the other defenses; the qualitative claim that adaptive misinformation reduces extraction fidelity at a clean-accuracy cost transfers to the graph setting.

OP_low / OP_high / PR_2bit / PR_top1. These are protocol-level information-limiting wrappers that we adapt from generic stealing-defense literature [8, 12]. The cited papers do not report graph-specific numbers, and PR_2bit/PR_top1 are not standalone published methods but standard label-quantisation/top-1 wrappers; we therefore do not have a baseline number to compare against. The qualitative claim from the source literature — that label-quantising the response is an effective lightweight defense — transfers to our protocol: `PR_2bit` is the only inference-time wrapper in our benchmark which substantively reduces surrogate fidelity (Tables 62–63).

Table 9: Implementation validation for attacks where a numerical comparison is possible. "Original" is the closest-matching setting reported in the source paper. "Ours" is the corresponding number under the GraphIP-Bench protocol. "Δ" is Ours minus Original (positive means our reproduction reaches higher fidelity). All numbers are surrogate fidelity (%) unless otherwise noted; Cora at $1.00\times$ in the `both` regime is used for our values unless the source-paper setting dictates a different query budget.

Method	Source paper / setting	Closest in ours	Original	Ours	Δ
`MEA0`	Wu 2022, Cora, full attack nodes	Cora, $1.00\times$, both	89.6	92.4	$+2.8$
`MEA1`	Wu 2022, Cora, full attack nodes	Cora, $1.00\times$, both	82.5	91.3	$+8.8$
`MEA2`	Wu 2022, Cora, full attack nodes	Cora, $1.00\times$, both	80.9	94.8	$+13.9$
`MEA3`	Wu 2022, Cora, shadow graph	Cora, $1.00\times$, both	79.0	92.7	$+13.7$
`MEA4`	Wu 2022, Cora, shadow graph	Cora, $1.00\times$, both	79.0	89.5	$+10.5$
`MEA5`	Wu 2022, Cora, shadow graph	Cora, $1.00\times$, both	80.7	92.5	$+11.8$
`AdvMEA`	DeFazio 2019, Cora, strong-adversary upper bound	Cora, $1.00\times$, both	$\sim$80	68.2	-11.8
`CEGA`	Wang 2025, CoauthorCS, $20C$ queries	CoauthorCS, $0.10\times$, both	93.4	$\sim$90.0	~ -3.4
`Realistic`	Guan 2024, Cora, Attack-0 (35 queries)	Cora, $0.05\times$, both	72.1	62.0	-10.1
`DFEA_I`	Zhuang 2024, Cora, Random-Graph baseline	Cora, $1.00\times$, data_free	73.7	90.2	$+16.5$
`DFEA_II`	Zhuang 2024, Cora, Attack II-E (real graph)[†]	Cora, $1.00\times$, data_free	92.8	96.8	$+4.0$
`DFEA_III`	Zhuang 2024, Cora, Attack III-E (real graph)[†]	Cora, $1.00\times$, data_free	93.0	92.7	-0.3

[†]The original paper does not separate Attack-II/III into "Random-Graph" rows the way it does for Attack-I; we cite the real-graph Attack-E numbers as the closest published reference.

Validation summary table. Table 9 compresses the comparable attack reproductions into one view; defenses are summarised in the paragraphs above because each family uses a different metric.

The takeaway is twofold. First, on attacks that share a clearly comparable setting with the source paper, our reproduction agrees with the original numbers within a band of $\sim \pm 14$ pp, with the direction of agreement consistent. Second, where the original paper uses a different protocol (image domain for PRADA / AdaptMisinfo / GradRedir, graph-classification metrics for SurviveWM, query-improvement multipliers for Integrity), a direct number-to-number comparison is not possible; we explicitly note these mismatches above and validate the qualitative claim instead.

E Supplementary Experimental Results and Discussion

E.1 Attack effectiveness results

This appendix reports the full results for attacks across the seven homophilic datasets of the core protocol; the three additional graphs (RomanEmpire, AmazonRatings, OGBN-Arxiv) are reported in Appendix E.4 (Tables 38–40). We first present compact overview tables which summarize, for each metric (Accuracy, F1, and Fidelity), the mean performance of twelve attacks across four query regimes (with an additional Overall column). Each number is averaged over the seven homophilic datasets and the five budget levels defined in the main text. These tables allow the reader to identify, at a glance, which attack performs best under each regime. We then provide the complete per-dataset matrices. For each dataset and each metric, we show a 2×2 panel that contains four sub-tables (one per regime). Each sub-table is a 12×5 matrix whose rows are the attacks and whose columns are the five query budgets. Bold font marks the best score in each budget column. All splits, budgets, and aggregation rules match the protocol in the main paper.

The overview table exposes three deep findings that the per-dataset detail tables (Tables 11–31) hide because of cell-level noise. *First, the ranking of attacks by mean fidelity is essentially identical across the three real-input regimes (`both`, `x_only`, `a_only`).* For example, the top-five strongest attacks by fidelity in the `both` column are `DFEA_III`, `DFEA_I`, `MEA5`, `MEA0`, `MEA3` (in order $89.77, 87.69, 83.92, 83.75, 83.26$); the same five attacks occupy the top-five positions in the `x_only` and `a_only` columns. The granularity of removing only one input modality at a time is therefore not sufficient to differentiate strong attacks — a conclusion that motivates our use of the more aggressive `data_free` regime as the discriminative axis. *Second, the data-free family (`DFEA_I/II/III` and `MEA2`) together with `AdvMEA`, `CEGA`, and `Realistic` are essentially regime-invariant*: their data_free fidelity is within ~ 1 pp of their `both` fidelity. This is a structural property of the attacks: `CEGA` retrains a centrality-based query selector even on synthetic graphs, `AdvMEA` learns adversarial features from scratch, `Realistic` reconstructs the structure with an auxiliary edge model, and the `DFEA` variants synthesise their own queries by design. They are the only candidates for an attacker who genuinely has no access to the real graph. *Third, the `Acc` and `F1` columns track each*

Table 10: RQ1 overview: regimes × metrics (%). Means across datasets and the five budgets (0.05–1.00).

	both			x_only			a_only			data_free		
Attack	Acc	F1	Fidelity	Acc	F1	Fidelity	Acc	F1	Fidelity	Acc	F1	Fidelity
MEA0	78.07	64.77	83.75	78.97	64.72	84.72	79.35	65.97	85.24	20.23	5.72	19.58
MEA1	57.08	43.79	60.33	57.07	43.96	60.34	57.08	43.80	60.32	21.06	5.68	18.98
MEA2	65.88	52.97	74.74	66.14	52.92	74.87	66.26	53.19	74.94	66.17	53.06	75.00
MEA3	78.74	65.31	83.26	79.19	65.28	83.35	78.65	64.29	83.16	22.88	6.59	21.56
MEA4	73.71	54.80	78.54	71.38	53.02	76.36	72.08	53.58	76.71	16.69	5.01	16.23
MEA5	79.34	65.77	83.92	79.64	65.72	84.31	79.30	65.67	84.03	21.20	6.34	20.19
AdvMEA	62.16	53.63	63.77	62.92	53.97	64.21	62.08	53.35	63.49	62.94	54.37	64.37
CEGA	75.01	64.61	83.08	74.94	64.64	82.68	75.58	64.71	83.80	74.02	63.83	82.08
Realistic	59.20	47.72	76.70	59.76	47.30	77.40	59.03	46.86	76.59	58.71	47.25	77.16
DFEA_I	77.22	66.28	87.69	77.21	66.27	87.69	77.21	66.26	87.68	77.20	66.25	87.70
DFEA_II	65.53	57.18	72.55	65.53	57.19	72.56	65.39	57.23	72.86	65.52	57.18	72.56
DFEA_III	77.84	67.50	89.77	77.80	67.34	89.65	77.82	67.40	89.68	77.80	67.36	89.69

Table 11: RQ1 detailed for dataset=Cora, metric=Acc (%). Rows are attacks; columns are budgets. Mean ± std across seeds; best per column is bold.

(a) Regime=both

Attack	0.05	0.10	0.25	0.50	1.00
MEA0	67.4±4.4	75.4±1.6	79.7±0.7	80.8±0.2	81.7±0.3
MEA1	52.7±0.5	63.5±2.0	81.5±0.7	80.8±0.1	82.3±0.2
MEA2	55.1±4.2	65.7±0.8	75.6±1.2	78.6±0.9	80.1±0.8
MEA3	67.1±3.4	74.3±1.9	79.6±1.5	81.2±0.6	81.1±0.3
MEA4	45.4±6.1	65.7±1.9	77.3±0.9	78.5±0.2	80.5±0.0
MEA5	72.1±2.9	75.4±0.8	79.9±0.7	81.4±0.6	81.2±0.3
AdvMEA	64.8±4.2	66.8±2.2	65.1±1.4	67.7±4.7	66.7±2.3
CEGA	71.0±5.2	76.5±0.9	79.7±0.2	79.3±0.6	79.3±0.3
Realistic	55.4±8.2	67.1±2.8	71.0±4.4	74.8±1.8	75.9±2.4
DFEA_I	76.3±2.3	78.6±0.4	80.2±1.0	80.9±0.2	80.7±0.6
DFEA_II	77.1±1.1	78.9±0.7	79.9±1.0	79.5±0.3	80.6±0.1
DFEA_III	77.0±0.9	79.4±1.5	80.4±1.2	80.7±0.8	81.6±0.5

(b) Regime=x_only

Attack	0.05	0.10	0.25	0.50	1.00
MEA0	68.7±4.2	75.1±0.7	80.1±0.2	80.4±1.3	81.2±0.5
MEA1	52.7±0.5	63.5±2.0	81.5±0.7	80.8±0.1	82.3±0.2
MEA2	55.7±1.6	67.7±0.3	76.3±0.4	79.2±0.8	80.1±0.8
MEA3	64.7±1.7	74.0±0.4	79.7±0.4	81.4±0.4	81.1±0.1
MEA4	42.9±8.4	63.7±3.7	76.8±0.4	78.5±0.2	80.5±0.0
MEA5	69.9±3.4	77.0±1.7	80.5±0.3	81.5±0.5	81.2±0.1
AdvMEA	65.5±3.3	68.8±2.5	65.4±2.0	63.6±0.8	65.0±3.0
CEGA	74.1±0.5	77.6±0.4	77.7±1.2	78.7±1.1	79.4±0.3
Realistic	55.7±8.3	64.2±5.0	71.0±4.3	74.8±3.4	75.5±2.7
DFEA_I	76.3±2.3	78.6±0.4	80.2±1.0	80.9±0.2	80.7±0.6
DFEA_II	77.1±1.1	78.9±0.7	79.9±1.0	79.5±0.3	80.6±0.1
DFEA_III	77.0±0.9	79.4±1.5	80.4±1.2	80.7±0.8	81.6±0.5

(c) Regime=a_only

Attack	0.05	0.10	0.25	0.50	1.00
MEA0	69.4±0.3	75.6±0.3	78.7±1.6	80.1±1.3	80.8±0.6
MEA1	52.7±0.5	63.5±2.0	81.5±0.7	80.8±0.1	82.3±0.2
MEA2	57.8±1.2	67.7±1.5	75.7±0.4	78.6±1.8	80.2±0.8
MEA3	63.0±1.3	75.2±1.8	79.7±0.8	81.0±0.6	81.3±0.2
MEA4	45.9±5.8	63.4±1.4	77.4±0.6	78.5±0.2	80.5±0.0
MEA5	65.6±6.9	76.5±1.5	79.6±1.1	81.5±0.5	81.3±0.1
AdvMEA	65.4±2.7	64.0±2.3	65.8±1.7	68.1±1.9	60.5±5.7
CEGA	69.6±3.6	78.0±0.4	78.0±0.8	79.6±0.5	79.2±0.6
Realistic	51.5±4.3	64.5±6.0	72.0±2.3	75.3±2.5	76.3±2.7
DFEA_I	76.3±2.3	78.6±0.4	80.2±1.0	80.9±0.2	80.7±0.6
DFEA_II	77.1±1.1	78.9±0.7	79.9±1.0	79.5±0.3	80.6±0.1
DFEA_III	77.1±0.9	79.4±1.5	80.4±1.2	80.7±0.8	81.6±0.5

(d) Regime=data_free

Attack	0.05	0.10	0.25	0.50	1.00
MEA0	10.9±2.5	14.6±0.2	19.3±8.9	20.2±8.2	19.0±9.3
MEA1	14.4±0.0	14.4±0.0	14.4±0.0	14.4±0.0	14.4±0.0
MEA2	60.5±1.8	69.4±1.8	76.1±1.2	78.2±0.6	80.2±0.8
MEA3	17.6±10.6	12.3±2.4	17.1±10.8	13.5±0.7	26.2±8.0
MEA4	17.1±10.8	19.9±8.5	18.5±9.7	10.9±2.5	18.0±10.0
MEA5	24.6±13.0	11.9±2.7	21.1±7.7	20.4±8.1	18.7±9.5
AdvMEA	68.6±2.4	68.5±1.5	65.1±6.3	65.8±2.9	67.9±3.7
CEGA	71.0±1.8	77.0±0.7	78.8±1.9	79.2±0.9	79.2±0.1
Realistic	67.9±2.3	70.8±1.6	69.0±3.6	66.5±2.6	69.1±1.6
DFEA_I	76.3±2.3	78.6±0.4	80.2±1.0	80.9±0.2	80.7±0.6
DFEA_II	77.1±1.1	78.9±0.7	79.9±1.0	79.5±0.3	80.6±0.1
DFEA_III	77.0±0.9	79.4±1.5	80.4±1.2	80.7±0.8	81.6±0.5

other except on heterophilic-style class distributions. On Cora-like datasets the F1 column tracks Acc within ~ 5 pp; the largest Acc/F1 gap appears for MEA0 (Acc 78.07, F1 64.77), reflecting a slight class-imbalance bias in the surrogate. Future attack design should therefore report F1 alongside accuracy, especially when targeting graphs with skewed class distributions such as OGBN-Arxiv.

Table 12: RQ1 detailed for dataset=Cora, metric=F1 (%). Rows are attacks; columns are budgets. Mean ± std across seeds; best per column is bold.

(a) Regime=both

Attack	0.05	0.10	0.25	0.50	1.00
MEA0	61.0±6.6	73.9±1.5	77.9±1.2	79.6±0.4	81.0±0.1
MEA1	50.5±0.5	58.2±4.1	80.3±0.7	80.2±0.2	81.8±0.0
MEA2	52.2±4.3	63.2±1.7	74.7±1.0	78.0±0.8	79.2±0.8
MEA3	60.6±5.9	70.4±2.8	78.4±1.6	79.5±0.9	80.2±0.2
MEA4	44.3±6.5	65.8±1.2	76.1±0.6	77.3±0.0	79.2±0.3
MEA5	67.9±4.1	70.3±3.8	78.8±0.8	80.3±0.6	80.2±0.4
AdvMEA	65.2±2.9	67.3±2.3	66.6±0.7	67.7±3.9	67.3±2.0
CEGA	69.9±4.4	75.6±0.9	79.1±0.1	78.6±0.3	78.4±0.2
Realistic	53.1±6.4	61.1±4.6	69.3±3.8	73.9±1.2	75.0±2.0
DFEA_I	72.7±5.1	75.5±1.0	78.9±1.1	79.6±0.2	79.3±1.1
DFEA_II	75.3±0.8	77.5±0.7	78.6±1.2	78.5±0.3	79.7±0.2
DFEA_III	74.4±2.4	77.6±1.6	79.3±1.1	79.7±0.6	80.7±0.5

(b) Regime=x_only

Attack	0.05	0.10	0.25	0.50	1.00
MEA0	63.2±4.5	68.7±0.4	78.8±0.2	79.0±1.8	80.4±0.6
MEA1	50.5±0.5	58.2±4.1	80.3±0.7	80.2±0.2	81.8±0.0
MEA2	50.5±1.8	66.1±0.7	75.1±0.5	78.5±0.7	79.2±0.8
MEA3	58.0±2.6	70.0±1.8	78.5±0.5	80.5±0.3	80.2±0.1
MEA4	27.9±6.9	62.2±4.5	75.8±0.5	77.3±0.0	79.2±0.3
MEA5	66.5±1.3	74.2±2.4	79.2±0.5	80.3±0.4	80.3±0.3
AdvMEA	66.3±2.8	67.0±3.0	65.3±3.1	64.0±0.5	66.4±2.2
CEGA	73.6±1.1	77.2±0.4	77.4±0.7	78.1±0.7	78.6±0.2
Realistic	50.9±6.5	58.8±4.9	68.2±6.1	74.0±3.1	75.2±2.6
DFEA_I	72.5±5.3	75.5±1.0	78.9±1.1	79.6±0.2	79.3±1.1
DFEA_II	75.3±0.7	77.5±0.7	78.6±1.2	78.5±0.3	79.7±0.2
DFEA_III	74.4±2.4	77.7±1.6	79.3±1.1	79.7±0.6	80.7±0.5

(c) Regime=a_only

Attack	0.05	0.10	0.25	0.50	1.00
MEA0	64.3±0.6	72.9±0.8	77.5±1.9	78.7±1.8	80.0±0.7
MEA1	50.4±0.5	58.2±4.1	80.3±0.7	80.2±0.2	81.8±0.0
MEA2	52.9±1.2	65.5±1.8	74.5±0.7	77.6±1.7	79.2±0.8
MEA3	55.7±3.0	70.3±3.0	78.3±1.4	80.0±0.3	80.4±0.2
MEA4	34.6±8.6	60.4±4.2	76.4±0.2	77.3±0.0	79.2±0.3
MEA5	58.8±11.2	73.7±2.4	77.7±1.0	80.7±0.4	80.2±0.2
AdvMEA	67.0±2.0	64.7±3.1	65.8±1.1	67.0±1.4	62.6±3.9
CEGA	68.7±1.4	77.5±0.6	77.4±0.9	79.0±0.8	78.4±0.6
Realistic	46.3±5.0	62.2±8.0	70.8±1.2	74.6±2.2	76.0±2.0
DFEA_I	72.7±5.1	75.5±1.0	78.9±1.1	79.6±0.2	79.3±1.1
DFEA_II	75.3±0.8	77.5±0.7	78.6±1.2	78.5±0.3	79.7±0.2
DFEA_III	74.5±2.3	77.7±1.6	79.3±1.1	79.7±0.6	80.7±0.5

(d) Regime=data_free

Attack	0.05	0.10	0.25	0.50	1.00
MEA0	2.8±0.6	3.6±0.1	4.5±1.7	4.7±1.6	4.4±1.8
MEA1	3.6±0.0	3.6±0.0	3.6±0.0	3.6±0.0	3.6±0.0
MEA2	55.4±0.5	69.0±0.4	74.8±1.1	77.5±0.5	79.2±0.8
MEA3	4.1±2.1	3.1±0.6	4.0±2.2	3.4±0.1	5.8±1.5
MEA4	4.0±2.2	4.6±1.6	4.3±1.9	2.8±0.6	4.2±2.0
MEA5	7.4±4.8	3.6±0.4	6.1±1.7	4.7±1.5	4.5±1.7
AdvMEA	68.4±0.6	68.4±1.1	64.7±6.1	66.3±2.2	68.0±2.7
CEGA	69.5±1.5	76.3±0.5	78.4±1.6	78.5±0.9	78.7±0.2
Realistic	63.1±3.3	67.8±3.2	67.1±3.7	63.0±4.0	67.2±1.8
DFEA_I	72.5±5.3	75.5±1.0	78.9±1.1	79.6±0.2	79.3±1.1
DFEA_II	75.3±0.8	77.5±0.7	78.6±1.2	78.5±0.3	79.7±0.2
DFEA_III	74.4±2.4	77.6±1.6	79.3±1.1	79.7±0.6	80.6±0.5

Table 13: RQ1 detailed for dataset=Cora, metric=Fidelity (%). Rows are attacks; columns are budgets. Mean ± std across seeds; best per column is bold.

(a) Regime=both

Attack	0.05	0.10	0.25	0.50	1.00
MEA0	69.3±3.1	82.6±1.6	87.5±0.9	89.7±0.7	92.4±0.6
MEA1	57.3±0.2	70.6±2.0	89.9±0.9	90.4±0.6	91.3±0.4
MEA2	57.4±3.2	68.8±0.9	82.8±1.2	89.3±0.3	94.8±0.2
MEA3	71.2±3.6	79.3±2.7	88.0±0.8	90.1±1.4	92.7±0.9
MEA4	49.2±6.2	71.9±1.7	85.0±1.3	87.6±0.6	89.5±0.2
MEA5	75.8±4.8	82.1±4.5	88.3±0.6	92.8±1.1	92.5±0.7
AdvMEA	67.6±4.0	68.8±2.8	67.4±1.6	69.0±4.9	68.2±4.0
CEGA	78.4±4.4	86.5±1.0	91.5±0.4	92.5±0.4	93.7±0.5
Realistic	62.0±4.5	68.1±1.8	78.6±0.7	83.7±0.6	88.5±1.7
DFEA_I	82.2±3.5	85.7±1.0	89.2±1.8	90.2±0.4	90.2±0.5
DFEA_II	79.9±0.7	84.1±0.8	88.5±0.3	93.1±0.4	96.8±0.5
DFEA_III	81.4±2.1	86.1±2.4	88.4±1.9	91.5±0.2	92.7±0.3

(b) Regime=x_only

Attack	0.05	0.10	0.25	0.50	1.00
MEA0	72.2±3.9	79.5±0.9	88.2±1.2	90.9±1.2	92.1±0.8
MEA1	57.3±0.2	70.6±2.0	89.9±0.9	90.4±0.5	91.3±0.4
MEA2	55.5±0.9	72.2±1.6	83.9±0.8	89.6±0.7	94.8±0.2
MEA3	69.1±0.8	77.7±0.5	88.0±0.9	90.9±1.1	92.5±1.3
MEA4	45.3±8.6	69.2±3.7	84.6±0.7	87.6±0.6	89.6±0.2
MEA5	73.9±1.8	83.2±0.3	88.8±0.8	91.9±0.5	92.3±1.1
AdvMEA	66.7±2.0	71.2±3.0	66.5±1.5	67.1±1.5	67.4±3.1
CEGA	82.5±1.7	86.8±0.8	90.8±1.1	92.8±0.8	93.7±0.1
Realistic	62.9±4.6	69.8±1.7	79.4±2.4	84.1±0.9	87.9±0.2
DFEA_I	82.2±3.5	85.7±1.0	89.2±1.8	90.2±0.4	90.2±0.5
DFEA_II	79.9±0.7	84.1±0.8	88.5±0.3	93.1±0.4	96.8±0.5
DFEA_III	81.3±2.2	86.1±2.4	88.4±1.9	91.5±0.2	92.7±0.3

(c) Regime=a_only

Attack	0.05	0.10	0.25	0.50	1.00
MEA0	74.1±0.8	81.9±1.4	87.2±1.1	89.5±1.3	92.4±1.2
MEA1	57.2±0.2	70.6±2.0	89.9±0.9	90.4±0.6	91.3±0.4
MEA2	56.8±2.1	69.9±2.2	82.9±0.3	90.0±1.0	94.8±0.2
MEA3	64.3±0.6	80.9±1.2	88.1±0.3	92.0±0.5	92.7±1.1
MEA4	48.3±4.1	68.2±1.8	85.6±0.5	87.6±0.6	89.5±0.2
MEA5	68.8±8.4	82.1±1.6	88.0±0.9	92.2±0.7	92.7±1.4
AdvMEA	67.5±3.0	66.1±2.3	67.4±3.6	68.9±2.5	62.7±4.3
CEGA	78.2±3.8	88.4±0.9	91.0±0.7	92.3±0.3	93.7±0.3
Realistic	56.5±4.1	69.3±3.9	79.8±0.3	84.3±1.9	89.1±0.9
DFEA_I	82.2±3.5	85.7±1.0	89.2±1.8	90.2±0.4	90.2±0.5
DFEA_II	79.9±0.7	84.1±0.8	88.5±0.3	93.1±0.4	96.8±0.5
DFEA_III	81.3±2.2	86.1±2.4	88.4±1.9	91.5±0.2	92.7±0.3

(d) Regime=data_free

Attack	0.05	0.10	0.25	0.50	1.00
MEA0	12.3±2.0	15.9±0.8	17.3±6.2	19.0±5.0	18.0±6.3
MEA1	15.3±0.2	15.3±0.2	15.3±0.2	15.3±0.1	15.3±0.2
MEA2	58.9±1.1	73.2±0.3	83.8±0.7	89.7±0.3	94.8±0.2
MEA3	16.2±7.9	13.3±2.5	15.3±8.0	13.8±1.0	23.1±4.3
MEA4	15.5±8.0	18.7±5.5	17.3±6.6	12.3±2.0	16.8±6.7
MEA5	21.9±10.9	12.5±2.6	20.2±4.3	19.5±4.8	17.2±6.6
AdvMEA	69.4±2.7	70.1±0.9	67.4±5.8	67.4±2.1	70.5±3.5
CEGA	79.8±2.7	88.0±0.4	91.0±1.5	92.5±0.0	93.5±0.6
Realistic	73.0±3.5	72.9±1.6	74.3±1.4	72.9±1.8	73.1±5.0
DFEA_I	82.2±3.5	85.7±1.0	89.2±1.8	90.2±0.4	90.2±0.5
DFEA_II	79.9±0.7	84.1±0.8	88.5±0.3	93.1±0.4	96.8±0.5
DFEA_III	81.4±2.1	86.1±2.4	88.4±1.9	91.5±0.2	92.7±0.3

Table 14: RQ1 detailed for dataset=CiteSeer, metric=Acc (%). Rows are attacks; columns are budgets. Mean ± std across seeds; best per column is bold.

(a) Regime=both

Attack	0.05	0.10	0.25	0.50	1.00
MEA0	55.4±6.9	62.4±2.4	69.0±0.7	70.1±0.9	70.1±0.6
MEA1	41.6±1.4	41.8±2.6	54.0±7.9	66.3±1.4	69.0±0.6
MEA2	36.7±2.8	47.0±3.0	59.6±1.2	66.3±0.7	69.3±0.3
MEA3	50.7±2.8	59.7±3.3	69.4±1.0	69.6±0.0	70.2±0.4
MEA4	44.9±1.0	57.9±3.7	67.1±0.2	69.9±0.4	70.6±0.4
MEA5	49.0±2.1	62.8±1.8	69.5±1.1	69.8±0.2	70.4±0.8
AdvMEA	51.8±8.1	46.3±4.2	53.2±0.7	52.3±1.7	51.3±5.1
CEGA	59.9±3.2	64.6±2.1	66.5±1.1	67.0±1.5	67.2±0.3
Realistic	47.2±2.0	57.7±4.2	64.3±2.3	64.5±0.4	65.2±1.1
DFEA_I	69.1±1.1	71.0±1.1	70.8±1.2	71.2±0.3	71.0±0.6
DFEA_II	70.3±1.4	70.0±0.4	69.5±0.6	69.7±0.8	70.3±0.5
DFEA_III	68.2±1.7	70.2±0.3	70.2±1.1	70.9±0.4	71.4±0.6

(b) Regime=x_only

Attack	0.05	0.10	0.25	0.50	1.00
MEA0	54.1±3.3	63.2±2.4	69.8±1.2	70.0±0.9	69.6±0.2
MEA1	41.6±1.4	41.8±2.6	54.0±7.9	66.3±1.4	68.9±0.6
MEA2	47.2±2.2	48.4±2.6	59.2±1.2	65.9±0.8	69.2±0.3
MEA3	57.9±4.1	64.6±1.8	68.7±1.0	69.9±0.8	69.9±0.7
MEA4	39.9±4.7	59.0±2.3	66.6±0.5	69.9±0.4	70.6±0.4
MEA5	55.3±1.9	65.9±0.7	70.3±0.6	70.3±0.7	70.0±0.5
AdvMEA	48.9±0.9	51.4±2.4	53.9±4.3	48.2±6.8	45.9±2.2
CEGA	61.3±1.9	65.2±1.1	66.7±0.6	67.3±0.6	67.8±0.5
Realistic	48.1±3.5	53.2±4.3	61.5±1.9	62.7±2.0	65.4±1.4
DFEA_I	69.1±1.1	71.0±1.1	70.8±1.2	71.2±0.3	71.0±0.6
DFEA_II	70.3±1.4	70.0±0.4	69.5±0.6	69.7±0.8	70.3±0.5
DFEA_III	68.3±1.7	70.2±0.3	70.2±1.1	70.9±0.4	71.4±0.6

(c) Regime=a_only

Attack	0.05	0.10	0.25	0.50	1.00
MEA0	52.5±3.1	64.5±1.5	70.2±0.9	69.3±0.8	70.1±1.1
MEA1	41.6±1.4	41.8±2.6	54.0±7.9	66.3±1.4	69.0±0.6
MEA2	35.9±1.2	49.6±1.5	59.0±0.9	65.9±1.4	69.2±0.3
MEA3	48.1±5.0	62.3±3.3	68.4±1.5	70.1±0.5	70.0±0.5
MEA4	43.9±1.3	56.8±1.3	66.2±0.6	69.9±0.4	70.6±0.4
MEA5	52.7±3.1	63.5±1.9	69.9±0.6	69.7±0.4	70.8±1.1
AdvMEA	47.5±4.0	51.2±4.3	54.0±4.7	49.9±5.4	46.5±0.3
CEGA	58.4±3.2	64.6±0.4	66.8±0.8	68.0±1.1	67.4±0.7
Realistic	40.7±7.3	55.1±4.9	62.8±0.2	63.2±2.2	64.1±1.2
DFEA_I	69.1±1.1	71.0±1.1	70.8±1.2	71.2±0.3	71.0±0.6
DFEA_II	70.3±1.4	70.0±0.4	69.5±0.6	69.7±0.8	70.3±0.5
DFEA_III	68.2±1.7	70.2±0.3	70.2±1.1	70.9±0.4	71.4±0.6

(d) Regime=data_free

Attack	0.05	0.10	0.25	0.50	1.00
MEA0	12.8±7.3	17.4±1.0	14.7±4.9	14.7±4.9	17.4±1.0
MEA1	21.4±2.4	21.4±2.4	21.4±2.4	21.4±2.4	21.4±2.4
MEA2	37.9±1.1	50.8±1.7	60.8±2.0	64.9±1.4	69.3±0.3
MEA3	18.1±0.0	19.5±2.6	16.7±5.4	17.7±0.6	16.6±0.4
MEA4	21.5±2.3	14.6±4.9	14.3±4.7	16.7±1.0	17.5±1.0
MEA5	18.8±3.1	17.3±0.6	19.8±2.3	17.3±0.6	14.0±4.5
AdvMEA	48.9±2.9	47.6±1.7	53.1±8.2	50.1±2.5	50.1±5.8
CEGA	60.9±2.4	64.4±0.8	67.8±0.8	67.6±0.7	67.5±0.6
Realistic	59.0±2.0	58.2±2.6	59.0±1.5	57.0±1.5	60.1±2.5
DFEA_I	69.1±1.1	71.0±1.1	70.8±1.2	71.2±0.3	71.0±0.6
DFEA_II	70.3±1.4	70.0±0.4	69.5±0.6	69.7±0.8	70.3±0.5
DFEA_III	68.2±1.7	70.2±0.3	70.1±1.0	70.9±0.4	71.4±0.6

Table 15: RQ1 detailed for dataset=CiteSeer, metric=F1 (%). Rows are attacks; columns are budgets. Mean ± std across seeds; best per column is bold.

(a) Regime=both

Attack	0.05	0.10	0.25	0.50	1.00
MEA0	50.9±4.6	55.4±1.7	63.7±0.6	66.0±0.8	66.6±0.2
MEA1	34.4±1.3	35.0±4.3	51.0±8.3	63.7±1.0	65.9±0.6
MEA2	34.6±2.9	44.7±3.1	57.2±1.7	63.3±1.1	66.1±0.4
MEA3	43.3±5.1	54.1±3.0	65.4±0.5	65.8±1.0	66.5±0.1
MEA4	36.5±2.6	55.1±4.6	63.8±0.1	66.4±0.5	67.2±0.3
MEA5	42.1±0.6	56.9±1.8	65.8±1.1	65.8±0.5	66.8±0.5
AdvMEA	47.8±5.1	41.3±5.4	46.7±0.4	45.6±1.6	46.8±6.4
CEGA	54.7±2.3	61.0±1.5	63.4±1.1	63.9±1.4	63.9±0.2
Realistic	42.4±3.0	53.0±3.3	59.2±2.6	60.4±1.1	61.3±1.2
DFEA_I	64.0±0.8	65.2±1.0	64.7±2.1	65.3±1.3	64.8±2.0
DFEA_II	65.2±2.0	66.0±0.2	66.5±0.6	66.8±1.0	67.4±0.6
DFEA_III	62.4±2.1	65.3±0.4	66.3±1.4	67.0±0.3	67.3±0.6

(b) Regime=x_only

Attack	0.05	0.10	0.25	0.50	1.00
MEA0	46.1±2.9	58.8±0.4	64.8±1.4	66.2±0.5	65.7±0.4
MEA1	34.4±1.3	35.0±4.3	51.0±8.3	63.7±1.0	65.8±0.6
MEA2	42.7±1.7	45.8±3.3	56.9±1.5	62.9±0.8	66.1±0.3
MEA3	51.9±4.4	57.7±0.5	63.4±1.0	65.0±0.4	66.3±0.7
MEA4	34.7±3.4	53.7±1.9	63.3±0.5	66.4±0.5	67.2±0.3
MEA5	47.0±5.4	59.9±1.6	65.4±0.7	65.8±0.7	66.3±0.5
AdvMEA	43.3±0.4	47.5±0.5	50.3±3.0	44.4±6.0	42.3±2.5
CEGA	57.4±1.1	61.4±0.8	63.3±0.5	63.9±0.5	64.5±0.8
Realistic	42.1±5.1	47.4±5.2	58.1±1.9	59.4±2.3	61.6±1.9
DFEA_I	64.0±0.8	65.2±1.0	64.7±2.1	65.3±1.3	64.8±2.0
DFEA_II	65.2±2.0	66.0±0.2	66.5±0.6	66.8±1.0	67.4±0.6
DFEA_III	62.4±2.1	65.3±0.4	66.3±1.4	67.0±0.3	67.3±0.6

(c) Regime=a_only

Attack	0.05	0.10	0.25	0.50	1.00
MEA0	46.0±3.1	57.1±3.2	65.8±1.3	65.6±0.6	66.6±1.1
MEA1	34.4±1.3	35.0±4.3	51.0±8.3	63.7±1.0	65.9±0.6
MEA2	33.5±1.4	46.8±1.0	56.4±0.7	63.0±1.4	66.1±0.3
MEA3	39.5±6.3	56.5±1.3	63.6±2.1	66.1±0.8	66.4±0.4
MEA4	33.0±4.6	54.5±1.7	63.1±0.7	66.4±0.5	67.2±0.3
MEA5	45.2±2.5	59.0±2.1	65.1±1.5	65.8±0.3	67.1±0.9
AdvMEA	44.2±6.2	46.2±4.9	47.9±7.8	47.3±3.3	41.5±1.2
CEGA	54.1±1.9	61.4±0.1	63.4±0.7	65.0±0.9	64.1±0.9
Realistic	33.2±10.0	50.1±4.6	58.5±0.3	58.9±2.7	60.6±1.0
DFEA_I	64.0±0.8	65.2±1.0	64.7±2.1	65.3±1.3	64.8±2.0
DFEA_II	65.2±2.0	66.0±0.2	66.5±0.6	66.8±1.0	67.4±0.6
DFEA_III	62.4±2.1	65.3±0.4	66.3±1.4	67.0±0.3	67.3±0.6

(d) Regime=data_free

Attack	0.05	0.10	0.25	0.50	1.00
MEA0	3.7±1.8	4.9±0.2	4.2±1.3	4.2±1.3	4.9±0.2
MEA1	5.9±0.5	5.9±0.5	5.9±0.5	5.9±0.5	5.9±0.5
MEA2	33.8±0.5	48.3±1.1	58.4±1.7	61.6±1.4	66.1±0.4
MEA3	5.1±0.0	6.0±0.6	5.6±0.6	5.0±0.1	4.7±0.1
MEA4	5.9±0.5	4.2±1.3	4.1±1.2	4.8±0.2	5.0±0.3
MEA5	5.4±0.7	4.9±0.1	5.5±0.5	4.9±0.1	4.0±1.2
AdvMEA	45.1±0.8	42.0±1.2	48.5±4.5	47.1±1.8	47.1±4.9
CEGA	56.0±2.0	61.0±1.1	64.3±1.1	64.2±0.7	64.2±0.4
Realistic	53.9±1.4	53.4±3.4	54.4±0.7	51.7±3.7	54.9±2.8
DFEA_I	64.0±0.8	65.2±1.0	64.7±2.1	65.3±1.3	64.8±2.0
DFEA_II	65.2±2.0	66.0±0.2	66.5±0.6	66.8±1.0	67.4±0.6
DFEA_III	62.4±2.1	65.3±0.4	66.2±1.3	67.0±0.3	67.3±0.6

Table 16: RQ1 detailed for dataset=CiteSeer, metric=Fidelity (%). Rows are attacks; columns are budgets. Mean ± std across seeds; best per column is bold.

(a) Regime=both

Attack	0.05	0.10	0.25	0.50	1.00
MEA0	62.9±6.1	69.9±3.6	82.8±1.5	86.7±1.0	90.0±0.7
MEA1	47.3±2.1	47.4±2.3	64.7±7.6	81.0±1.7	83.4±0.9
MEA2	42.4±4.3	55.5±3.2	74.4±2.3	83.8±0.4	91.5±0.2
MEA3	55.6±3.6	69.0±3.6	82.5±1.5	86.3±2.2	88.5±0.5
MEA4	48.3±2.9	65.4±5.3	79.4±0.8	83.3±1.5	84.1±1.3
MEA5	56.5±1.5	72.1±2.9	83.0±0.7	87.2±0.4	87.9±0.8
AdvMEA	55.9±6.8	50.0±4.2	54.5±2.5	57.2±1.0	52.7±6.0
CEGA	68.6±2.0	79.8±0.7	83.2±0.9	86.3±0.8	87.2±1.0
Realistic	54.1±3.8	64.5±1.5	73.3±1.4	78.3±3.5	84.1±0.8
DFEA_I	80.5±1.7	83.7±0.6	83.8±1.4	85.3±0.9	85.6±1.5
DFEA_II	76.9±1.3	80.8±1.1	85.6±0.8	90.1±1.0	93.6±0.9
DFEA_III	77.0±0.7	82.3±0.1	87.7±0.7	90.4±0.2	91.5±0.1

(b) Regime=x_only

Attack	0.05	0.10	0.25	0.50	1.00
MEA0	58.5±2.3	73.2±0.6	82.0±0.2	85.8±0.5	89.2±0.8
MEA1	47.3±2.1	47.4±2.3	64.7±7.6	81.0±1.7	83.4±1.0
MEA2	51.4±2.4	54.9±2.0	74.0±1.7	84.5±1.3	91.5±0.2
MEA3	63.4±5.5	69.8±0.5	81.0±0.6	85.2±1.1	88.8±0.4
MEA4	43.5±4.9	67.1±2.3	79.7±1.8	83.3±1.5	84.1±1.3
MEA5	61.9±3.9	72.7±0.7	83.4±0.5	86.2±1.6	88.5±0.5
AdvMEA	52.4±3.0	55.2±3.2	57.7±3.7	52.7±6.8	50.7±3.0
CEGA	73.1±1.8	78.6±1.8	83.7±0.9	86.4±0.9	87.0±1.1
Realistic	54.5±3.8	60.3±2.7	74.5±1.8	80.0±2.9	84.4±1.1
DFEA_I	80.5±1.7	83.7±0.6	83.8±1.4	85.3±0.9	85.6±1.5
DFEA_II	77.0±1.3	80.8±1.1	85.6±0.8	90.1±1.0	93.6±0.9
DFEA_III	77.0±0.7	82.3±0.1	87.6±0.7	90.4±0.2	91.5±0.1

(c) Regime=a_only

Attack	0.05	0.10	0.25	0.50	1.00
MEA0	57.6±3.5	73.1±4.4	82.9±0.5	85.8±0.5	89.8±0.7
MEA1	47.3±2.1	47.4±2.3	64.7±7.6	81.0±1.7	83.4±0.9
MEA2	40.1±1.3	58.3±1.3	72.1±0.6	84.8±1.1	91.5±0.2
MEA3	54.4±4.3	72.5±3.2	80.8±0.7	87.1±0.3	87.9±0.5
MEA4	44.5±4.3	66.6±2.9	80.0±1.6	83.3±1.5	84.1±1.3
MEA5	58.2±2.7	73.7±2.3	84.0±1.7	86.2±1.5	88.5±0.8
AdvMEA	52.2±3.8	53.6±3.0	56.1±6.6	53.5±5.3	50.6±2.2
CEGA	69.9±3.5	79.6±2.4	81.9±0.9	87.2±0.3	88.8±0.5
Realistic	48.1±7.3	61.3±4.2	73.8±0.7	81.1±0.8	84.2±0.3
DFEA_I	80.5±1.7	83.7±0.6	83.8±1.4	85.3±0.9	85.6±1.5
DFEA_II	77.0±1.3	80.8±1.1	85.6±0.8	90.1±1.0	93.6±0.9
DFEA_III	77.1±0.6	82.3±0.1	87.6±0.7	90.4±0.2	91.5±0.1

(d) Regime=data_free

Attack	0.05	0.10	0.25	0.50	1.00
MEA0	12.2±3.6	18.4±0.9	16.1±4.7	15.9±4.5	18.6±0.9
MEA1	18.1±0.7	18.1±0.7	18.1±0.7	18.1±0.7	18.1±0.7
MEA2	43.1±1.0	59.3±2.2	73.5±2.2	85.3±1.1	91.5±0.2
MEA3	19.0±0.4	18.0±0.9	16.1±2.0	18.3±1.1	17.2±0.3
MEA4	17.6±0.6	15.9±4.5	15.4±4.3	17.9±0.8	18.7±1.0
MEA5	17.6±0.5	17.9±1.0	19.0±0.6	17.6±0.7	15.3±4.3
AdvMEA	54.3±3.5	52.7±1.0	56.3±6.5	53.3±2.1	54.6±3.1
CEGA	71.9±2.1	77.4±0.1	85.2±0.7	86.4±1.0	86.9±0.9
Realistic	70.6±2.6	69.8±3.7	67.3±1.1	67.2±2.3	70.8±3.1
DFEA_I	80.5±1.7	83.7±0.6	83.8±1.4	85.3±0.9	85.6±1.5
DFEA_II	77.0±1.3	80.8±1.1	85.6±0.8	90.1±1.0	93.6±0.9
DFEA_III	77.1±0.6	82.3±0.1	87.6±0.7	90.4±0.2	91.5±0.1

Table 17: RQ1 detailed for dataset=CoauthorCS, metric=Acc (%). Rows are attacks; columns are budgets. Mean ± std across seeds; best per column is bold.

(a) Regime=both

Attack	0.05	0.10	0.25	0.50	1.00
MEA0	84.3±3.8	88.4±1.8	90.8±1.1	91.2±1.2	92.2±0.9
MEA1	71.1±0.8	74.4±0.7	77.2±0.3	89.2±0.7	89.5±0.4
MEA2	48.5±1.5	56.2±0.8	70.8±0.6	80.6±1.1	84.6±1.5
MEA3	86.2±0.6	88.8±0.7	90.8±0.5	91.8±0.3	92.8±0.3
MEA4	68.4±8.5	79.4±7.5	85.8±3.7	90.3±0.5	91.0±0.2
MEA5	87.3±0.7	88.5±0.3	91.4±0.8	92.2±0.1	92.0±0.4
AdvMEA	92.0±0.4	91.8±0.2	91.7±0.4	91.8±0.4	91.9±0.3
CEGA	89.0±1.0	90.4±0.7	91.6±0.4	91.8±0.0	91.7±0.6
Realistic	71.9±5.8	81.1±4.4	81.0±3.4	79.1±3.4	77.7±2.1
DFEA_I	89.7±1.1	89.7±0.7	89.6±0.4	89.8±0.6	89.4±0.6
DFEA_II	91.3±1.4	90.9±0.2	90.1±0.8	88.6±0.8	87.4±0.2
DFEA_III	89.6±0.7	89.4±0.8	89.3±0.9	88.6±0.2	88.3±0.2

(b) Regime=x_only

Attack	0.05	0.10	0.25	0.50	1.00
MEA0	83.5±2.7	89.1±0.2	91.5±0.6	92.3±0.2	92.2±1.6
MEA1	71.1±0.8	74.4±0.7	77.2±0.3	89.2±0.7	89.5±0.4
MEA2	46.6±1.6	55.6±2.0	71.0±1.2	80.5±0.5	84.6±1.5
MEA3	79.2±3.8	89.0±1.0	90.2±0.7	91.2±0.5	91.6±0.3
MEA4	65.3±10.4	73.3±0.6	86.9±1.5	89.7±0.2	91.0±0.3
MEA5	83.2±2.8	89.7±1.9	91.0±0.4	91.6±1.2	91.7±1.1
AdvMEA	91.7±0.3	91.8±0.6	91.8±0.6	91.6±0.4	91.8±0.4
CEGA	88.7±0.8	90.3±0.4	91.0±0.1	91.7±0.5	91.9±0.4
Realistic	68.8±8.3	77.2±4.3	81.2±2.2	78.9±2.4	79.3±1.2
DFEA_I	89.8±1.1	89.7±0.7	89.6±0.5	89.8±0.6	89.4±0.6
DFEA_II	91.3±1.4	90.9±0.2	90.1±0.8	88.7±0.8	87.4±0.2
DFEA_III	89.6±0.7	89.4±0.8	89.3±0.9	88.6±0.2	88.3±0.2

(c) Regime=a_only

Attack	0.05	0.10	0.25	0.50	1.00
MEA0	85.1±2.1	89.0±1.4	90.5±0.5	91.0±0.3	91.4±0.7
MEA1	71.1±0.8	74.4±0.7	77.2±0.3	89.2±0.7	89.5±0.4
MEA2	46.7±1.7	59.5±0.9	73.3±1.0	81.1±0.8	84.6±1.5
MEA3	87.6±0.4	89.5±1.3	90.8±0.7	91.9±0.3	92.5±0.4
MEA4	58.5±15.4	82.6±3.3	87.2±0.2	90.0±0.7	91.0±0.4
MEA5	86.5±1.2	89.2±0.7	91.3±0.0	92.0±0.9	92.0±0.6
AdvMEA	91.8±0.2	91.7±0.3	91.9±0.2	91.8±0.4	91.6±0.5
CEGA	90.0±0.2	90.4±0.2	91.8±0.5	91.3±0.8	91.7±0.7
Realistic	74.5±3.2	80.8±2.0	84.4±4.4	77.1±3.0	77.3±2.3
DFEA_I	89.8±1.1	89.7±0.7	89.6±0.4	89.8±0.7	89.4±0.6
DFEA_II	91.3±1.4	90.9±0.2	90.1±0.8	88.6±0.8	87.4±0.2
DFEA_III	89.6±0.7	89.4±0.8	89.3±0.9	88.6±0.2	88.3±0.2

(d) Regime=data_free

Attack	0.05	0.10	0.25	0.50	1.00
MEA0	7.4±2.7	33.5±23.5	7.4±3.8	3.5±2.7	22.1±19.8
MEA1	0.5±0.4	0.5±0.4	0.5±0.4	0.5±0.4	0.5±0.4
MEA2	45.2±1.7	54.3±2.6	73.8±1.0	81.5±1.1	84.6±1.5
MEA3	21.5±20.3	22.1±19.9	17.5±23.1	37.2±18.2	18.9±19.5
MEA4	4.0±2.4	22.6±19.5	18.4±22.5	20.1±21.5	7.1±3.0
MEA5	17.0±12.7	26.4±23.8	18.1±22.7	6.2±4.3	7.8±5.0
AdvMEA	91.7±0.3	91.9±0.2	91.8±0.3	91.8±0.4	91.8±0.3
CEGA	88.8±1.0	91.1±0.6	91.4±0.3	91.3±0.8	91.1±0.6
Realistic	74.9±2.2	77.4±2.8	75.1±2.0	79.7±1.1	79.9±1.9
DFEA_I	89.7±1.1	89.7±0.7	89.6±0.4	89.8±0.6	89.5±0.6
DFEA_II	91.3±1.4	90.9±0.2	90.1±0.8	88.6±0.8	87.4±0.2
DFEA_III	89.6±0.7	89.4±0.8	89.3±0.9	88.6±0.2	88.3±0.1

Table 18: RQ1 detailed for dataset=CoauthorCS, metric=F1 (%). Rows are attacks; columns are budgets. Mean ± std across seeds; best per column is bold.

(a) Regime=both

Attack	0.05	0.10	0.25	0.50	1.00
MEA0	51.8±1.1	61.1±3.9	70.1±3.4	73.7±3.8	77.1±2.5
MEA1	34.5±0.3	36.7±0.4	42.1±1.7	61.2±0.9	64.3±1.3
MEA2	32.7±1.4	38.9±3.3	52.1±4.0	57.5±5.4	59.5±4.5
MEA3	54.8±2.8	64.2±4.6	71.6±4.2	76.8±0.6	76.4±1.5
MEA4	25.2±4.7	38.0±4.8	52.3±8.8	67.1±1.9	71.3±1.1
MEA5	54.6±1.0	59.5±1.4	71.8±5.1	77.6±1.4	77.7±0.1
AdvMEA	75.0±1.6	73.7±0.8	74.0±1.8	74.9±2.2	75.3±1.0
CEGA	67.6±2.1	72.6±1.5	74.7±2.0	76.5±0.9	74.1±2.4
Realistic	42.9±6.9	53.4±2.3	61.3±3.9	56.6±5.6	54.2±3.5
DFEA_I	81.9±2.0	82.0±0.9	81.6±0.8	81.3±0.6	80.5±0.8
DFEA_II	83.1±1.3	82.1±0.4	81.6±2.1	78.2±2.3	77.0±1.6
DFEA_III	81.8±1.0	80.7±0.6	80.6±2.0	78.8±0.5	78.6±0.9

(b) Regime=x_only

Attack	0.05	0.10	0.25	0.50	1.00
MEA0	44.4±3.8	60.9±4.1	74.5±0.4	76.1±1.7	74.8±4.7
MEA1	34.5±0.3	36.7±0.4	42.1±1.7	61.2±0.9	64.3±1.3
MEA2	31.8±1.1	41.5±1.6	55.6±3.9	58.8±3.0	59.5±4.5
MEA3	45.6±0.8	62.5±6.8	67.6±3.0	74.1±1.6	73.5±1.6
MEA4	20.8±8.6	36.1±6.9	52.2±4.5	64.5±0.7	71.1±0.8
MEA5	50.4±3.0	66.6±5.2	71.6±4.0	73.1±6.9	74.4±3.6
AdvMEA	74.7±0.7	74.7±2.0	74.6±1.6	74.3±1.0	73.2±1.9
CEGA	70.0±0.9	70.8±1.5	74.0±2.8	72.5±1.3	72.8±1.4
Realistic	46.1±1.1	46.4±3.0	56.5±1.7	56.9±3.7	55.8±0.6
DFEA_I	81.9±2.0	82.0±1.0	81.6±0.8	81.3±0.6	80.5±0.8
DFEA_II	83.1±1.3	82.1±0.4	81.6±2.1	78.2±2.3	77.0±1.6
DFEA_III	81.8±1.0	80.7±0.6	80.6±2.0	78.8±0.5	78.6±0.9

(c) Regime=a_only

Attack	0.05	0.10	0.25	0.50	1.00
MEA0	56.0±6.3	65.7±4.6	71.3±2.8	73.2±1.6	73.4±3.3
MEA1	34.5±0.3	36.7±0.4	42.1±1.7	61.2±0.9	64.3±1.3
MEA2	31.6±6.0	43.5±3.7	54.7±1.8	58.9±4.6	59.5±4.5
MEA3	57.1±0.9	64.4±7.1	70.5±4.1	74.8±2.2	75.8±0.9
MEA4	21.3±4.2	47.2±8.5	52.4±0.9	66.1±2.5	71.3±1.4
MEA5	53.6±3.3	67.3±4.9	74.1±1.1	77.3±1.9	74.1±2.0
AdvMEA	75.0±0.8	75.2±1.0	74.7±1.1	74.6±1.1	74.4±1.0
CEGA	69.4±2.1	71.2±0.9	73.9±0.9	73.3±3.0	72.3±1.3
Realistic	41.5±6.9	56.2±2.7	61.6±5.3	54.4±5.0	54.5±0.8
DFEA_I	81.9±2.0	82.0±0.9	81.6±0.8	81.3±0.7	80.5±0.8
DFEA_II	83.1±1.3	82.1±0.4	81.6±2.1	78.2±2.3	77.0±1.6
DFEA_III	81.8±1.0	80.7±0.6	80.6±2.0	78.8±0.5	78.6±0.9

(d) Regime=data_free

Attack	0.05	0.10	0.25	0.50	1.00
MEA0	0.9±0.3	3.0±2.1	0.9±0.5	0.4±0.3	2.1±1.6
MEA1	0.1±0.0	0.1±0.0	0.1±0.0	0.1±0.0	0.1±0.0
MEA2	32.0±2.6	38.9±7.7	55.3±3.7	59.8±6.4	59.5±4.5
MEA3	2.4±1.5	3.4±1.9	1.6±2.0	3.9±0.8	2.9±2.8
MEA4	0.5±0.3	2.2±1.6	1.7±2.0	1.9±1.8	0.9±0.4
MEA5	2.7±2.2	5.5±5.0	1.8±1.9	0.8±0.5	3.6±2.6
AdvMEA	75.1±1.0	74.9±0.8	73.9±0.9	74.7±0.9	74.6±0.7
CEGA	65.1±3.0	72.6±2.4	71.9±1.0	75.5±0.8	72.0±1.0
Realistic	52.0±1.7	55.1±3.3	54.1±1.5	59.5±0.8	56.9±2.8
DFEA_I	81.9±2.0	82.0±1.0	81.6±0.8	81.3±0.6	80.5±0.7
DFEA_II	83.1±1.3	82.1±0.4	81.6±2.1	78.2±2.3	77.0±1.6
DFEA_III	81.8±1.0	80.7±0.6	80.6±2.0	78.8±0.5	78.5±0.9

Table 19: RQ1 detailed for dataset=CoauthorCS, metric=Fidelity (%). Rows are attacks; columns are budgets. Mean ± std across seeds; best per column is bold.

(a) Regime=both

Attack	0.05	0.10	0.25	0.50	1.00
MEA0	83.7±4.0	87.9±1.6	91.2±1.2	92.8±0.3	94.5±0.3
MEA1	71.0±0.8	74.2±0.5	76.9±0.5	89.8±0.8	90.2±0.7
MEA2	47.8±1.2	57.3±1.4	73.0±2.3	84.2±1.7	87.7±2.9
MEA3	85.2±1.8	88.2±1.3	90.8±1.0	91.7±0.2	93.1±0.6
MEA4	66.7±8.4	79.1±7.2	86.9±3.4	93.5±0.7	96.3±0.5
MEA5	85.8±0.2	87.8±0.3	91.1±0.2	92.4±0.4	93.6±0.8
AdvMEA	92.3±0.5	92.3±0.4	92.0±0.4	92.1±0.3	92.3±0.4
CEGA	90.3±0.6	91.7±0.7	93.5±0.7	94.9±0.8	94.8±0.5
Realistic	72.6±5.2	81.5±4.3	82.5±3.2	80.4±3.7	80.9±2.0
DFEA_I	91.6±0.5	93.2±0.2	94.7±0.4	95.7±1.1	96.9±0.9
DFEA_II	89.6±1.2	91.1±1.1	93.1±0.7	96.1±0.4	100.0±0.0
DFEA_III	91.0±0.7	92.6±0.4	94.8±0.0	96.8±0.7	98.9±0.3

(b) Regime=x_only

Attack	0.05	0.10	0.25	0.50	1.00
MEA0	83.3±2.8	88.8±0.5	92.3±0.7	93.3±0.5	93.7±0.2
MEA1	71.0±0.8	74.2±0.5	76.9±0.5	89.8±0.8	90.2±0.7
MEA2	46.2±1.8	56.5±2.5	74.3±2.6	83.7±2.2	87.7±2.9
MEA3	77.8±4.5	88.6±0.9	90.0±0.6	91.7±0.4	93.4±0.5
MEA4	63.8±10.0	72.2±0.8	87.7±1.2	92.9±0.3	96.4±0.4
MEA5	83.5±2.4	89.2±2.0	91.0±0.3	92.0±0.7	93.1±1.0
AdvMEA	92.0±0.4	92.1±0.3	92.2±0.6	92.0±0.3	92.2±0.2
CEGA	90.2±0.6	92.7±0.3	92.8±0.4	94.5±0.3	96.2±0.3
Realistic	68.4±8.8	78.1±4.7	81.4±1.7	80.8±1.9	80.5±1.1
DFEA_I	91.7±0.5	93.2±0.2	94.6±0.4	95.6±1.0	96.9±0.9
DFEA_II	89.6±1.2	91.1±1.1	93.1±0.7	96.1±0.4	100.0±0.0
DFEA_III	91.0±0.7	92.6±0.4	94.8±0.0	96.8±0.7	98.9±0.3

(c) Regime=a_only

Attack	0.05	0.10	0.25	0.50	1.00
MEA0	84.6±2.4	89.4±1.4	91.9±0.6	92.9±0.4	94.6±0.4
MEA1	71.0±0.8	74.2±0.5	76.9±0.5	89.8±0.8	90.2±0.7
MEA2	46.3±1.1	60.7±0.8	76.0±0.3	84.0±1.6	87.7±2.9
MEA3	86.5±0.5	89.5±1.4	90.8±0.9	92.0±0.4	93.5±0.1
MEA4	57.4±15.1	81.4±2.8	88.5±0.3	92.8±1.3	96.6±0.4
MEA5	86.2±1.6	89.0±0.6	91.1±0.4	92.4±0.7	93.7±1.0
AdvMEA	92.0±0.3	92.0±0.4	92.3±0.4	91.9±0.3	91.9±0.3
CEGA	90.2±1.0	92.5±0.5	93.8±0.5	94.2±0.3	95.8±0.3
Realistic	73.9±3.3	82.2±1.5	85.7±4.5	78.6±3.7	79.0±2.6
DFEA_I	91.7±0.5	93.2±0.2	94.7±0.4	95.7±1.0	96.9±0.9
DFEA_II	89.6±1.2	91.1±1.1	93.1±0.7	96.1±0.4	100.0±0.0
DFEA_III	91.0±0.7	92.6±0.4	94.8±0.0	96.8±0.7	98.9±0.3

(d) Regime=data_free

Attack	0.05	0.10	0.25	0.50	1.00
MEA0	6.6±2.5	32.2±22.7	7.0±3.9	3.4±2.8	21.2±19.1
MEA1	0.6±0.7	0.6±0.7	0.6±0.7	0.6±0.7	0.6±0.7
MEA2	45.1±2.4	55.9±2.2	75.3±2.4	84.1±1.9	87.7±2.9
MEA3	20.4±19.6	21.2±19.1	16.8±22.4	36.1±17.3	18.7±18.9
MEA4	3.9±2.2	22.1±18.8	17.4±21.7	19.4±20.5	7.0±3.1
MEA5	16.3±12.3	25.8±23.0	17.3±21.8	5.8±3.7	8.0±5.0
AdvMEA	91.9±0.4	92.2±0.4	92.2±0.4	92.0±0.5	92.1±0.5
CEGA	90.0±1.2	92.3±0.6	93.1±0.3	93.8±0.7	95.5±0.5
Realistic	77.8±2.5	78.9±2.1	76.4±2.5	80.3±1.9	81.5±2.1
DFEA_I	91.7±0.5	93.2±0.2	94.7±0.4	95.6±1.0	96.9±0.8
DFEA_II	89.6±1.2	91.1±1.1	93.1±0.7	96.1±0.4	100.0±0.0
DFEA_III	91.0±0.7	92.6±0.4	94.8±0.0	96.8±0.7	98.9±0.3

Table 20: RQ1 detailed for dataset=CoauthorPhysics, metric=Acc (%). Rows are attacks; columns are budgets. Mean ± std across seeds; best per column is bold.

(a) Regime=both

Attack	0.05	0.10	0.25	0.50	1.00
MEA0	82.2±4.9	89.6±0.4	90.9±0.2	90.7±0.4	92.8±1.0
MEA1	3.5±0.0	10.1±0.6	17.2±0.2	44.0±1.9	79.5±7.9
MEA2	33.3±2.4	44.2±1.4	66.8±1.0	73.6±4.4	84.0±3.1
MEA3	74.0±1.4	81.1±2.6	89.5±1.4	89.8±0.7	90.6±1.8
MEA4	70.1±10.5	74.0±10.0	87.7±2.0	89.6±0.5	89.5±0.6
MEA5	75.4±4.8	78.4±4.7	89.8±1.6	91.0±0.8	91.3±1.0
AdvMEA	91.4±1.2	91.6±0.7	91.3±0.2	90.6±1.3	91.4±0.9
CEGA	90.9±1.3	90.4±2.8	91.5±0.6	91.0±0.5	90.8±0.3
Realistic	79.6±3.8	77.0±6.5	79.3±1.7	76.1±3.1	73.0±1.5
DFEA_I	90.7±0.2	90.8±0.2	90.8±0.5	90.8±0.2	90.6±0.2
DFEA_II	90.9±0.2	90.0±0.6	90.6±0.4	90.1±0.4	89.5±0.4
DFEA_III	90.5±0.4	90.1±0.6	90.5±0.4	90.3±0.5	90.4±0.3

(b) Regime=x_only

Attack	0.05	0.10	0.25	0.50	1.00
MEA0	80.9±4.2	90.4±1.8	89.3±1.5	91.5±0.9	91.3±0.8
MEA1	3.5±0.0	10.1±0.6	17.2±0.2	44.0±1.9	79.5±7.9
MEA2	31.0±2.1	41.2±2.2	64.9±4.1	71.9±6.2	83.9±3.1
MEA3	75.3±1.5	84.0±2.4	89.8±0.9	91.6±0.5	91.4±0.5
MEA4	39.5±17.4	83.4±4.5	88.7±1.6	90.2±0.6	89.9±0.3
MEA5	76.2±5.5	78.9±5.5	89.0±1.5	91.5±0.7	91.2±1.4
AdvMEA	90.8±1.2	91.2±1.0	90.7±0.4	91.6±0.4	90.9±0.9
CEGA	90.9±0.4	91.2±1.0	91.6±0.3	91.2±0.5	91.2±0.4
Realistic	79.0±5.6	83.0±4.6	79.4±2.7	78.6±2.6	74.4±0.5
DFEA_I	90.7±0.2	90.8±0.2	90.8±0.5	90.8±0.2	90.6±0.2
DFEA_II	90.9±0.2	90.0±0.6	90.6±0.4	90.1±0.4	89.5±0.4
DFEA_III	90.4±0.4	90.1±0.6	90.5±0.4	90.3±0.5	90.4±0.3

(c) Regime=a_only

Attack	0.05	0.10	0.25	0.50	1.00
MEA0	85.3±2.4	89.0±0.8	91.1±0.4	90.1±2.0	92.0±0.6
MEA1	3.5±0.0	10.1±0.6	17.2±0.2	44.0±1.9	79.5±7.9
MEA2	34.0±1.0	46.1±0.6	65.9±2.4	76.1±2.6	83.9±3.1
MEA3	70.5±6.3	83.9±2.6	89.6±1.0	90.7±1.1	91.3±0.5
MEA4	61.6±24.8	77.9±6.2	86.0±3.0	89.4±0.5	89.7±0.6
MEA5	73.1±9.3	83.9±1.0	89.4±1.5	90.7±0.7	90.4±0.6
AdvMEA	91.4±0.4	91.0±0.7	91.6±1.0	90.9±1.1	91.0±0.7
CEGA	90.7±1.0	91.8±0.6	91.6±0.3	91.3±0.1	91.5±0.8
Realistic	72.2±5.2	84.5±1.3	72.7±7.7	74.1±1.2	69.8±2.1
DFEA_I	90.7±0.2	90.8±0.2	90.8±0.5	90.8±0.2	90.7±0.3
DFEA_II	90.9±0.2	90.0±0.6	90.6±0.4	90.1±0.4	89.5±0.4
DFEA_III	90.5±0.4	90.1±0.6	90.5±0.4	90.3±0.5	90.4±0.3

(d) Regime=data_free

Attack	0.05	0.10	0.25	0.50	1.00
MEA0	5.5±2.9	27.6±18.8	3.5±0.0	15.7±10.1	20.8±20.3
MEA1	3.5±0.0	3.5±0.0	3.5±0.0	3.5±0.0	3.5±0.0
MEA2	31.5±1.3	43.1±2.3	64.7±2.0	75.4±4.3	83.9±3.1
MEA3	6.7±2.3	19.5±21.1	28.6±19.9	35.8±22.7	18.8±21.6
MEA4	4.9±1.9	13.7±11.6	5.5±2.9	14.4±11.3	12.3±12.5
MEA5	3.5±0.0	34.0±21.6	29.9±12.2	25.0±18.8	18.8±21.6
AdvMEA	91.1±0.5	91.6±0.7	91.1±0.9	91.2±0.8	91.0±0.4
CEGA	89.0±1.5	90.7±0.7	91.6±0.5	91.0±0.2	91.4±0.3
Realistic	70.1±1.6	73.5±1.7	71.5±1.4	71.5±2.7	69.6±3.6
DFEA_I	90.7±0.2	90.8±0.2	90.8±0.5	90.8±0.2	90.6±0.2
DFEA_II	90.9±0.2	90.0±0.6	90.6±0.4	90.1±0.4	89.5±0.4
DFEA_III	90.5±0.4	90.1±0.6	90.5±0.4	90.3±0.5	90.4±0.3

Table 21: RQ1 detailed for dataset=CoauthorPhysics, metric=F1 (%). Rows are attacks; columns are budgets. Mean ± std across seeds; best per column is bold.

(a) Regime=both

Attack	0.05	0.10	0.25	0.50	1.00
MEA0	71.3±6.1	78.7±2.0	80.3±0.6	80.9±0.8	84.2±1.5
MEA1	1.4±0.0	10.4±1.8	18.5±1.1	44.0±1.2	71.6±5.2
MEA2	32.1±2.9	41.2±2.4	55.3±2.5	57.0±8.9	57.5±8.9
MEA3	61.1±3.7	70.1±2.5	79.9±2.3	79.5±0.9	80.4±3.1
MEA4	38.8±7.7	48.9±6.7	68.6±1.4	74.8±1.7	76.1±0.9
MEA5	62.6±6.6	67.6±4.2	78.6±2.6	79.3±1.6	81.6±0.6
AdvMEA	82.9±2.3	82.9±1.7	82.9±1.0	81.5±2.2	82.5±2.0
CEGA	80.5±1.4	80.3±3.9	80.3±1.6	79.8±1.3	80.2±0.2
Realistic	64.7±4.0	64.9±5.4	65.2±1.1	62.9±3.2	60.0±1.1
DFEA_I	81.3±0.5	81.5±0.2	81.8±0.7	81.9±0.5	81.7±0.3
DFEA_II	82.0±0.3	80.3±1.2	81.7±1.0	80.7±1.0	79.4±0.6
DFEA_III	81.1±0.9	80.4±1.2	81.4±0.9	81.2±1.1	81.1±0.3

(b) Regime=x_only

Attack	0.05	0.10	0.25	0.50	1.00
MEA0	63.9±4.3	78.5±3.6	77.5±2.1	79.4±1.4	81.9±1.0
MEA1	1.4±0.0	10.4±1.8	18.5±1.1	44.0±1.2	71.6±5.2
MEA2	26.3±2.6	39.0±0.2	52.9±5.7	54.1±8.1	57.4±8.8
MEA3	58.1±4.4	71.1±2.8	79.4±0.5	81.4±0.8	81.5±1.6
MEA4	21.8±5.2	61.3±8.0	69.3±4.0	75.1±1.9	76.9±0.6
MEA5	63.0±6.6	68.0±3.4	78.6±2.6	81.1±1.4	81.0±1.6
AdvMEA	81.9±2.2	82.1±1.9	81.7±1.1	83.2±0.9	81.6±2.2
CEGA	79.8±1.9	81.6±1.2	81.8±0.5	81.2±1.0	81.1±0.7
Realistic	63.4±4.6	68.1±5.3	65.6±4.9	64.1±3.9	60.6±0.3
DFEA_I	81.3±0.5	81.5±0.2	81.8±0.7	81.9±0.5	81.7±0.3
DFEA_II	82.0±0.3	80.3±1.2	81.7±1.0	80.7±1.0	79.4±0.6
DFEA_III	81.0±1.0	80.4±1.2	81.4±0.9	81.2±1.1	81.1±0.3

(c) Regime=a_only

Attack	0.05	0.10	0.25	0.50	1.00
MEA0	70.1±6.9	78.0±1.8	80.6±0.4	79.9±3.5	82.7±1.6
MEA1	1.4±0.0	10.4±1.8	18.5±1.1	44.0±1.2	71.6±5.2
MEA2	29.8±2.9	37.7±1.8	57.0±3.8	58.9±7.7	57.5±8.9
MEA3	62.6±2.9	72.7±1.8	78.8±1.7	79.9±3.0	81.4±1.0
MEA4	42.8±15.8	51.2±5.7	64.2±3.1	76.4±2.3	76.6±0.9
MEA5	60.1±9.1	72.1±0.8	78.0±2.2	79.9±1.2	79.1±1.1
AdvMEA	82.8±1.1	82.1±1.7	82.9±2.2	81.8±1.8	82.1±1.5
CEGA	79.2±2.1	80.7±0.7	81.6±0.7	81.3±1.2	80.6±0.5
Realistic	52.4±8.7	70.5±2.6	60.2±6.0	60.1±2.4	56.2±1.3
DFEA_I	81.3±0.5	81.5±0.2	81.8±0.7	81.9±0.5	81.7±0.4
DFEA_II	82.0±0.3	80.3±1.2	81.7±1.0	80.7±1.0	79.4±0.6
DFEA_III	81.1±0.9	80.4±1.2	81.4±0.9	81.2±1.1	81.1±0.3

(d) Regime=data_free

Attack	0.05	0.10	0.25	0.50	1.00
MEA0	2.1±1.0	7.9±4.9	1.4±0.0	5.2±2.9	6.0±5.2
MEA1	1.4±0.0	1.4±0.0	1.4±0.0	1.4±0.0	1.4±0.0
MEA2	31.4±2.6	39.8±0.8	55.2±2.1	58.4±8.2	57.5±8.9
MEA3	3.5±2.1	6.2±5.1	10.2±7.7	17.1±9.7	5.3±5.6
MEA4	1.8±0.7	4.5±3.4	2.1±1.0	4.7±3.3	4.0±3.7
MEA5	1.4±0.0	9.3±5.6	12.3±4.0	9.0±5.4	5.3±5.6
AdvMEA	82.5±1.3	82.7±1.6	82.2±2.0	82.7±1.6	82.3±0.9
CEGA	77.8±1.5	79.5±2.5	80.4±0.9	80.4±0.5	80.8±1.0
Realistic	56.4±3.0	58.3±1.0	58.5±1.9	56.0±2.7	55.1±2.9
DFEA_I	81.3±0.5	81.5±0.2	81.8±0.7	81.9±0.5	81.7±0.3
DFEA_II	82.0±0.3	80.3±1.2	81.7±1.0	80.7±1.0	79.4±0.6
DFEA_III	81.1±0.9	80.4±1.2	81.4±0.9	81.2±1.1	81.1±0.3

Table 22: RQ1 detailed for dataset=CoauthorPhysics, metric=Fidelity (%). Rows are attacks; columns are budgets. Mean ± std across seeds; best per column is bold.

(a) Regime=both

Attack	0.05	0.10	0.25	0.50	1.00
MEA0	81.9±4.5	89.3±0.9	92.5±0.7	92.8±0.9	94.2±0.1
MEA1	2.7±0.5	9.5±0.3	15.3±0.7	44.4±1.6	78.6±7.3
MEA2	32.5±2.5	44.8±1.9	69.0±1.0	76.1±4.9	85.8±3.2
MEA3	74.4±2.1	80.8±3.0	89.1±1.0	90.4±1.7	93.0±0.7
MEA4	69.2±11.7	75.4±11.2	90.7±0.9	95.5±0.6	97.8±0.4
MEA5	74.3±5.8	77.5±4.9	89.5±1.5	91.2±1.4	91.9±0.2
AdvMEA	90.0±0.5	90.2±0.5	89.7±0.8	89.5±0.9	90.2±0.4
CEGA	91.0±1.4	91.6±1.3	94.1±0.0	94.9±0.3	96.8±0.3
Realistic	80.5±4.1	77.5±6.4	82.2±1.6	77.4±2.2	74.3±1.4
DFEA_I	95.4±0.3	96.4±0.6	97.3±0.3	97.6±0.7	97.7±0.7
DFEA_II	93.6±0.7	94.4±0.5	96.3±0.2	97.3±0.1	99.6±0.1
DFEA_III	93.7±0.3	95.1±0.4	96.8±0.4	97.7±0.4	98.7±0.1

(b) Regime=x_only

Attack	0.05	0.10	0.25	0.50	1.00
MEA0	80.4±4.7	89.9±1.2	92.0±1.5	93.6±0.7	93.3±0.8
MEA1	2.7±0.5	9.5±0.3	15.3±0.7	44.4±1.6	78.6±7.3
MEA2	30.4±2.2	41.2±2.5	66.3±4.1	74.0±6.2	85.7±3.1
MEA3	74.5±1.4	83.1±2.9	90.1±1.2	92.6±1.4	92.9±0.4
MEA4	40.3±18.5	84.0±4.2	90.9±0.1	94.4±0.4	98.1±0.6
MEA5	75.8±5.7	77.8±6.2	89.1±1.4	92.4±1.1	93.4±0.9
AdvMEA	89.8±0.6	90.4±0.2	89.8±0.2	90.0±0.3	89.9±0.3
CEGA	92.3±1.3	93.0±1.3	94.1±0.6	94.7±0.8	96.3±0.8
Realistic	79.1±6.6	84.3±4.3	81.0±2.9	79.2±2.2	76.7±1.1
DFEA_I	95.4±0.3	96.4±0.6	97.3±0.3	97.6±0.7	97.7±0.7
DFEA_II	93.6±0.7	94.4±0.5	96.3±0.2	97.3±0.1	99.6±0.1
DFEA_III	93.6±0.2	95.1±0.4	96.8±0.4	97.7±0.4	98.7±0.1

(c) Regime=a_only

Attack	0.05	0.10	0.25	0.50	1.00
MEA0	84.5±3.8	88.6±0.5	91.9±0.8	91.8±1.0	94.5±0.4
MEA1	2.7±0.5	9.5±0.3	15.3±0.7	44.4±1.6	78.6±7.3
MEA2	33.7±0.6	46.5±1.1	68.5±2.6	77.9±3.1	85.8±3.2
MEA3	69.7±6.2	84.3±3.2	89.8±0.5	90.7±0.3	93.7±0.8
MEA4	61.1±25.0	78.4±6.6	89.0±1.9	94.6±0.7	97.9±0.3
MEA5	72.1±9.2	84.0±1.2	90.4±1.9	92.6±0.9	94.4±0.3
AdvMEA	90.0±0.9	90.1±0.1	90.1±0.4	89.9±0.8	90.1±0.3
CEGA	91.5±0.4	93.3±0.6	93.5±0.4	95.6±1.1	96.2±0.4
Realistic	72.8±4.6	85.6±2.4	73.0±7.3	75.6±1.1	72.0±3.2
DFEA_I	95.4±0.3	96.4±0.6	97.3±0.3	97.6±0.7	97.7±0.7
DFEA_II	93.6±0.7	94.4±0.5	96.3±0.2	97.3±0.1	99.6±0.1
DFEA_III	93.7±0.3	95.1±0.4	96.8±0.4	97.7±0.4	98.7±0.1

(d) Regime=data_free

Attack	0.05	0.10	0.25	0.50	1.00
MEA0	4.6±2.8	27.6±18.8	2.7±0.5	16.3±11.3	19.5±20.3
MEA1	2.7±0.5	2.7±0.5	2.7±0.5	2.7±0.5	2.7±0.5
MEA2	31.1±1.6	43.4±2.3	67.7±1.7	77.6±4.8	85.8±3.2
MEA3	6.2±2.2	18.9±20.8	28.8±20.2	35.8±22.6	17.8±21.4
MEA4	4.6±2.7	14.6±12.7	4.6±2.8	14.7±12.6	12.5±13.9
MEA5	2.7±0.5	33.3±21.6	30.5±12.9	24.6±18.9	17.9±21.9
AdvMEA	89.7±0.6	90.5±0.9	89.9±0.6	90.0±0.7	89.7±0.3
CEGA	89.6±1.7	92.8±0.7	95.0±0.2	95.1±1.0	96.5±0.4
Realistic	72.7±2.0	75.2±2.1	73.5±0.7	73.5±2.0	71.6±4.1
DFEA_I	95.4±0.3	96.4±0.6	97.3±0.3	97.6±0.7	97.7±0.7
DFEA_II	93.6±0.7	94.4±0.5	96.3±0.2	97.3±0.1	99.6±0.1
DFEA_III	93.7±0.3	95.1±0.4	96.8±0.4	97.7±0.4	98.7±0.1

Table 23: RQ1 detailed for dataset=Computers, metric=Acc (%). Rows are attacks; columns are budgets. Mean ± std across seeds; best per column is bold.

(a) Regime=both

Attack	0.05	0.10	0.25	0.50	1.00
MEA0	51.7±7.0	60.4±4.2	65.7±2.4	67.3±2.3	71.4±1.4
MEA1	46.4±19.1	31.3±14.7	48.1±2.6	51.9±1.4	53.0±5.3
MEA2	40.2±23.5	43.0±22.8	42.1±25.4	40.8±26.2	41.5±26.7
MEA3	61.6±2.2	69.8±2.0	66.0±1.3	69.3±2.5	70.7±3.1
MEA4	41.7±14.8	35.0±19.2	65.9±4.1	66.5±3.7	71.7±0.3
MEA5	67.8±2.0	68.8±2.9	69.4±3.1	70.5±3.3	70.1±4.2
AdvMEA	34.7±17.3	20.8±22.8	22.4±23.3	46.8±13.1	16.8±11.4
CEGA	29.8±21.9	27.8±20.7	34.8±14.0	45.4±24.1	39.6±25.5
Realistic	2.4±1.1	1.1±0.7	1.1±0.7	1.5±1.2	1.1±0.7
DFEA_I	39.2±24.6	40.5±15.6	39.9±22.8	36.9±22.9	45.4±13.7
DFEA_II	31.5±19.0	30.1±18.0	30.1±18.0	30.1±18.0	30.1±18.0
DFEA_III	45.2±22.1	41.3±16.4	44.1±21.4	46.4±21.2	46.1±21.7

(b) Regime=x_only

Attack	0.05	0.10	0.25	0.50	1.00
MEA0	54.7±8.8	63.8±1.1	64.4±5.4	64.7±6.9	67.0±4.9
MEA1	46.4±19.1	31.3±14.7	48.0±2.5	51.7±1.3	52.9±5.6
MEA2	41.5±23.0	42.1±21.0	41.8±24.8	41.4±25.6	41.5±26.7
MEA3	63.7±3.0	68.4±1.8	69.2±3.4	70.3±3.9	70.1±1.8
MEA4	31.7±4.2	37.0±22.1	61.4±4.3	67.2±0.9	71.4±1.1
MEA5	69.9±2.3	67.7±2.3	67.9±3.1	71.1±3.3	72.1±1.9
AdvMEA	27.6±23.9	33.1±21.1	31.6±22.4	29.5±21.4	40.4±26.8
CEGA	27.9±17.2	27.5±20.0	43.6±25.0	25.1±22.5	41.6±29.1
Realistic	12.9±15.6	13.2±16.7	1.1±0.7	13.6±16.6	10.9±13.6
DFEA_I	38.5±24.2	40.6±15.7	39.9±22.8	37.0±22.9	45.4±13.7
DFEA_II	31.5±19.0	30.1±18.0	30.1±18.0	30.1±18.0	30.1±18.0
DFEA_III	44.2±22.0	41.2±16.4	44.1±21.4	46.6±21.3	45.7±21.6

(c) Regime=a_only

Attack	0.05	0.10	0.25	0.50	1.00
MEA0	62.9±5.2	64.4±2.9	62.3±1.6	67.7±2.6	67.6±3.3
MEA1	46.4±19.1	31.3±14.7	48.1±2.6	51.9±1.4	53.0±5.3
MEA2	38.9±21.1	41.3±23.3	41.3±24.3	41.4±26.5	41.5±26.7
MEA3	62.1±2.2	67.2±1.0	68.1±4.2	65.2±5.8	71.7±1.7
MEA4	40.2±16.5	44.6±19.3	54.0±17.1	62.2±7.8	68.4±0.5
MEA5	64.5±4.1	69.9±0.5	68.3±1.8	71.5±4.9	71.7±1.6
AdvMEA	36.9±14.9	40.3±16.2	27.0±23.9	31.6±24.1	17.2±8.3
CEGA	29.1±16.6	31.0±20.7	39.7±23.2	36.1±25.4	39.3±28.1
Realistic	12.7±16.1	1.5±1.2	15.0±19.4	1.1±0.7	14.6±18.4
DFEA_I	39.1±24.5	40.1±15.4	39.9±22.8	37.0±22.9	45.5±13.8
DFEA_II	31.2±18.8	30.1±18.0	30.1±18.0	25.4±15.7	30.1±18.0
DFEA_III	44.2±22.0	41.3±16.4	44.1±21.4	46.6±21.3	46.1±21.7

(d) Regime=data_free

Attack	0.05	0.10	0.25	0.50	1.00
MEA0	25.7±22.9	11.7±7.5	29.7±18.9	44.1±16.9	8.6±8.2
MEA1	56.1±0.0	56.1±0.0	56.1±0.0	56.1±0.0	56.1±0.0
MEA2	40.1±21.2	41.5±21.8	42.5±22.9	40.1±25.0	41.5±26.7
MEA3	38.6±24.7	41.7±20.4	27.3±20.9	25.6±23.0	19.8±25.7
MEA4	25.6±23.0	4.7±5.8	19.0±26.2	5.7±5.3	4.7±5.8
MEA5	19.3±26.0	20.9±25.0	25.4±22.0	26.5±21.2	24.8±22.8
AdvMEA	42.6±13.0	32.0±16.6	23.6±21.7	20.7±17.0	39.4±10.4
CEGA	30.4±15.3	17.2±17.0	39.6±28.3	34.9±26.8	36.4±24.5
Realistic	13.6±17.4	1.3±0.5	10.8±13.4	8.2±9.7	1.0±0.6
DFEA_I	38.7±24.3	40.4±15.6	39.9±22.8	37.0±23.0	45.5±13.8
DFEA_II	31.2±18.8	30.1±18.0	30.1±18.0	30.1±18.0	30.1±18.0
DFEA_III	44.2±22.0	41.3±16.4	44.1±21.4	46.6±21.3	45.7±21.6

Table 24: RQ1 detailed for dataset=Computers, metric=F1 (%). Rows are attacks; columns are budgets. Mean ± std across seeds; best per column is bold.

(a) Regime=both

Attack	0.05	0.10	0.25	0.50	1.00
MEA0	22.0±6.0	44.3±4.0	46.4±8.0	44.1±2.0	60.0±0.6
MEA1	13.0±6.0	7.6±3.7	17.2±5.5	19.3±7.8	22.7±4.6
MEA2	20.3±12.7	27.3±15.1	27.8±18.1	26.5±18.2	27.1±18.8
MEA3	20.6±4.3	41.7±4.6	44.0±4.2	54.5±4.0	58.8±2.5
MEA4	13.8±1.8	16.5±9.6	28.0±6.6	36.7±9.7	46.8±4.4
MEA5	29.8±1.1	39.5±4.5	56.3±4.8	53.5±1.9	53.7±8.7
AdvMEA	21.7±13.1	14.9±14.0	15.5±16.6	30.0±8.0	12.0±9.9
CEGA	26.8±18.9	22.8±15.0	31.3±15.1	39.5±23.5	33.4±21
Realistic	2.0±1.2	0.2±0.1	0.2±0.1	0.5±0.3	0.2±0.1
DFEA_I	32.3±22.5	29.9±16.3	33.4±19.9	28.2±20.8	29.6±19.0
DFEA_II	11.7±9.4	4.3±2.4	4.3±2.4	4.3±2.4	4.3±2.4
DFEA_III	34.2±18.1	27.6±15.8	32.1±18.4	38.0±20.3	38.7±20.9

(b) Regime=x_only

Attack	0.05	0.10	0.25	0.50	1.00
MEA0	29.9±7.4	41.9±4.5	43.1±8.7	42.5±18.6	50.8±7.5
MEA1	13.0±6.0	7.6±3.7	17.1±5.5	19.9±8.5	27.8±2.7
MEA2	25.4±14.1	26.3±12.6	26.6±15.9	27.5±18.5	27.1±18.8
MEA3	29.0±3.6	40.5±2.5	50.5±7.4	51.0±12.1	56.9±3.9
MEA4	12.7±4.4	15.6±5.3	24.6±5.1	34.5±9.6	47.8±1.1
MEA5	32.9±4.8	39.0±4.6	50.6±8.6	52.5±4.6	59.5±1.9
AdvMEA	17.3±13.6	17.5±12.9	22.8±16.0	18.8±11.7	27.5±18.8
CEGA	29.1±17.2	27.1±19.3	36.9±20.2	21.0±20.3	35.8±25.5
Realistic	3.9±4.3	5.1±6.8	0.2±0.1	5.5±7.2	3.2±4.1
DFEA_I	31.9±22.1	30.0±16.4	33.2±19.7	27.8±20.3	29.6±19.0
DFEA_II	11.7±9.4	4.3±2.4	4.3±2.4	4.3±2.4	4.3±2.4
DFEA_III	30.4±15.7	26.8±14.8	32.1±18.4	38.1±20.4	37.6±20.3

(c) Regime=a_only

Attack	0.05	0.10	0.25	0.50	1.00
MEA0	33.3±3.9	44.3±5.7	35.8±10.0	55.1±0.6	52.9±5.0
MEA1	13.0±6.0	7.6±3.7	17.2±5.5	19.3±7.8	22.7±4.6
MEA2	22.1±12.5	25.9±15.4	26.8±16.7	27.2±18.7	27.1±18.8
MEA3	24.9±1.6	34.9±1.8	45.5±9.0	42.4±18.4	60.8±2.4
MEA4	15.1±4.4	16.4±9.1	27.8±5.7	32.1±8.9	40.6±5.5
MEA5	32.5±5.3	38.5±1.8	48.9±5.2	57.0±9.1	58.4±1.5
AdvMEA	23.1±12.3	25.9±11.9	17.8±16.5	20.0±15.2	11.9±6.3
CEGA	21.5±15.5	22.0±23.1	33.2±19.2	31.4±19.8	34.6±25.0
Realistic	4.0±5.2	0.4±0.3	4.3±5.6	0.2±0.1	4.8±5.8
DFEA_I	31.9±22.1	29.6±15.9	33.4±19.9	27.8±20.3	29.3±18.7
DFEA_II	11.6±9.4	4.3±2.4	4.3±2.4	6.1±4.3	4.3±2.4
DFEA_III	30.4±15.7	27.6±15.8	32.1±18.4	38.1±20.3	38.7±20.9

(d) Regime=data_free

Attack	0.05	0.10	0.25	0.50	1.00
MEA0	3.6±2.9	2.0±1.2	4.3±2.1	5.9±1.8	1.5±1.3
MEA1	7.2±0.0	7.2±0.0	7.2±0.0	7.2±0.0	7.2±0.0
MEA2	24.2±11.6	25.1±13.5	25.3±13.9	26.2±17.5	27.1±18.8
MEA3	5.0±3.1	5.6±2.3	5.1±3.5	3.5±2.9	2.7±3.2
MEA4	3.5±2.9	0.8±1.0	2.5±3.3	1.0±0.9	0.8±1.0
MEA5	2.7±3.2	3.3±2.9	4.8±3.0	4.4±2.1	4.4±2.9
AdvMEA	31.8±11.4	21.1±13.9	13.9±11.5	16.2±13.4	23.3±8.1
CEGA	21.7±13.3	15.7±18.4	32.8±22.6	28.1±20.6	35.5±22.6
Realistic	5.2±6.9	1.0±1.1	3.6±4.7	2.2±2.7	0.2±0.1
DFEA_I	31.7±22.0	29.8±16.1	33.4±19.9	27.8±20.3	29.3±18.7
DFEA_II	11.5±9.3	4.3±2.4	4.3±2.4	4.3±2.4	4.3±2.4
DFEA_III	30.4±15.7	27.6±15.8	32.0±18.4	38.1±20.4	37.6±20.3

Table 25: RQ1 detailed for dataset=Computers, metric=Fidelity (%). Rows are attacks; columns are budgets. Mean ± std across seeds; best per column is bold.

(a) Regime=both

Attack	0.05	0.10	0.25	0.50	1.00
MEA0	51.0±7.0	67.3±3.1	67.0±1.5	71.4±2.7	80.5±4.6
MEA1	41.5±15.5	27.7±14.0	46.2±5.5	49.4±5.6	56.3±12.6
MEA2	51.0±7.5	58.8±6.0	65.2±2.4	66.2±6.3	68.3±8.0
MEA3	53.8±3.0	64.8±5.5	67.6±6.2	74.9±4.3	79.5±5.2
MEA4	38.4±13.4	37.9±12.6	63.6±4.0	74.3±5.0	83.7±4.3
MEA5	61.3±4.3	65.6±6.4	66.5±2.1	73.9±3.5	76.3±4.2
AdvMEA	35.5±17.8	25.7±24.7	26.9±22.4	46.1±12.5	22.8±11.8
CEGA	36.0±25.0	36.7±23.0	43.4±17.5	53.9±29.2	54.1±33.4
Realistic	64.5±33.7	67.9±45.4	67.7±45.3	67.4±44.0	67.0±44.8
DFEA_I	67.5±12.4	73.7±18.1	60.3±25.5	64.8±15.9	55.8±28.2
DFEA_II	43.9±8.1	28.4±20.5	28.4±20.5	28.4±20.5	28.4±20.5
DFEA_III	72.9±5.5	66.7±14.2	72.9±3.1	82.5±3.1	82.1±2.8

(b) Regime=x_only

Attack	0.05	0.10	0.25	0.50	1.00
MEA0	54.8±10.5	65.4±7.0	70.6±2.9	69.7±10.9	79.8±3.1
MEA1	41.5±15.5	27.7±14.0	46.2±5.5	49.1±5.7	57.1±11.4
MEA2	53.9±6.6	58.6±6.4	63.9±0.6	68.4±5.0	68.3±8.0
MEA3	56.5±7.4	61.9±5.6	68.2±4.2	71.7±4.9	77.6±3.1
MEA4	33.7±0.4	34.7±18.5	65.6±4.0	75.7±0.8	84.6±3.4
MEA5	59.4±3.4	65.5±5.2	71.0±3.6	75.4±5.6	79.5±3.5
AdvMEA	29.0±24.1	33.6±19.9	34.5±23.4	28.7±16.6	39.8±25.8
CEGA	30.9±16.1	33.6±25.2	49.2±24.3	33.1±30.1	49.8±33.8
Realistic	75.1±25.8	78.7±30.0	67.9±45.4	81.0±25.5	78.6±25.1
DFEA_I	67.3±12.1	73.5±18.1	60.7±25.9	64.9±16.2	55.4±27.8
DFEA_II	43.9±8.1	28.4±20.5	28.4±20.5	28.4±20.5	28.4±20.5
DFEA_III	69.9±2.4	65.7±13.4	72.9±3.1	82.2±2.9	82.3±2.9

(c) Regime=a_only

Attack	0.05	0.10	0.25	0.50	1.00
MEA0	60.7±2.6	66.5±6.5	66.1±1.6	77.1±2.9	78.8±0.9
MEA1	41.5±15.5	27.7±14.0	46.2±5.5	49.4±5.6	56.3±12.6
MEA2	47.8±10.2	59.6±4.5	64.3±1.1	66.8±7.2	68.3±8.0
MEA3	58.0±4.7	62.7±5.5	68.4±4.2	65.1±4.4	79.5±4.4
MEA4	42.3±14.5	38.0±15.4	54.9±16.2	64.1±4.0	81.2±2.2
MEA5	57.7±4.0	62.8±3.9	69.7±5.2	72.5±3.9	80.9±3.3
AdvMEA	39.9±16.5	40.0±16.3	32.3±22.2	32.2±23.3	20.2±8.3
CEGA	37.9±19.9	37.9±23.5	50.1±27.4	45.4±30.8	51.6±32.9
Realistic	69.5±26.3	64.5±43.1	77.2±30.2	67.8±45.4	80.8±26.0
DFEA_I	67.3±12.2	73.2±17.9	60.3±25.5	64.9±16.2	55.8±28.1
DFEA_II	44.2±7.8	28.4±20.4	28.4±20.5	38.9±12.6	28.4±20.5
DFEA_III	69.9±2.4	66.7±14.2	72.9±3.1	82.4±3.1	82.1±2.8

(d) Regime=data_free

Attack	0.05	0.10	0.25	0.50	1.00
MEA0	22.2±16.0	9.5±6.5	22.7±14.2	33.7±11.0	14.2±10.6
MEA1	40.4±1.6	40.4±1.6	40.4±1.6	40.4±1.6	40.4±1.6
MEA2	54.3±7.2	57.0±7.2	66.0±2.4	67.1±4.5	68.4±8.0
MEA3	31.8±13.7	29.5±15.1	22.4±13.8	19.9±16.5	15.6±18.0
MEA4	23.9±16.7	3.3±3.6	15.1±19.0	6.7±5.1	4.4±4.7
MEA5	16.1±17.6	15.7±16.2	18.4±13.6	22.6±12.8	23.1±14.1
AdvMEA	44.9±13.6	34.2±18.1	21.6±17.4	24.3±18.1	40.7±12.2
CEGA	33.6±15.6	21.0±18.4	49.4±31.1	46.2±32.9	50.0±30.4
Realistic	82.1±22.2	70.2±41.7	82.5±24.8	75.5±34.6	66.5±44.5
DFEA_I	67.3±12.2	73.8±18.2	60.3±25.5	65.1±16.3	55.8±28.1
DFEA_II	44.2±7.8	28.4±20.5	28.4±20.5	28.4±20.5	28.4±20.4
DFEA_III	69.9±2.4	66.7±14.2	73.0±2.9	82.2±2.9	82.3±2.9

Table 26: RQ1 detailed for dataset=Photo, metric=Acc (%). Rows are attacks; columns are budgets. Mean ± std across seeds; best per column is bold.

(a) Regime=both

Attack	0.05	0.10	0.25	0.50	1.00
MEA0	55.1±30.4	90.2±3.8	94.9±0.6	96.4±0.2	95.5±0.4
MEA1	2.0±0.2	39.5±26.2	42.2±28.9	62.7±33.5	67.0±36.5
MEA2	84.4±2.3	89.0±1.9	90.1±2.2	91.4±2.0	92.4±2.3
MEA3	78.9±14.6	93.9±2.4	96.2±0.4	96.5±0.2	96.3±0.5
MEA4	74.6±2.4	83.0±8.4	95.1±0.3	95.5±0.4	96.0±0.5
MEA5	80.2±7.1	92.8±1.3	95.0±1.6	95.5±0.8	96.4±0.2
AdvMEA	49.0±22.8	38.0±24.8	47.3±27.6	36.8±26.7	40.9±24.8
CEGA	79.6±5.4	83.0±14.5	89.8±6.4	94.8±0.6	88.9±9.3
Realistic	49.0±1.1	47.7±8.3	64.5±19.4	63.3±20.6	50.3±7.0
DFEA_I	91.0±2.5	91.1±2.9	91.4±2.7	91.4±3.0	91.7±3.1
DFEA_II	30.2±33.7	28.7±31.6	15.8±6.6	11.1±6.6	14.4±6.1
DFEA_III	92.3±1.6	92.6±1.8	90.6±3.6	92.4±1.8	92.7±1.9

(b) Regime=x_only

Attack	0.05	0.10	0.25	0.50	1.00
MEA0	84.5±5.9	91.1±2.3	95.4±0.8	95.9±0.8	96.0±0.4
MEA1	2.0±0.2	39.6±26.4	42.2±28.9	62.7±33.5	67.0±36.5
MEA2	87.8±2.0	89.3±2.2	90.6±1.9	91.1±2.4	92.4±2.3
MEA3	83.0±5.1	92.8±2.1	95.7±0.1	95.8±0.8	96.2±0.3
MEA4	67.2±18.6	86.0±2.1	87.8±8.1	96.0±0.4	96.0±0.1
MEA5	82.5±13.8	94.5±1.7	95.9±0.1	96.4±0.2	96.1±0.6
AdvMEA	48.7±30.4	40.1±24.6	42.7±26.8	44.0±25.6	57.3±17.0
CEGA	84.9±6.6	85.9±6.1	82.7±7.0	93.8±1.9	94.1±3.0
Realistic	53.5±5.7	34.5±15.1	51.7±5.8	61.5±14.2	56.9±15.7
DFEA_I	91.0±2.4	91.1±2.9	91.4±2.7	91.4±3.0	91.7±3.1
DFEA_II	30.2±33.7	28.7±31.6	15.8±6.6	11.1±6.6	14.4±6.1
DFEA_III	92.3±1.6	92.6±1.8	90.6±3.6	92.4±1.8	92.7±1.9

(c) Regime=a_only

Attack	0.05	0.10	0.25	0.50	1.00
MEA0	87.2±5.3	92.2±1.8	93.9±1.5	95.9±0.2	95.7±0.5
MEA1	2.0±0.2	39.4±26.0	42.2±28.9	62.7±33.5	67.0±36.5
MEA2	87.3±1.8	88.8±2.4	90.5±2.2	91.5±2.4	92.4±2.3
MEA3	81.6±3.9	92.5±1.8	95.6±0.2	96.0±0.2	96.7±0.3
MEA4	69.2±15.5	75.7±19.8	90.5±2.4	95.9±0.2	96.0±0.3
MEA5	75.5±4.4	94.2±1.3	95.7±0.4	96.0±0.2	96.6±0.4
AdvMEA	47.8±27.0	52.5±30.7	33.5±28.0	47.0±31.9	38.9±6.2
CEGA	90.0±3.4	84.9±8.2	95.1±0.7	95.5±0.9	94.2±2.5
Realistic	47.0±7.1	33.5±13.4	51.8±7.0	59.2±19.6	66.4±19.5
DFEA_I	90.9±2.5	91.1±2.9	91.4±2.7	91.4±3.0	91.7±3.1
DFEA_II	30.2±33.7	28.7±31.6	15.8±6.6	11.1±6.6	14.4±6.1
DFEA_III	92.3±1.6	92.6±1.8	90.6±3.6	92.4±1.8	92.7±1.9

(d) Regime=data_free

Attack	0.05	0.10	0.25	0.50	1.00
MEA0	10.4±6.9	28.0±13.5	15.8±0.8	16.9±0.0	11.7±7.5
MEA1	10.2±7.2	10.2±7.2	10.2±7.2	10.2±7.2	10.2±7.2
MEA2	85.9±2.1	89.2±1.4	90.4±2.0	91.4±2.4	92.4±2.3
MEA3	21.2±19.2	10.8±7.5	5.7±6.8	6.1±7.7	15.3±0.0
MEA4	11.3±8.0	11.2±7.0	11.0±7.3	11.7±7.4	5.9±7.8
MEA5	32.0±21.4	27.1±14.2	10.9±6.3	10.4±6.4	22.1±19.1
AdvMEA	49.3±29.1	50.8±30.7	36.9±25.8	46.9±29.3	40.9±24.7
CEGA	51.2±32.0	89.9±7.7	95.1±0.5	92.7±2.8	92.8±1.5
Realistic	42.1±18.6	63.2±19.3	61.1±20.5	33.7±13.0	57.9±17.0
DFEA_I	90.9±2.5	91.1±2.9	91.4±2.7	91.4±3.0	91.7±3.1
DFEA_II	30.2±33.7	28.7±31.6	15.8±6.6	11.1±6.6	14.4±6.1
DFEA_III	92.3±1.6	92.6±1.8	90.6±3.6	92.4±1.8	92.7±1.9

Table 27: RQ1 detailed for dataset=Photo, metric=F1 (%). Rows are attacks; columns are budgets. Mean ± std across seeds; best per column is bold.

(a) Regime=both

Attack	0.05	0.10	0.25	0.50	1.00
MEA0	31.9±15.5	54.4±4.2	59.6±4.6	64.4±2.4	62.0±3.0
MEA1	2.0±0.2	22.6±14.3	25.7±19.3	33.5±21.6	41.6±27.2
MEA2	42.2±2.4	49.7±8.8	56.4±6.6	57.4±8.7	59.0±9.6
MEA3	52.0±9.1	66.9±7.6	64.5±1.7	66.9±4.1	64.9±5.5
MEA4	32.6±2.7	37.6±7.0	50.1±2.0	49.6±1.5	55.3±2.8
MEA5	56.8±9.0	66.4±4.1	60.2±3.6	61.7±5.3	62.7±0.7
AdvMEA	28.5±14.3	25.6±14.7	28.6±15.2	20.1±16.2	21.8±13.3
CEGA	45.7±3.0	50.3±11.3	55.4±4.3	58.5±1.2	55.1±8.4
Realistic	15.4±4.7	15.9±4.8	28.0±18.4	28.6±19.9	17.0±5.2
DFEA_I	48.3±3.5	51.4±6.5	49.8±9.2	51.0±11.5	51.8±11.9
DFEA_II	16.9±21.7	14.0±17.7	10.0±6.0	5.4±5.5	5.6±4.5
DFEA_III	51.2±4.7	57.4±9.6	53.6±12.3	57.9±7.3	56.2±11.7

(b) Regime=x_only

Attack	0.05	0.10	0.25	0.50	1.00
MEA0	46.4±7.7	59.5±6.0	58.4±2.4	66.3±2.7	65.7±1.0
MEA1	2.0±0.2	22.7±14.5	25.7±19.3	33.5±21.6	41.6±27.2
MEA2	43.5±1.7	45.4±2.8	48.2±2.8	58.0±10.2	59.0±9.6
MEA3	54.0±9.8	61.5±5.0	63.3±5.3	68.0±2.2	69.5±4.5
MEA4	24.8±15.5	43.3±4.7	43.0±5.1	60.1±4.7	55.9±2.4
MEA5	48.2±17.8	61.7±4.6	60.4±3.9	69.9±5.0	62.9±2.7
AdvMEA	28.7±14.8	23.3±13.4	24.0±15.4	29.0±16.3	34.3±10.8
CEGA	48.6±8.1	53.1±4.3	45.6±7.4	59.3±3.3	58.5±3.0
Realistic	15.3±4.5	13.0±4.5	15.6±5.0	26.5±15.7	22.5±12.1
DFEA_I	48.7±3.1	51.4±6.5	49.8±9.2	51.0±11.5	51.8±11.9
DFEA_II	16.9±21.7	14.0±17.7	10.0±6.0	5.4±5.5	5.6±4.5
DFEA_III	51.2±4.7	57.4±9.6	53.6±12.3	57.9±7.3	56.2±11.7

(c) Regime=a_only

Attack	0.05	0.10	0.25	0.50	1.00
MEA0	57.9±4.5	63.7±7.0	57.5±9.1	64.2±3.5	64.0±4.5
MEA1	2.0±0.2	22.7±14.5	25.7±19.3	33.5±21.6	41.6±27.2
MEA2	48.6±10.0	48.5±6.9	52.2±8.7	58.3±10.5	59.0±9.6
MEA3	45.1±7.8	57.7±3.2	60.5±2.4	65.9±3.7	65.3±2.1
MEA4	33.8±6.9	33.0±17.0	46.4±4.7	51.1±3.2	56.1±4.1
MEA5	43.2±7.8	62.0±1.4	64.6±5.2	64.1±5.3	65.4±5.1
AdvMEA	29.5±14.9	32.1±17.1	19.4±17.3	26.8±17.8	21.6±3.4
CEGA	54.2±3.2	49.3±8.7	62.0±2.1	62.0±3.6	58.2±3.0
Realistic	15.0±3.0	10.0±5.7	17.1±5.6	26.5±17.5	32.6±24.6
DFEA_I	48.6±3.2	51.4±6.5	49.8±9.2	51.0±11.5	51.8±11.9
DFEA_II	16.9±21.7	14.0±17.7	10.0±6.0	5.4±5.5	5.6±4.5
DFEA_III	51.2±4.7	57.4±9.6	53.6±12.3	57.9±7.3	56.2±11.7

(d) Regime=data_free

Attack	0.05	0.10	0.25	0.50	1.00
MEA0	2.3±1.5	5.3±1.9	3.4±0.1	3.6±0.0	2.5±1.6
MEA1	2.2±1.6	2.2±1.6	2.2±1.6	2.2±1.6	2.2±1.6
MEA2	43.3±2.6	46.6±3.1	46.0±3.5	59.1±9.5	59.0±9.6
MEA3	3.9±3.2	2.9±0.8	1.6±1.6	1.3±1.6	3.3±0.0
MEA4	2.4±1.7	2.4±1.5	2.4±1.6	2.5±1.6	1.3±1.7
MEA5	5.8±3.1	7.0±2.2	3.1±0.3	2.6±1.7	4.0±3.2
AdvMEA	29.9±15.9	30.8±17.4	22.9±14.2	29.2±19.0	23.3±11.7
CEGA	31.0±17.9	55.3±6.1	62.7±1.6	59.0±3.2	60.0±4.9
Realistic	13.7±4.1	28.6±18.2	27.0±17.7	10.3±6.3	24.6±15.1
DFEA_I	48.6±3.2	51.4±6.5	49.8±9.2	51.0±11.5	51.8±11.9
DFEA_II	16.9±21.7	14.0±17.7	10.0±6.0	5.4±5.5	5.6±4.5
DFEA_III	51.2±4.7	57.4±9.6	53.6±12.3	57.9±7.3	56.2±11.7

Table 28: RQ1 detailed for dataset=Photo, metric=Fidelity (%). Rows are attacks; columns are budgets. Mean ± std across seeds; best per column is bold.

(a) Regime=both

Attack	0.05	0.10	0.25	0.50	1.00
MEA0	54.7±30.8	90.8±4.1	95.4±1.4	96.6±1.1	96.8±0.1
MEA1	1.9±0.3	39.2±26.6	42.0±29.2	62.1±33.8	67.0±37.2
MEA2	85.2±3.2	89.2±2.4	93.3±2.0	95.4±1.6	96.1±1.9
MEA3	78.3±15.0	93.9±3.0	96.5±0.8	96.9±0.9	97.8±1.0
MEA4	74.3±2.6	83.1±8.2	95.2±0.4	96.7±1.1	97.4±0.8
MEA5	80.1±6.6	92.4±0.8	95.0±2.3	95.9±0.9	97.5±0.6
AdvMEA	49.5±22.9	38.6±24.6	48.0±27.4	37.3±26.7	41.3±24.7
CEGA	80.6±5.0	83.7±15.1	91.4±6.8	95.9±1.2	90.4±9.5
Realistic	70.7±15.3	72.5±13.9	83.6±10.3	86.9±5.1	77.5±11.1
DFEA_I	92.6±3.9	93.8±1.9	91.6±4.4	91.5±4.6	91.4±4.8
DFEA_II	30.1±31.7	29.2±30.5	16.1±5.2	11.4±5.4	13.8±6.1
DFEA_III	92.9±3.0	93.3±2.5	91.8±5.2	94.2±2.3	95.4±2.4

(b) Regime=x_only

Attack	0.05	0.10	0.25	0.50	1.00
MEA0	84.2±5.8	91.0±3.3	96.0±0.8	96.8±1.0	96.6±1.2
MEA1	1.9±0.3	39.3±26.8	42.0±29.2	62.1±33.8	67.0±37.2
MEA2	86.8±3.4	90.2±1.8	92.9±2.0	95.4±1.8	96.1±1.9
MEA3	82.4±5.2	92.6±0.8	96.1±0.7	96.3±1.1	96.7±0.8
MEA4	67.3±18.7	85.8±1.8	88.5±7.8	97.0±0.9	97.3±0.9
MEA5	81.9±13.2	94.0±1.1	96.2±0.7	96.9±1.4	97.8±0.8
AdvMEA	49.5±30.4	40.3±24.6	43.1±26.5	44.7±25.5	57.6±17.4
CEGA	85.5±7.2	86.6±5.8	83.7±7.5	94.8±2.3	95.5±2.9
Realistic	76.1±11.1	53.1±24.5	72.3±16.7	81.6±9.4	85.5±5.4
DFEA_I	93.0±3.4	93.8±1.9	91.6±4.4	91.5±4.6	91.4±4.8
DFEA_II	30.1±31.7	29.2±30.5	16.1±5.2	11.4±5.4	13.8±6.1
DFEA_III	92.9±3.0	93.3±2.5	91.8±5.2	94.2±2.3	95.4±2.4

(c) Regime=a_only

Attack	0.05	0.10	0.25	0.50	1.00
MEA0	87.3±5.7	92.4±1.1	94.3±2.3	96.5±0.9	97.5±0.9
MEA1	1.9±0.3	39.1±26.5	42.0±29.2	62.1±33.8	67.0±37.2
MEA2	88.5±2.5	90.1±2.0	92.8±2.1	95.4±1.7	96.1±1.9
MEA3	81.4±3.8	92.4±2.3	95.8±1.0	96.8±0.8	97.6±0.7
MEA4	69.0±16.2	76.0±19.4	90.9±2.0	96.1±0.6	98.2±0.5
MEA5	75.2±4.1	94.2±1.4	95.9±0.5	96.8±0.7	97.7±1.1
AdvMEA	48.3±26.7	53.1±30.6	34.1±28.0	47.7±31.8	39.1±6.0
CEGA	90.6±3.9	85.5±8.8	95.4±1.1	97.3±0.8	96.4±1.8
Realistic	69.3±14.6	62.2±32.2	78.4±11.1	84.9±7.0	85.2±8.0
DFEA_I	92.9±3.6	93.8±1.9	91.6±4.4	91.5±4.6	91.4±4.8
DFEA_II	30.1±31.7	29.2±30.5	16.1±5.2	11.4±5.4	13.8±6.1
DFEA_III	92.9±3.0	93.3±2.5	91.8±5.2	94.2±2.3	95.4±2.4

(d) Regime=data_free

Attack	0.05	0.10	0.25	0.50	1.00
MEA0	10.3±7.0	28.3±13.4	15.6±0.6	16.2±0.6	11.6±7.6
MEA1	10.3±6.6	10.3±6.6	10.3±6.6	10.3±6.6	10.3±6.6
MEA2	86.4±2.8	89.3±1.6	92.8±2.6	95.2±1.9	96.1±1.9
MEA3	21.1±19.3	10.3±7.2	5.3±7.2	6.2±7.2	14.9±0.5
MEA4	11.1±8.0	10.7±6.7	10.0±6.9	10.9±7.0	5.9±7.4
MEA5	31.9±21.7	26.9±14.6	10.1±6.4	10.3±6.5	22.2±19.2
AdvMEA	50.3±29.2	51.6±30.7	37.6±25.6	47.6±29.1	41.1±24.3
CEGA	51.7±32.2	91.0±7.8	95.9±1.0	93.8±2.4	94.2±1.4
Realistic	70.4±15.5	86.8±4.3	86.0±5.6	61.8±31.4	85.0±5.8
DFEA_I	92.9±3.5	93.8±1.9	91.6±4.4	91.5±4.6	91.4±4.8
DFEA_II	30.1±31.7	29.2±30.5	16.1±5.2	11.4±5.4	13.8±6.1
DFEA_III	92.9±3.0	93.3±2.5	91.8±5.2	94.2±2.3	95.4±2.4

Table 29: RQ1 detailed for dataset=PubMed, metric=Acc (%). Rows are attacks; columns are budgets. Mean ± std across seeds; best per column is bold.

(a) Regime=both

Attack	0.05	0.10	0.25	0.50	1.00
MEA0	70.6±1.5	75.8±1.8	77.4±0.3	76.7±0.4	78.2±0.3
MEA1	68.6±2.3	70.6±5.0	74.8±3.4	75.3±3.5	75.5±3.9
MEA2	69.9±0.9	72.8±0.6	76.1±1.0	77.7±0.5	77.8±0.2
MEA3	72.1±1.9	73.4±1.6	76.6±0.7	79.0±1.1	77.3±1.7
MEA4	67.8±0.6	71.2±3.8	75.3±0.9	78.2±0.5	78.6±0.8
MEA5	72.3±3.4	75.9±0.1	77.8±0.8	77.8±0.7	78.1±1.1
AdvMEA	60.4±3.2	66.5±1.9	65.5±2.6	62.6±6.7	66.0±2.6
CEGA	78.3±0.4	77.9±1.6	78.2±0.2	79.1±0.2	78.7±0.7
Realistic	72.7±1.5	71.5±1.0	74.7±0.2	75.6±1.8	76.8±0.8
DFEA_I	78.2±0.2	78.5±0.3	78.5±0.2	78.4±0.4	78.7±0.2
DFEA_II	78.7±0.5	78.9±0.5	79.7±0.4	79.6±0.4	79.1±0.3
DFEA_III	78.3±0.1	78.5±0.4	78.8±0.1	78.9±0.1	78.9±0.2

(b) Regime=x_only

Attack	0.05	0.10	0.25	0.50	1.00
MEA0	72.1±3.2	76.8±1.1	76.8±1.7	78.0±0.5	78.5±0.3
MEA1	68.6±2.3	70.6±5.0	74.8±3.4	75.3±3.5	75.5±3.9
MEA2	69.4±0.1	73.9±0.7	76.4±1.2	77.6±0.2	77.8±0.2
MEA3	73.2±1.1	75.4±1.4	77.2±0.6	77.4±0.7	78.0±0.6
MEA4	51.5±4.7	65.7±6.3	77.0±1.3	77.4±0.9	78.6±0.8
MEA5	70.6±2.8	74.5±1.0	77.0±1.4	77.7±0.5	77.5±0.9
AdvMEA	64.3±9.4	64.2±5.4	64.0±6.3	62.5±3.1	61.6±3.1
CEGA	74.8±1.2	78.7±0.7	78.7±0.4	79.1±0.2	78.9±0.3
Realistic	67.1±1.7	74.2±0.6	76.7±1.0	75.7±0.4	76.0±0.8
DFEA_I	78.2±0.2	78.5±0.3	78.5±0.2	78.4±0.4	78.7±0.2
DFEA_II	78.7±0.5	78.9±0.5	79.7±0.4	79.6±0.4	79.1±0.2
DFEA_III	78.3±0.1	78.5±0.4	78.8±0.1	78.9±0.1	78.9±0.2

(c) Regime=a_only

Attack	0.05	0.10	0.25	0.50	1.00
MEA0	71.1±0.9	76.3±0.6	77.3±1.0	78.4±0.5	78.3±0.6
MEA1	68.6±2.3	70.6±5.0	74.8±3.4	75.3±3.5	75.5±3.9
MEA2	68.9±2.0	73.4±0.9	75.8±1.5	77.4±0.1	77.8±0.2
MEA3	70.7±3.4	73.8±1.3	77.7±0.4	77.6±0.4	79.1±0.5
MEA4	54.4±7.9	71.4±0.5	76.6±1.2	78.0±1.0	78.8±1.0
MEA5	72.1±3.5	76.9±1.0	77.6±1.1	77.8±0.9	77.8±0.9
AdvMEA	59.3±7.4	63.2±6.2	62.5±5.0	63.6±2.0	63.8±2.6
CEGA	74.9±2.4	77.7±1.3	78.3±0.5	78.9±0.5	78.8±0.3
Realistic	69.6±1.5	72.7±0.8	74.9±0.6	76.5±0.9	76.6±0.4
DFEA_I	78.2±0.2	78.5±0.3	78.5±0.2	78.4±0.4	78.7±0.2
DFEA_II	78.7±0.5	78.9±0.5	79.7±0.4	79.6±0.4	79.1±0.2
DFEA_III	78.3±0.1	78.5±0.4	78.8±0.1	78.9±0.1	78.9±0.2

(d) Regime=data_free

Attack	0.05	0.10	0.25	0.50	1.00
MEA0	33.1±10.7	41.3±0.0	40.9±0.3	40.9±0.3	40.9±0.3
MEA1	41.3±0.0	41.3±0.0	41.3±0.0	41.3±0.0	41.3±0.0
MEA2	70.4±1.3	73.2±0.7	76.2±0.2	77.2±0.3	77.8±0.2
MEA3	38.3±3.8	33.3±10.8	33.5±11.0	40.9±0.3	40.9±0.3
MEA4	40.7±0.0	33.1±10.7	33.3±10.8	33.3±10.8	41.1±0.3
MEA5	18.1±0.1	40.9±0.3	26.0±10.4	25.6±10.7	41.2±0.4
AdvMEA	62.1±6.5	66.9±1.9	65.3±4.1	62.0±6.2	62.7±3.6
CEGA	75.7±2.4	78.0±1.1	78.6±0.4	78.5±0.4	78.6±0.3
Realistic	76.1±0.6	77.2±0.4	76.6±0.5	76.2±0.8	75.9±0.5
DFEA_I	78.2±0.2	78.5±0.3	78.5±0.2	78.4±0.4	78.7±0.2
DFEA_II	78.7±0.5	78.9±0.5	79.7±0.4	79.6±0.4	79.1±0.2
DFEA_III	78.3±0.1	78.5±0.4	78.8±0.1	78.9±0.1	78.9±0.2

Table 30: RQ1 detailed for dataset=PubMed, metric=F1 (%). Rows are attacks; columns are budgets. Mean ± std across seeds; best per column is bold.

(a) Regime=both

Attack	0.05	0.10	0.25	0.50	1.00
MEA0	68.2±2.8	74.7±1.4	76.3±0.2	76.0±0.5	77.2±0.4
MEA1	50.2±1.7	68.3±6.2	74.0±3.5	74.6±3.5	74.9±3.9
MEA2	65.4±1.0	69.5±0.5	74.4±1.2	76.7±0.6	77.2±0.3
MEA3	70.3±2.3	72.2±2.0	75.4±0.5	78.0±0.9	76.3±1.6
MEA4	64.4±3.3	66.2±7.9	73.8±0.7	76.8±0.6	77.0±0.7
MEA5	71.3±3.0	74.1±0.5	76.5±0.9	76.7±0.5	77.1±1.2
AdvMEA	55.6±1.7	65.8±2.1	64.8±2.6	60.9±8.1	63.9±1.7
CEGA	77.3±0.3	76.9±1.5	77.4±0.1	78.3±0.1	77.7±0.6
Realistic	71.9±1.0	70.6±1.2	73.9±0.1	74.6±1.7	76.2±0.7
DFEA_I	77.5±0.2	77.8±0.3	77.7±0.2	77.7±0.4	78.0±0.2
DFEA_II	78.0±0.5	78.5±0.6	79.1±0.4	79.0±0.4	78.4±0.3
DFEA_III	77.6±0.1	77.8±0.4	78.0±0.1	78.2±0.2	78.2±0.1

(b) Regime=x_only

Attack	0.05	0.10	0.25	0.50	1.00
MEA0	70.7±4.1	75.7±0.8	75.9±1.4	77.2±0.4	77.5±0.6
MEA1	50.2±1.7	68.3±6.2	74.0±3.5	74.6±3.5	74.9±3.9
MEA2	64.3±0.6	71.1±1.1	74.9±1.1	76.9±0.6	77.2±0.3
MEA3	71.6±1.3	74.1±1.4	75.7±0.8	76.3±0.7	76.9±0.9
MEA4	46.5±5.0	62.1±7.7	75.3±1.6	75.8±0.8	77.0±0.8
MEA5	68.2±2.9	73.0±0.5	75.5±2.1	76.5±0.3	76.6±0.8
AdvMEA	62.3±11.3	63.1±5.7	61.3±6.6	59.8±2.0	60.4±2.9
CEGA	74.4±0.9	77.8±0.6	77.8±0.4	78.2±0.2	78.1±0.3
Realistic	66.1±1.2	72.6±0.3	76.1±0.8	75.3±0.4	75.4±0.7
DFEA_I	77.5±0.2	77.8±0.3	77.7±0.2	77.7±0.4	78.0±0.2
DFEA_II	78.0±0.5	78.5±0.6	79.1±0.4	79.0±0.4	78.5±0.2
DFEA_III	77.6±0.1	77.8±0.4	78.0±0.1	78.2±0.2	78.2±0.1

(c) Regime=a_only

Attack	0.05	0.10	0.25	0.50	1.00
MEA0	68.6±2.2	75.3±0.5	76.0±1.3	77.4±0.5	77.5±0.4
MEA1	50.2±1.7	68.3±6.2	74.0±3.5	74.6±3.5	74.9±3.9
MEA2	63.3±2.6	70.2±1.8	74.3±1.8	76.6±0.3	77.2±0.3
MEA3	68.8±5.0	72.9±1.2	76.4±0.6	76.4±0.3	78.0±0.5
MEA4	43.5±15.2	69.3±0.5	74.9±1.6	76.5±1.1	77.2±1.0
MEA5	69.1±3.1	75.9±1.0	76.5±1.1	76.8±0.8	76.9±0.8
AdvMEA	56.1±10.3	60.4±7.9	58.8±5.1	62.0±2.4	61.8±1.8
CEGA	74.0±2.1	77.1±1.2	77.4±0.5	77.8±0.5	77.8±0.3
Realistic	69.0±0.9	71.2±1.9	74.6±0.6	75.7±0.9	76.1±0.3
DFEA_I	77.5±0.2	77.8±0.3	77.7±0.2	77.7±0.4	78.0±0.2
DFEA_II	78.0±0.4	78.5±0.6	79.1±0.4	79.0±0.4	78.5±0.2
DFEA_III	77.6±0.1	77.8±0.4	78.0±0.1	78.2±0.2	78.2±0.1

(d) Regime=data_free

Attack	0.05	0.10	0.25	0.50	1.00
MEA0	16.2±4.3	19.5±0.0	19.4±0.1	19.4±0.1	19.4±0.1
MEA1	19.5±0.0	19.5±0.0	19.5±0.0	19.5±0.0	19.5±0.0
MEA2	65.1±0.8	69.9±0.9	74.7±0.4	76.5±0.4	77.2±0.3
MEA3	20.2±1.2	16.9±4.8	16.4±4.4	19.4±0.1	19.4±0.1
MEA4	19.3±0.0	16.2±4.3	16.3±4.3	16.3±4.3	19.4±0.1
MEA5	10.3±0.2	19.4±0.1	14.0±3.9	13.3±4.2	20.2±1.2
AdvMEA	59.5±8.3	64.7±1.6	63.6±5.3	60.1±8.6	61.3±3.4
CEGA	75.0±2.2	77.3±1.1	77.8±0.4	77.4±0.4	77.7±0.3
Realistic	75.4±0.4	76.6±0.4	75.9±0.6	75.7±0.7	75.4±0.5
DFEA_I	77.5±0.2	77.8±0.3	77.7±0.2	77.7±0.4	78.0±0.2
DFEA_II	78.0±0.5	78.5±0.6	79.1±0.4	79.0±0.4	78.5±0.2
DFEA_III	77.6±0.1	77.8±0.4	78.0±0.1	78.2±0.2	78.2±0.1

Table 31: RQ1 detailed for dataset=PubMed, metric=Fidelity (%). Rows are attacks; columns are budgets. Mean ± std across seeds; best per column is bold.

(a) Regime=both

Attack	0.05	0.10	0.25	0.50	1.00
MEA0	80.0±0.6	87.1±2.4	90.6±1.8	92.9±0.8	94.2±0.6
MEA1	72.9±2.0	79.0±6.1	81.9±3.4	83.2±4.5	85.3±4.6
MEA2	80.5±2.0	85.3±0.2	91.3±0.6	94.5±0.7	96.8±0.3
MEA3	80.8±2.1	83.3±1.5	87.0±1.4	89.6±0.7	89.7±1.3
MEA4	71.6±1.9	77.7±4.1	83.5±1.1	87.7±0.9	89.1±0.9
MEA5	82.2±4.6	86.4±1.6	89.3±1.3	90.6±1.1	90.9±0.9
AdvMEA	63.5±6.4	70.6±3.6	69.5±4.2	65.1±8.9	69.8±4.5
CEGA	89.5±0.4	89.9±1.3	92.6±0.3	94.4±0.4	94.2±0.3
Realistic	81.2±1.3	83.5±1.1	88.1±1.0	89.5±1.6	91.4±0.8
DFEA_I	94.5±0.3	94.5±0.4	94.6±0.3	94.9±0.3	94.8±0.6
DFEA_II	89.7±1.4	91.1±1.5	92.9±1.3	93.6±1.0	93.5±1.1
DFEA_III	93.5±0.6	93.9±0.7	94.8±0.6	95.2±0.4	95.1±0.4

(b) Regime=x_only

Attack	0.05	0.10	0.25	0.50	1.00
MEA0	82.9±0.9	87.5±1.5	91.7±0.7	92.6±0.3	93.3±1.1
MEA1	72.9±2.0	79.0±6.1	81.9±3.4	83.2±4.5	85.3±4.6
MEA2	78.4±0.8	85.8±0.6	91.6±0.0	94.8±0.4	96.8±0.3
MEA3	82.8±2.2	84.8±2.4	88.7±0.6	88.7±2.3	90.8±0.8
MEA4	52.8±4.6	72.6±5.9	86.0±1.4	87.2±1.4	89.2±0.9
MEA5	80.0±3.1	84.7±2.4	88.0±0.8	89.9±0.8	90.4±0.5
AdvMEA	67.8±11.8	66.1±8.4	65.7±8.6	65.2±6.3	64.1±5.7
CEGA	85.4±2.4	91.0±0.9	93.5±0.4	93.5±1.3	95.3±0.7
Realistic	77.6±3.0	83.8±2.8	88.1±2.9	90.8±0.9	91.7±0.4
DFEA_I	94.5±0.3	94.5±0.4	94.6±0.3	94.9±0.3	94.8±0.6
DFEA_II	89.7±1.4	91.1±1.5	92.9±1.3	93.6±1.0	93.5±1.1
DFEA_III	93.5±0.6	93.9±0.7	94.8±0.6	95.2±0.4	95.1±0.4

(c) Regime=a_only

Attack	0.05	0.10	0.25	0.50	1.00
MEA0	79.6±1.8	89.5±0.4	92.7±0.9	91.8±0.5	93.4±0.6
MEA1	72.9±2.0	79.0±6.1	81.9±3.4	83.2±4.5	85.3±4.6
MEA2	77.7±2.2	84.8±0.8	91.1±0.8	94.6±0.4	96.8±0.3
MEA3	79.1±2.3	84.5±1.3	88.1±0.9	89.3±0.4	90.7±0.2
MEA4	59.3±7.1	78.5±1.7	84.9±1.5	86.8±1.5	89.2±0.9
MEA5	80.9±2.2	86.6±1.4	89.4±0.4	89.8±0.8	90.6±0.4
AdvMEA	59.0±9.8	66.2±9.0	66.4±8.2	69.1±3.4	65.6±4.6
CEGA	84.7±2.2	91.8±1.3	93.2±0.4	93.0±1.2	94.8±0.5
Realistic	79.7±2.2	82.7±2.3	89.0±0.7	91.0±1.3	92.4±1.6
DFEA_I	94.5±0.3	94.5±0.4	94.6±0.3	94.9±0.3	94.8±0.6
DFEA_II	89.7±1.3	91.0±1.4	92.9±1.3	93.6±1.0	93.5±1.1
DFEA_III	93.5±0.6	93.9±0.7	94.8±0.6	95.2±0.4	95.1±0.4

(d) Regime=data_free

Attack	0.05	0.10	0.25	0.50	1.00
MEA0	30.7±9.8	45.5±0.5	40.0±3.6	40.0±3.6	40.0±3.6
MEA1	45.5±0.5	45.5±0.5	45.5±0.5	45.5±0.5	45.5±0.5
MEA2	78.4±1.4	84.7±0.9	91.0±0.5	94.9±0.5	96.8±0.3
MEA3	37.6±6.1	32.8±11.7	36.0±13.6	40.0±3.6	40.0±3.6
MEA4	37.7±0.5	31.0±10.0	33.7±12.4	33.4±12.1	43.2±3.6
MEA5	16.9±0.1	40.0±3.6	24.4±9.8	23.6±9.5	43.4±3.7
AdvMEA	63.9±8.6	70.4±2.9	69.9±6.7	64.5±8.3	64.1±6.5
CEGA	87.2±2.8	90.9±1.0	93.4±0.6	93.8±0.3	94.4±0.2
Realistic	92.2±1.3	92.3±0.2	92.1±1.0	91.4±0.9	92.1±1.3
DFEA_I	94.5±0.3	94.5±0.4	94.6±0.3	94.9±0.3	94.8±0.6
DFEA_II	89.7±1.4	91.1±1.5	92.9±1.3	93.6±1.0	93.5±1.1
DFEA_III	93.5±0.6	93.9±0.7	94.8±0.6	95.2±0.4	95.1±0.4

E.1.1 Seed sensitivity of data-free extraction

For `DFEA_II` on *Computers*, the original three seeds at budgets $0.10\times$ through $1.00\times$ each produced a surrogate that predicted a single class. A constant predictor's accuracy equals the frequency of that class in the test labels, whereas its fidelity equals the frequency in the target's predictions. The repeated means in Table 1 therefore reflect these seeds rather than duplicate log entries. The ten-seed rerun below reports fidelity across all seeds, including collapsed runs.

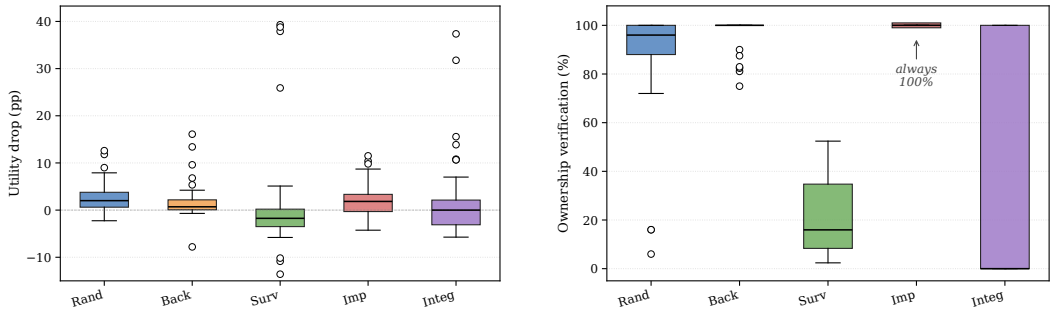
Table 32: DFEA_II fidelity on Computers (mean $\pm$ SD, %).

Budget	Unique queries	Original (3 seeds)	Audit (10 seeds)	Collapsed
$0.05\times$	687	43.9 ± 8.1	47.2 ± 14.6	3/10
$0.10\times$	1,375	28.4 ± 20.5	50.7 ± 21.0	3/10
$0.25\times$	3,438	28.4 ± 20.5	48.2 ± 23.6	4/10
$0.50\times$	6,876	28.4 ± 20.5	44.3 ± 22.6	5/10
$1.00\times$	13,752	28.4 ± 20.5	44.1 ± 23.9	6/10

E.2 Defense performance results

This subsection contains the per-dataset defense performance and the boxplot view that the main text references. Figure 5 aggregates utility drop and ownership verification across all ten datasets and three seeds (30 points per defense except Integrity (44 dataset–seed pairs)), and the per-dataset numbers follow. Table 33 reports task utility measured by macro F1 (%); Table 34 reports behavioural alignment with the original target measured by fidelity (%) on the same test inputs; Table 35 summarises ownership verification on a standardised verification set. Together these views separate downstream utility, behavioural consistency, and ownership verification, so that the trade-offs across defenses are explicit on every dataset.

Watermark profile across six axes. Tables 33–35 report the three primary metrics separately. To make the trade-offs across the five watermarking and integrity defenses visible at a glance, Figure 6 reports the same numbers as a radar chart together with two efficiency axes (training time and peak memory, both inverted to a higher-is-better score on a log scale to match the other axes). Three patterns become explicit which the per-metric tables only show implicitly. *First*, no defense dominates on every axis. `BackdoorWM` encloses the largest area on the verification, fidelity, and utility axes but sits in the middle of the speed and memory axes. The radar axes summarize performance and compute costs separately. `ImperceptibleWM` achieves perfect verification at the cost of being the slowest and heaviest defense, which gives it a visibly indented profile on the speed and memory axes. *Second*, `SurviveWM` keeps utility almost unchanged but loses on the verification axis, which is consistent with the bimodal verification numbers in Table 35; this is a clear stability–verification trade-off rather than a generic weakness. *Third*, the gap between `RandomWM` and the other watermarks is structural rather than a per-dataset artefact: `RandomWM` loses on every metric except utility, which suggests the random-graph watermark is not competitive with trigger-based or query-based mechanisms under our protocol.



(a) Utility drop.

(b) Ownership verification.

Figure 5: Defense effectiveness across all ten datasets: (a) utility drop and (b) ownership verification. Each box aggregates one point per (dataset, seed), giving 30 points per defense except Integrity (44 dataset–seed pairs).

Dataset	backdoorwm	randomwm	survivewm	imperceptiblewm	integrity
Cora	79.37 ± 0.45	76.06 ± 0.81	79.07 ± 0.33	71.94 ± 0.27	75.39 ± 0.36
CiteSeer	64.74 ± 0.35	64.99 ± 0.69	67.47 ± 0.27	58.07 ± 0.79	57.61 ± 0.38
PubMed	77.00 ± 0.59	73.77 ± 0.26	25.32 ± 1.19	76.00 ± 0.17	75.68 ± 0.37
Computers	55.39 ± 2.89	58.49 ± 2.93	37.62 ± 24.96	67.04 ± 1.66	37.70 ± 19.20
Photo	57.47 ± 2.27	52.15 ± 5.30	58.47 ± 3.84	61.90 ± 0.43	51.05 ± 11.55
CoauthorCS	69.13 ± 1.21	66.09 ± 6.69	72.75 ± 0.46	72.52 ± 0.73	73.43 ± 0.32
CoauthorPhysics	76.23 ± 1.03	57.32 ± 12.15	81.11 ± 0.89	80.50 ± 0.75	80.91 ± 0.81

Table 33: Defense results: F1 (mean $\pm$ std, in %).

Dataset	backdoorwm	randomwm	survivewm	imperceptiblewm	integrity
Cora	80.07 ± 0.40	76.13 ± 1.17	79.93 ± 0.26	71.97 ± 0.31	76.03 ± 0.37
CiteSeer	67.47 ± 0.40	67.90 ± 0.57	70.87 ± 0.12	60.30 ± 1.00	60.10 ± 0.29
PubMed	77.60 ± 0.79	74.13 ± 0.26	39.17 ± 1.01	76.37 ± 0.12	76.33 ± 0.38
Computers	68.27 ± 2.74	71.47 ± 2.49	45.97 ± 31.21	78.90 ± 0.73	11.97 ± 5.56
Photo	92.73 ± 1.50	85.33 ± 6.07	93.20 ± 3.89	96.70 ± 0.08	61.80 ± 20.58
CoauthorCS	88.43 ± 0.77	89.27 ± 2.46	91.70 ± 0.36	89.63 ± 0.76	90.97 ± 0.12
CoauthorPhysics	89.33 ± 0.37	68.60 ± 10.96	90.97 ± 0.33	90.20 ± 0.40	90.60 ± 0.65

Table 34: Defense results: Fidelity (mean $\pm$ std, in %).

Dataset	backdoorwm	randomwm	survivewm	imperceptiblewm	integrity
Cora	100.00 ± 0.00	75.33 ± 9.98	54.07 ± 5.79	100.00 ± 0.00	100.00 ± 0.00
CiteSeer	100.00 ± 0.00	72.00 ± 4.32	55.72 ± 4.51	100.00 ± 0.00	100.00 ± 0.00
PubMed	100.00 ± 0.00	64.00 ± 11.31	34.97 ± 0.71	100.00 ± 0.00	100.00 ± 0.00
Computers	93.33 ± 9.43	94.67 ± 1.89	11.08 ± 0.81	100.00 ± 0.00	20.00 ± 40.00
Photo	100.00 ± 0.00	98.67 ± 0.94	13.25 ± 1.10	100.00 ± 0.00	10.00 ± 30.00
CoauthorCS	100.00 ± 0.00	45.33 ± 3.77	8.51 ± 0.34	100.00 ± 0.00	33.33 ± 47.14
CoauthorPhysics	100.00 ± 0.00	56.67 ± 13.70	21.76 ± 0.49	100.00 ± 0.00	66.67 ± 47.14

Table 35: Target-side verification (mean $\pm$ SD, %). For Integrity this is the bit-flip detection rate, not fingerprint self-agreement. Integrity uses ten seeds on Computers and Photo.

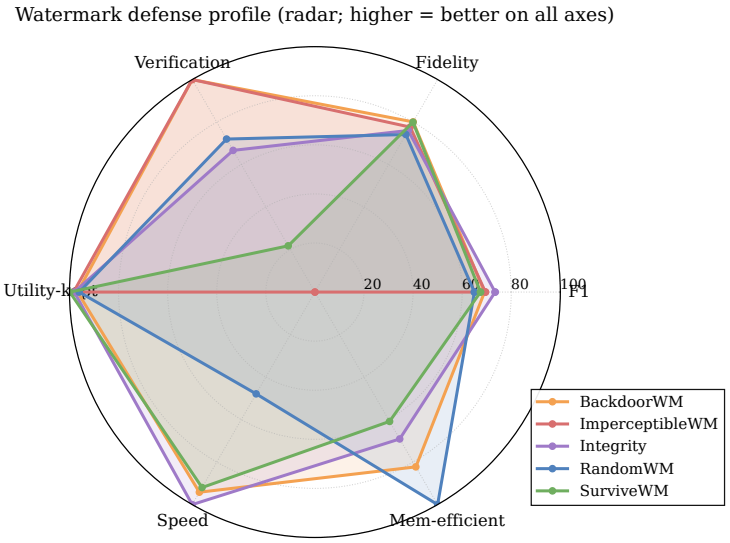


Figure 6: Radar profile of the five watermarking and integrity defenses across six axes. F1, fidelity, verification, and utility-kept come from Tables 33–35; speed and memory-efficiency are obtained from the RQ4 numbers (Tables 4–5 and Figure 8) by inverting and log-normalising to a 0–100 scale. Higher is better on every axis. No defense dominates; `BackdoorWM` is the largest envelope, `ImperceptibleWM` pays for perfect verification with the worst speed and memory profile.

E.2.1 Integrity target training

For `Integrity`, we apply the bit-flip verifier to a copy of the model so that it cannot modify the target subsequently queried by the attacker. On *Computers* and *Photo*, we also aligned the optimizer with the shared configuration (learning rate 0.01, weight decay 5×10^{-4}). Across ten seeds on each dataset, target accuracy was 44.5% and 86.4%, respectively, with no constant-class targets. The remaining eight datasets use the isolated verifier with three seeds.

Table 36: Integrity target accuracy (%) before and after optimizer alignment.

Dataset	Original accuracy	Aligned accuracy	Collapsed after alignment
Computers	16.5	44.5	0/10
Photo	49.1	86.4	0/10

E.3 Baseline utility across backbones

To allow utility-drop numbers in the main text to be compared across defenses that use different backbones, Table 37 reports the test accuracy of an undefended target on each of the ten datasets and for each of the three backbones used in the benchmark. The first column reports a DGL GCN with hidden dimension 16, which is the backbone used by every original watermarking defense and by every information-limiting defense. The second column reports a DGL GraphSAGE with hidden dimension 128, which is the backbone used by `RandomWM`. The third column reports a PyG GCN with hidden dimension 128, which is the backbone used by `ImperceptibleWM`.

The baseline-utility table reveals one pattern that has direct consequences for any cross-defense comparison in the main text: the per-dataset gap between the two backbones used by watermark methods can be huge, and it is largest exactly on the graphs where defenses are evaluated as "most informative". On *RomanEmpire*, the GraphSAGE-128 baseline of $77.5\,\%$ is 34.7 pp higher than the GCN-16 baseline of $42.8\,\%$; on *Computers* the gap is 15.2 pp; on *OGBN-Arxiv* it is 17.2 pp. This means that any utility-drop number in the main text that compares `RandomWM` (GraphSAGE-128) against the GCN-16 baseline implicitly attributes the entire backbone gap to the defense, which would over-estimate `RandomWM`'s damage by 15–35 pp on these three graphs; we therefore always compare each defense against its own matched-backbone baseline rather than against a single shared GCN baseline.

E.4 Attack effectiveness on the three additional datasets

We report the per-attack and per-budget fidelity for all twelve attacks on the three additional graphs (RomanEmpire, AmazonRatings, OGBN-Arxiv) in the four regimes. Constant values across budgets reflect attacks whose surrogate is independent of the query budget (e.g., the data-free `DFEA` variants, which always train on the same synthesized queries).

E.5 Standard deviations for information-limiting defenses

Tables 41–42 extend Table 3 of the main text with standard deviations for each protected-model accuracy and verification proxy. The seven defenses are split across two tables for readability: the four output-perturbation / prediction-rounding defenses are in Table 41, and the three query-detection defenses are in Table 42.

Heatmap view of the seven information-limiting defenses. Figure 7 reports the same numbers as Tables 41–42 as a 10×7 heatmap, with protected-model accuracy on the left panel and the verification proxy on the right panel. The two-panel view exposes three patterns which are not visible in the per-defense tables. *First, the verification proxy clusters into two regimes.* The four output-perturbation and rounding defenses (`OP_low`, `OP_high`, `PR_2bit`, `PR_top1`) plus `GradRedir` verify at $\geq 80\%$ on every dataset, while the two query-detection defenses (`PRADA`, `AdaptMisinfo`) verify at $\sim 50\%$ on most homophilic graphs and below 50% on *RomanEmpire*; this is consistent with the joint-evaluation behaviour reported in Appendix E.8, where the same two defenses are also the strongest at reducing surrogate fidelity. *Second, the accuracy panel is largely flat across defenses on the eight non-Computers datasets.* The output-perturbation methods leave protected

Table 37: Baseline utility (test accuracy, %) for an undefended target across three backbones. Mean ± standard deviation over three seeds.

Dataset	GCN (DGL, hidden=16)	GraphSAGE (DGL, hidden=128)	GCN (PyG, hidden=128)
Cora	79.4 ± 0.5	79.1 ± 0.3	80.7 ± 0.4
CiteSeer	67.8 ± 1.1	70.1 ± 0.2	70.9 ± 0.4
PubMed	78.0 ± 0.6	77.1 ± 0.3	79.5 ± 0.2
Computers	44.6 ± 22.4	59.8 ± 18.4	75.2 ± 0.7
Photo	90.1 ± 4.8	94.5 ± 0.5	95.3 ± 0.2
CoauthorCS	87.4 ± 0.3	92.9 ± 0.3	90.3 ± 0.2
CoauthorPhysics	89.3 ± 0.4	91.2 ± 0.1	89.8 ± 0.2
OGBN-Arxiv	37.7 ± 3.2	54.9 ± 0.0	52.3 ± 0.1
RomanEmpire	42.8 ± 0.2	77.5 ± 0.5	46.0 ± 0.3
AmazonRatings	41.7 ± 0.3	45.5 ± 0.5	43.4 ± 0.3

Table 38: Detailed RQ1 results on *RomanEmpire*. Fidelity (%) at five budget multipliers across four regimes. Mean ± standard deviation over three seeds.

(a) Regime=`both`

Attack	0.05	0.10	0.25	0.50	1.00
MEA0	72.9±0.4	75.9±1.7	77.0±0.8	77.2±1.5	77.4±1.5
MEA1	54.0±2.2	59.7±3.5	68.7±1.1	72.6±1.0	77.4±1.5
MEA2	27.0±0.1	34.0±1.3	47.8±0.7	49.8±1.9	32.7±9.8
MEA3	61.2±1.0	65.2±1.1	74.1±1.1	77.2±1.6	77.4±1.5
MEA4	63.6±1.0	70.9±2.1	73.3±2.6	76.0±1.1	77.4±1.5
MEA5	65.8±1.2	70.0±0.9	76.7±1.2	77.6±1.0	77.4±1.5
AdvMEA	22.0±6.5	23.5±6.5	21.9±6.2	19.1±3.3	15.7±3.7
CEGA	72.1±0.5	73.3±1.2	73.4±2.3	71.4±2.1	71.4±2.1
Realistic	53.7±2.3	57.5±2.1	58.2±1.5	57.9±1.9	75.4±1.9
DFEA_I	71.7±1.1	71.4±2.1	72.1±2.7	72.3±2.7	72.7±2.2
DFEA_II	69.2±0.7	74.9±0.5	80.8±1.0	83.3±0.4	84.3±0.3
DFEA_III	73.4±0.3	76.2±0.6	75.7±2.1	77.2±1.1	77.3±1.4

(b) Regime=`x_only`

Attack	0.05	0.10	0.25	0.50	1.00
MEA0	72.5±1.1	76.5±0.6	75.8±2.6	77.4±0.6	77.4±1.5
MEA1	54.0±2.2	59.7±3.5	68.7±1.1	72.6±1.0	77.4±1.5
MEA2	26.9±0.6	33.4±0.3	47.1±1.4	47.3±2.5	32.7±9.8
MEA3	61.2±0.4	65.2±0.9	74.3±1.1	77.4±1.4	77.4±1.5
MEA4	63.8±0.4	70.9±2.1	73.4±2.6	76.0±1.1	77.4±1.5
MEA5	65.9±0.5	69.9±0.3	76.1±2.5	77.2±1.5	77.4±1.5
AdvMEA	23.2±7.3	23.0±7.1	21.5±4.3	19.3±3.8	16.2±3.9
CEGA	72.1±1.3	72.0±2.9	73.6±2.9	71.4±2.1	71.4±2.1
Realistic	54.4±1.5	56.7±1.7	58.3±2.0	57.9±2.0	75.7±1.8
DFEA_I	71.7±1.1	71.4±2.1	72.1±2.7	72.3±2.7	72.7±2.2
DFEA_II	69.2±0.7	74.9±0.5	80.8±1.0	83.3±0.4	84.3±0.3
DFEA_III	73.4±0.3	76.2±0.6	75.7±2.1	77.2±1.1	77.3±1.4

(c) Regime=`a_only`

Attack	0.05	0.10	0.25	0.50	1.00
MEA0	73.3±0.8	75.4±0.3	77.4±0.4	77.3±1.7	77.4±1.5
MEA1	54.0±2.2	59.7±3.5	68.7±1.1	72.6±1.0	77.4±1.5
MEA2	25.5±1.2	33.7±0.2	47.7±0.8	50.5±2.1	32.7±9.8
MEA3	62.1±1.3	66.7±0.4	75.2±0.7	77.4±1.7	77.4±1.5
MEA4	63.3±1.0	70.6±2.4	73.4±2.5	76.0±1.1	77.4±1.5
MEA5	65.5±0.4	70.3±1.0	76.7±1.3	77.5±1.1	77.4±1.5
AdvMEA	22.4±6.5	22.8±5.9	20.8±6.3	17.8±4.2	15.1±4.1
CEGA	71.5±2.6	72.9±2.9	73.4±2.7	71.4±2.1	71.4±2.1
Realistic	55.3±2.2	58.1±1.0	56.8	58.1±1.9	75.7±1.7
DFEA_I	71.7±1.1	71.4±2.1	72.1±2.7	72.3±2.7	72.7±2.2
DFEA_II	69.2±0.7	74.9±0.5	80.8±1.0	83.3±0.4	84.3±0.3
DFEA_III	73.4±0.3	76.2±0.6	75.7±2.1	77.2±1.1	77.3±1.4

(d) Regime=`data_free`

Attack	0.05	0.10	0.25	0.50	1.00
MEA0	72.8±1.1	74.7±1.3	76.0±1.5	76.9±2.1	77.4±1.5
MEA1	54.0±2.2	59.7±3.5	68.7±1.1	72.6±1.0	77.4±1.5
MEA2	26.4±0.5	33.8±0.8	47.4±0.5	51.1±2.1	32.7±9.8
MEA3	62.6±0.3	65.8±0.7	74.0±1.5	77.2±1.5	77.4±1.5
MEA4	63.1±1.1	71.1±1.7	73.3±2.3	75.8±1.5	77.4±1.5
MEA5	64.8±1.2	69.5±1.0	76.2±2.3	77.2±1.3	77.4±1.5
AdvMEA	23.4±6.6	23.0±7.1	21.7±6.9	18.3±4.6	15.3±4.4
CEGA	71.2±2.2	73.0±1.9	73.3±2.7	71.4±2.1	71.4±2.1
Realistic	54.4±2.3	56.3±2.4	58.3±1.4	57.8±2.5	75.6±1.6
DFEA_I	71.7±1.1	71.4±2.1	72.1±2.7	72.3±2.7	72.7±2.2
DFEA_II	69.2±0.7	74.9±0.5	80.8±1.0	83.3±0.4	84.3±0.3
DFEA_III	73.4±0.3	76.2±0.6	75.7±2.1	77.2±1.1	77.3±1.4

accuracy within ~ 2 pp of the undefended baseline on *Cora*, *CiteSeer*, *PubMed*, *Photo*, *CoauthorCS*, *CoauthorPhysics*, *OGBN-Arxiv*, and *AmazonRatings*, which means the protection signal in those rows is carried entirely by the verification panel. *Third, Computers is the only dataset where the accuracy panel is heterogeneous*: every defense produces high variance, and three defenses (`OP_high`, `PR_2bit`, `AdaptMisinfo`) push protected accuracy below 40%, which mirrors the high variance of the same dataset in Tables 33–34 and is consistent with the structural-property analysis (high average degree) in Appendix E.10.

E.6 Peak GPU memory of attacks and defenses (RQ4)

Figure 8 reports the peak GPU memory of every attack (panel a) and every defense (panel b) on a symmetric-log y-axis, aggregated over all ten datasets. The symlog scale is necessary because the workloads span more than two orders of magnitude on the same axis: `MEA0`, `CEGA`, and the lightweight defenses sit near 0.05–0.1 GB, while `MEA2`, `Realistic`, the `DFEA` family, and `ImperceptibleWM` reach several gigabytes. Two findings supplement the time-based discussion in the main text. *First, peak memory is a more discriminative signal than wall-clock time for separating attack families.* The fast `MEA0/1/3/4/5/CEGA` group is tightly clustered around 0.05–0.15 GB across every dataset, while the data-free `DFEA` family and `Realistic` sit at 1–5 GB; the within-group variance is much smaller than the between-group gap, which means an operator who watches GPU memory can infer the attack family without timing the queries. *Second, the watermarking-versus-information-limiting*

Table 39: Detailed RQ1 results on *AmazonRatings*. Fidelity (%) at five budget multipliers across four regimes. Mean ± standard deviation over three seeds.

(a) Regime=`both`

Attack	0.05	0.10	0.25	0.50	1.00
MEA0	92.3±0.6	93.1±1.4	93.8±0.7	93.9±0.5	94.4±1.0
MEA1	88.8±1.0	91.9±0.5	94.2±0.6	94.8±0.7	94.4±1.0
MEA2	82.0±1.4	87.3±0.6	92.4±0.8	93.9±1.3	94.5±0.5
MEA3	88.0±0.7	91.2±1.3	93.8±1.3	94.6±1.0	94.4±1.0
MEA4	85.1±0.4	87.1±0.5	90.1±0.8	92.4±1.1	94.4±1.0
MEA5	89.9±0.6	91.4±1.1	94.7±0.9	94.5±0.9	94.4±1.0
AdvMEA	70.4±1.5	66.2±7.3	68.7±3.4	70.1±1.3	66.9±5.4
CEGA	87.1±0.9	87.3±1.2	89.1±1.2	89.7±2.0	89.7±2.0
Realistic	89.9±2.7	90.8±3.0	90.6±2.6	92.8±1.0	94.9±0.3
DFEA_I	88.6±1.1	89.2±2.3	89.6±1.7	89.6±1.4	89.4±1.3
DFEA_II	90.4±1.2	92.6±0.6	94.5±0.7	95.1±0.6	95.6±0.2
DFEA_III	92.4±0.9	93.5±1.2	94.6±0.5	94.5±0.6	94.5±0.7

(b) Regime=`x_only`

Attack	0.05	0.10	0.25	0.50	1.00
MEA0	92.1±0.6	93.5±0.9	94.1±1.2	94.3±0.9	94.4±1.0
MEA1	88.8±1.0	91.9±0.5	94.1±0.7	94.8±0.7	94.4±1.0
MEA2	82.7±1.5	86.9±1.7	91.8±0.9	93.7±1.3	94.5±0.5
MEA3	87.4±2.1	90.5±1.3	93.8±0.4	94.6±1.1	94.4±1.0
MEA4	85.8±0.5	86.7±0.5	90.1±0.8	92.4±1.1	94.4±1.0
MEA5	89.1±1.4	92.0±1.2	94.4±0.6	94.2±0.9	94.4±1.0
AdvMEA	69.1±2.4	68.0±5.5	69.5±1.7	65.3±7.2	67.0±4.1
CEGA	88.2±0.7	87.4±1.1	89.5±1.7	89.7±2.0	89.7±2.0
Realistic	90.7±1.9	91.0±2.4	92.2±1.0	93.5±0.5	94.9±0.4
DFEA_I	88.6±1.1	89.2±2.3	89.6±1.7	89.6±1.4	89.4±1.3
DFEA_II	90.4±1.2	92.5±0.6	94.5±0.7	95.1±0.6	95.6±0.2
DFEA_III	92.4±1.0	93.5±1.2	94.6±0.5	94.4±0.7	94.5±0.7

(c) Regime=`a_only`

Attack	0.05	0.10	0.25	0.50	1.00
MEA0	92.3±0.6	93.0±0.7	94.6±0.9	94.2±0.9	94.4±1.0
MEA1	88.8±1.0	91.9±0.5	94.1±0.7	94.8±0.7	94.4±1.0
MEA2	82.2±0.7	87.0±1.8	92.2±0.8	94.1±1.2	94.5±0.5
MEA3	88.6±0.1	90.7±1.2	94.0±0.9	94.7±1.1	94.4±1.0
MEA4	85.3±0.3	87.2±0.4	90.1±0.8	92.4±1.1	94.4±1.0
MEA5	89.4±0.9	91.5±1.7	94.3±0.8	94.5±1.0	94.4±1.0
AdvMEA	70.4±1.5	69.5±3.0	67.3±5.8	63.9±9.1	68.2±3.5
CEGA	87.5±1.2	88.8±1.9	88.8±2.0	89.7±2.0	89.7±2.0
Realistic	89.5±2.2	92.3±0.7	92.7±1.0	93.6±0.3	95.0±0.3
DFEA_I	88.6±1.1	89.2±2.3	89.6±1.7	89.6±1.4	89.4±1.3
DFEA_II	90.4±1.3	92.5±0.6	94.5±0.7	95.2±0.5	95.6±0.2
DFEA_III	92.4±0.9	93.5±1.3	94.6±0.5	94.5±0.6	94.5±0.7

(d) Regime=`data_free`

Attack	0.05	0.10	0.25	0.50	1.00
MEA0	91.7±0.5	93.3±1.0	93.5±0.7	94.3±0.9	94.4±1.0
MEA1	88.8±1.0	91.9±0.5	94.1±0.7	94.8±0.7	94.4±1.0
MEA2	81.8±0.9	86.6±0.7	91.9±1.0	93.9±1.0	94.5±0.6
MEA3	87.9±0.5	91.0±1.5	94.0±1.0	94.6±1.0	94.4±1.0
MEA4	85.4±0.4	87.0±0.6	90.1±0.8	92.4±1.1	94.4±1.0
MEA5	89.5±1.0	91.5±1.6	94.4±0.7	94.6±0.9	94.4±1.0
AdvMEA	70.0±2.0	67.3±5.0	68.0±3.5	64.7±8.0	67.5±4.0
CEGA	87.6±1.0	87.8±1.5	89.1±1.5	89.7±2.0	89.7±2.0
Realistic	89.7±2.4	91.5±2.0	91.7±1.5	93.0±0.7	94.9±0.4
DFEA_I	88.6±1.1	89.2±2.3	89.6±1.7	89.6±1.4	89.4±1.3
DFEA_II	90.3±1.3	92.6±0.6	94.5±0.7	95.2±0.5	95.6±0.2
DFEA_III	92.4±1.0	93.5±1.2	94.6±0.5	94.4±0.7	94.5±0.7

Table 40: Detailed RQ1 results on *OGBN-Arxiv*. Fidelity (%) at five budget multipliers across four regimes. Mean ± standard deviation over three seeds. The 169,343-node graph requires sub-sampled edge construction at large budgets for the `Realistic` attack and the data-free variants.

(a) Regime=`both`

Attack	0.05	0.10	0.25	0.50	1.00
MEA0	77.2±4.2	77.4±4.7	77.1±4.6	77.2±4.7	77.2±4.8
MEA1	74.2±1.2	79.0±1.3	81.7±2.9	81.6±3.4	77.2±4.8
MEA2	52.8±3.6	52.8±3.6	52.8±3.6	52.8±3.6	52.8±3.6
MEA3	64.0±4.5	66.9±5.4	74.2±5.1	77.5±4.8	77.3±4.8
MEA4	62.2±4.8	63.2±5.2	65.5±6.0	70.6±4.9	77.1±5.1
MEA5	64.9±4.1	69.5±4.8	77.2±4.8	77.6±4.4	77.3±4.8
AdvMEA	26.9±22.7	28.7±21.1	26.2±21.2	23.0±17.1	20.4±17.2
CEGA	77.9±3.0	77.7±4.1	77.4±4.6	75.5±4.2	75.5±4.2
Realistic	74.5±3.7	74.4±2.7	75.3±2.7	75.6±3.0	75.0±3.2
DFEA_I	80.7±4.5	80.8±4.6	81.0±4.2	81.1±4.0	81.0±3.9
DFEA_II	75.1±1.2	76.0±1.6	76.4±1.5	76.3±1.3	76.7±1.3
DFEA_III	76.9±4.5	77.6±4.4	77.7±4.6	77.6±4.5	77.1±4.7

(b) Regime=`x_only`

Attack	0.05	0.10	0.25	0.50	1.00
MEA0	76.6±4.7	77.5±4.6	77.4±4.1	77.3±4.8	77.2±4.8
MEA1	74.2±1.2	79.0±1.2	81.7±2.9	81.6±3.4	77.3±4.8
MEA2	52.8±3.5	52.8±3.6	52.8±3.6	52.8±3.6	52.8±3.6
MEA3	64.5±4.8	67.3±4.7	74.3±4.8	77.4±4.8	77.2±4.8
MEA4	62.6±4.8	63.3±5.1	65.4±5.6	70.6±5.0	77.1±5.0
MEA5	64.8±4.6	69.4±4.8	77.2±4.8	77.5±4.7	77.2±4.8
AdvMEA	20.7±20.4	23.1±21.9	24.9±23.1	22.7±23.9	18.8±16.7
CEGA	77.6±4.9	78.0±4.8	77.1±5.1	75.5±4.2	75.5±4.2
Realistic	73.9±2.5	74.9±1.9	74.9±2.4	75.6±3.0	75.0±3.1
DFEA_I	80.7±4.5	80.7±4.7	81.0±4.2	81.1±4.0	81.0±3.9
DFEA_II	75.1±1.3	76.0±1.3	76.3±1.6	76.3±1.6	76.8±1.2
DFEA_III	76.9±4.5	77.6±4.4	77.7±4.5	77.6±4.5	77.1±4.7

(c) Regime=`a_only`

Attack	0.05	0.10	0.25	0.50	1.00
MEA0	77.1±5.2	77.5±4.3	77.3±4.1	77.1±4.9	77.3±4.8
MEA1	74.2±1.2	79.0±1.2	81.7±2.9	81.6±3.4	77.3±4.8
MEA2	52.8±3.6	52.8±3.6	52.8±3.6	52.8±3.6	52.8±3.6
MEA3	64.1±4.7	67.9±4.9	74.5±4.9	77.5±4.4	77.3±4.8
MEA4	62.6±4.5	63.4±5.6	65.2±6.0	70.6±4.8	77.1±5.0
MEA5	65.3±4.7	69.7±4.4	77.2±4.7	77.3±4.7	77.2±4.8
AdvMEA	23.1±18.5	24.8±18.8	24.4±20.2	24.0±19.1	21.4±16.3
CEGA	77.6±4.5	77.3±4.6	76.7±4.5	75.5±4.2	75.5±4.2
Realistic	74.3±3.3	74.6±2.1	75.2±2.5	74.9±2.3	75.1±3.2
DFEA_I	80.7±4.5	80.7±4.6	81.0±4.2	81.1±4.0	81.0±3.9
DFEA_II	75.0±1.4	75.8±1.4	76.4±1.5	76.5±1.5	76.6±1.3
DFEA_III	76.9±4.5	77.6±4.4	77.7±4.5	77.6±4.5	77.1±4.8

(d) Regime=`data_free`

Attack	0.05	0.10	0.25	0.50	1.00
MEA0	77.2±4.2	77.0±4.7	77.2±4.9	77.3±4.8	77.3±4.8
MEA1	74.2±1.2	79.0±1.3	81.7±2.9	81.6±3.4	77.2±4.8
MEA2	52.8±3.6	52.8±3.6	52.8±3.6	52.8±3.6	52.8±3.6
MEA3	64.4±4.8	66.9±5.0	74.4±4.8	77.4±4.7	77.2±4.8
MEA4	63.0±5.1	63.4±5.5	65.1±6.0	70.1±5.5	77.1±5.0
MEA5	65.0±4.8	69.3±5.0	77.4±4.5	77.6±4.4	77.3±4.8
AdvMEA	30.4±21.8	26.0±20.8	24.4±22.6	22.0±21.7	22.6±18.2
CEGA	77.9±4.8	77.5±4.8	76.7±4.9	75.5±4.2	75.5±4.2
Realistic	74.2±3.1	75.1±3.3	75.4±3.0	74.8±2.2	75.1±3.1
DFEA_I	80.7±4.5	80.8±4.5	81.0±4.2	81.1±4.0	81.0±3.9
DFEA_II	75.2±1.3	76.0±1.3	76.3±1.4	76.6±1.8	76.5±1.5
DFEA_III	76.9±4.5	77.7±4.3	77.7±4.6	77.7±4.5	77.1±4.7

split is sharp on the defense panel. The five watermarking defenses (left of the dashed line) all train an in-model artefact and so allocate proportional buffers (0.1–5 GB depending on the watermarking technique), whereas the seven information-limiting defenses (right of the dashed line) are inference-time wrappers and use less than 0.05 GB on every dataset — they essentially add no memory cost on top of the protected model itself. This explains why output-perturbation defenses are attractive in deployment: they cost nothing in memory while providing the protection summarised in the main text.

Table 41: Detailed results for the four output-perturbation and prediction-rounding defenses across all ten datasets. Each cell reports protected-model accuracy (%) with the verification proxy (%) in parentheses, both as mean ± standard deviation over three seeds. The target backbone is a DGL GCN with hidden dimension 16.

Dataset	`OP_low`	`OP_high`	`PR_2bit`	`PR_top1`
Cora	79.4±0.7 (98.6±0.7)	79.2±1.5 (93.9±1.3)	73.3±0.8 (83.7±0.1)	79.6±0.5 (100.0±0.0)
CiteSeer	67.6±0.8 (97.8±0.6)	66.3±0.8 (91.0±1.5)	53.9±3.4 (70.3±5.1)	68.8±0.4 (100.0±0.0)
PubMed	77.9±0.2 (99.0±0.4)	75.9±0.7 (94.7±0.3)	77.6±0.4 (93.4±1.0)	78.2±0.3 (100.0±0.0)
Computers	44.0±21.1 (89.2±13.0)	37.6±27.0 (55.3±37.8)	36.1±26.4 (61.7±37.1)	34.8±23.6 (100.0±0.0)
Photo	89.1±3.7 (98.9±0.5)	**90.7±5.7** (96.6±3.7)	**90.4±2.6** (96.7±2.1)	**95.5±0.6** (100.0±0.0)
CoauthorCS	87.8±0.1 (99.5±0.2)	88.2±0.7 (98.8±0.4)	87.5±0.8 (98.1±0.7)	88.1±0.7 (100.0±0.0)
CoauthorPhysics	**89.4±0.3** (99.8±0.2)	89.1±0.2 (99.3±0.1)	90.2±0.1 (98.7±0.4)	89.5±0.6 (100.0±0.0)
OGBN-Arxiv	37.7±2.9 (95.5±0.3)	37.8±0.7 (81.2±1.0)	30.2±2.0 (59.6±3.8)	39.5±0.5 (100.0±0.0)
RomanEmpire	42.7±0.3 (95.3±0.1)	40.6±1.4 (82.2±1.3)	35.2±0.7 (56.4±1.2)	42.7±0.5 (100.0±0.0)
AmazonRatings	42.0±0.3 (94.8±0.6)	41.2±0.1 (80.0±0.7)	39.4±0.6 (70.6±2.8)	41.6±0.2 (100.0±0.0)

Table 42: Detailed results for the three query-detection defenses across all ten datasets. Each cell reports protected-model accuracy (%) with the verification proxy (%) in parentheses, both as mean ± standard deviation over three seeds.

Dataset	`PRADA`	`AdaptMisinfo`	`GradRedir`
Cora	40.2±2.1 (43.0±1.3)	41.0±0.1 (48.5±0.0)	79.8±0.2 (100.0±0.0)
CiteSeer	69.3±0.7 (100.0±0.0)	39.8±0.3 (52.5±0.0)	68.4±0.9 (100.0±0.0)
PubMed	78.0±0.7 (100.0±0.0)	44.1±0.8 (48.6±0.0)	78.3±0.5 (100.0±0.0)
Computers	46.0±18.0 (100.0±0.0)	28.0±13.9 (64.3±0.0)	52.4±20.9 (100.0±0.0)
Photo	**87.0±10.6** (100.0±0.0)	46.3±0.4 (49.6±0.0)	66.6±17.6 (100.0±0.0)
CoauthorCS	75.0±0.8 (79.6±1.3)	52.4±0.5 (58.7±0.0)	88.2±0.7 (100.0±0.0)
CoauthorPhysics	83.4±0.7 (89.0±0.9)	**59.0±0.2** (63.1±0.0)	**89.7±0.3** (100.0±0.0)
OGBN-Arxiv	37.0±0.3 (100.0±0.0)	19.9±0.3 (52.3±0.0)	38.2±1.0 (100.0±0.0)
RomanEmpire	19.7±0.2 (25.4±0.7)	22.5±0.4 (50.8±0.0)	42.5±0.3 (100.0±0.0)
AmazonRatings	41.8±0.4 (100.0±0.0)	33.9±0.1 (48.9±0.0)	41.7±0.3 (100.0±0.0)

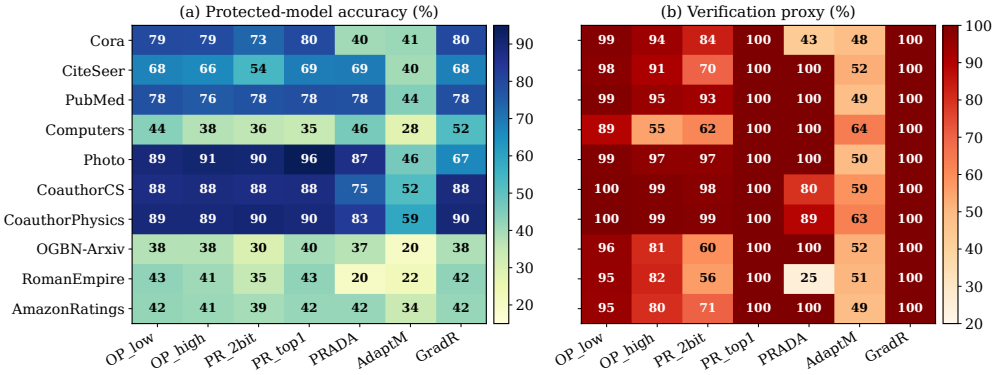
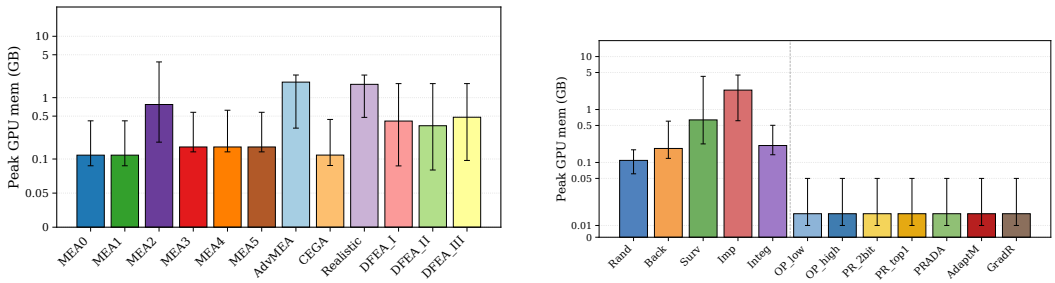


Figure 7: Heatmap view of the seven information-limiting and query-detection defenses across all ten datasets. Left panel: protected-model accuracy (%); right panel: verification proxy (%). Numbers are the same as in Tables 41–42. The two-panel view makes explicit that verification splits into two regimes: output-perturbation/rounding defenses and `GradRedir` verify at high rates, whereas `PRADA` and `AdaptMisinfo` are more variable and often closer to random; protected accuracy is largely flat across defenses except on *Computers*.

Wall-clock cost. Figure 9 aggregates total wall-clock time across all datasets for the twelve attacks (panel a) and the five watermarking defenses (panel b), again on a symmetric-log scale because the workloads span more than three orders of magnitude. The median bars and IQR error bars summarise Tables 4–5, and three patterns are sharper here than in the per-dataset tables. *First, on the attack side the cost cleaves into three groups.* The fast `MEA` family and `CEGA` sit between 0.7 and 2 minutes per run, the data-free `DFEA` family and `MEA2` sit slightly above at 1–3 minutes, and only `Realistic` and (more variably) `AdvMEA` sit one to three orders of magnitude higher; the upper IQR



(a) Attacks: peak memory.

(b) Defenses: peak memory.

Figure 8: Peak GPU memory (GB) on a symmetric-log scale, aggregated across all ten datasets. Bars show median and error bars show the inter-quartile range across (dataset, seed) combinations. Panel (b) covers all twelve defenses; the dashed line separates the five watermarking defenses (`Rand`, `Back`, `Surv`, `Imp`, `Integ`) on the left from the seven information-limiting / query-detection defenses on the right.

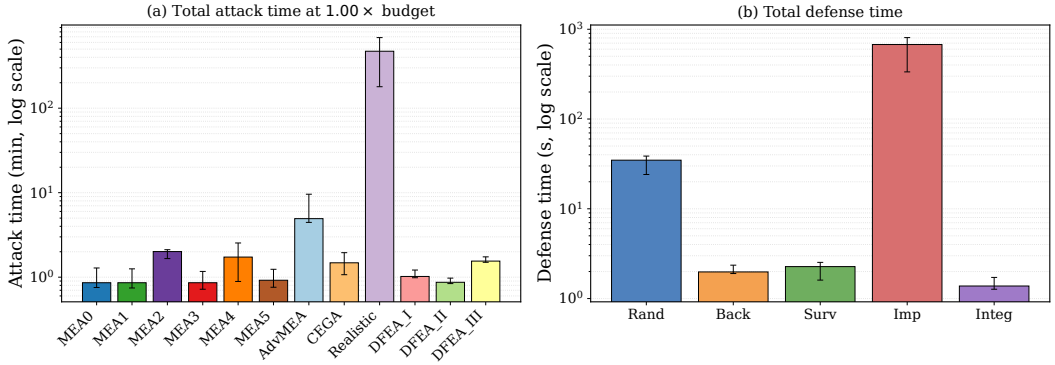


Figure 9: Wall-clock cost summary on a log scale. (a) Total attack time (min) at $1.00\times$ budget; bars are median and error bars are the inter-quartile range across the seven homophilic datasets. (b) Total defense time (s); same conventions. Numbers from Tables 4–5. Three groupings emerge on the attack side (fast `MEA/CEGA`, intermediate `DFEA/MEA2`, slow `Realistic/AdvMEA`) and two on the defense side (fast watermarks vs. `ImperceptibleWM`).

of `Realistic` reaches ~ 1000 minutes which is the largest single value in the benchmark. The cost gap is large enough that the *cost–fidelity* ordering is non-trivial, since RQ1 shows that simple attacks already saturate near $0.25\times$ budget. *Second, the defense panel separates into a fast tier (*1–$60\,s$*) and a slow tier (*$\sim 500\,s$*)*: `BackdoorWM` and `SurviveWM` train in seconds, `RandomWM` sits one order of magnitude higher because of its independent watermark graph training, and `ImperceptibleWM` sits two orders of magnitude higher because of its representation-level losses. *Third, the IQR error bars are narrow on every fast method and wide only on `Realistic` and `ImperceptibleWM`*, which means that empirical efficiency is essentially deterministic for the recommended configurations and that the cost numbers in the per-dataset tables are reproducible across hardware.

E.7 Extended statistical analysis of attack effectiveness (RQ1)

We complement the per-dataset RQ1 tables (Tables 10–31 and Tables 38–40) with eight aggregated views (Figure 10, Figure 11, and Figures 12–15) which average across datasets, regimes, or seeds to expose patterns that are hard to read off the raw tables.

Full ten-dataset budget–metric grid. Figure 10 reports the budget–metric curves on all ten datasets, in the same format as the six-dataset main-text Figure 2. The four datasets which the main text omits (CiteSeer, Photo, CoauthorCS, AmazonRatings) reproduce the qualitative behaviour of the chosen six: CiteSeer and Photo track the homophilic-citation/coauthor pattern of Cora and CoauthorPhysics; CoauthorCS sits between them; and AmazonRatings reproduces the heterophilic

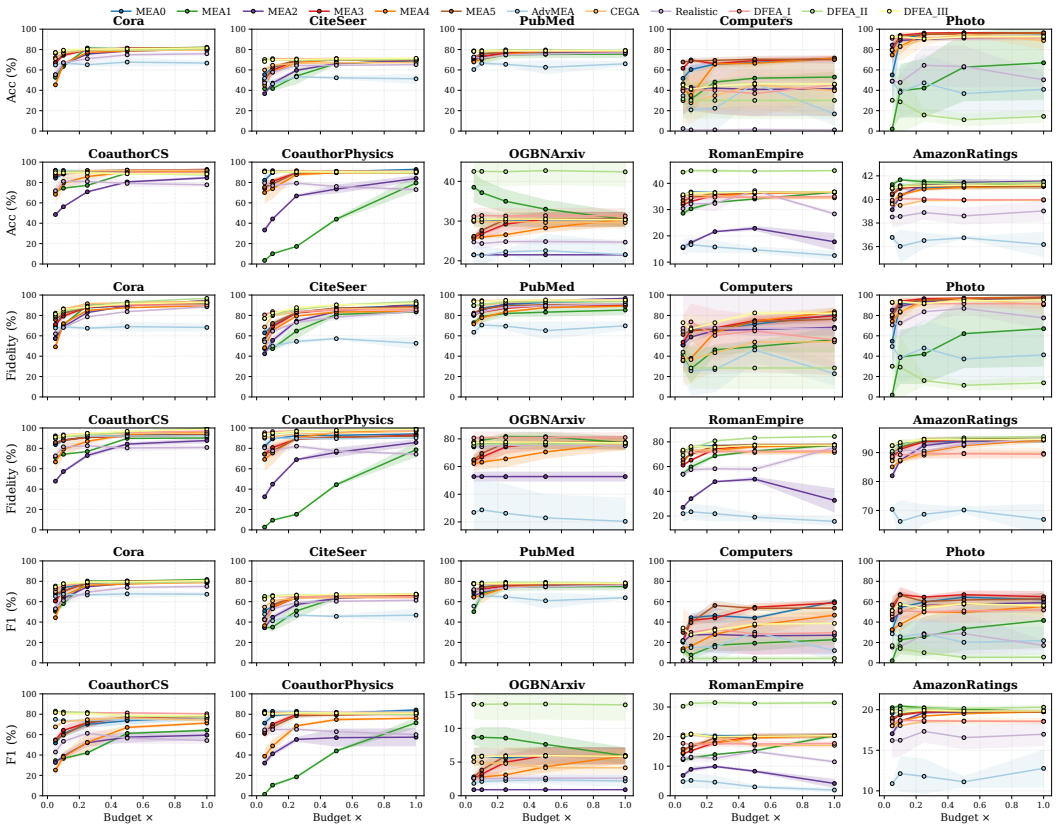


Figure 10: Budget–metric curves on all ten datasets (columns) for accuracy, fidelity, and macro F1 (rows). Lines are the twelve attacks (mean over three seeds, shaded bands ± 1 std). The seven homophilic graphs share a 0–100% y-axis; OGBN-Arxiv, RomanEmpire, and AmazonRatings use per-subplot ranges since their target accuracy is bounded by intrinsic task difficulty. The six-dataset version that appears in the main text (Figure 2) is a subset of this figure.

behaviour of RomanEmpire although its ordinal 5-class label space inflates absolute fidelity. The qualitative conclusions of RQ1 therefore hold uniformly across all ten datasets.

Regime sensitivity heatmap. Figure 11 reports the regime sensitivity across the standard five-budget grid: each cell is the ratio between fidelity in a constrained regime (`x_only`, `a_only`, `data_free`) and fidelity in the `both` regime for the same attack at the same budget, aggregated over all ten datasets. The heatmap exposes two patterns. *First, the left two blocks (`x_only`, `a_only`) are uniformly green at ratio ≈ 1.0 for every attack at every budget*: removing one input modality is essentially a no-op for the strong attacks, because the surrogate is trained on the target's labelled responses and label information dominates whichever single input remains. *Second, the right block (`data_free`) is bimodal*: the strong-MEA family (rows MEA0/3/4/5) drops to ratios in the 0.42–0.53 band across every budget, while `AdvMEA`, `CEGA`, `Realistic`, and the three `DFEA` variants stay at ratios around 1.0. The data-driven attacks (MEA family) collapse without a real graph because they rely on the target's responses to real-graph queries; the data-free attacks (`DFEA`, `Realistic`) by design synthesize their own queries and so are insensitive to the absence of a real graph; `CEGA` and `AdvMEA` retrain a query selector on whichever input is provided, including a synthetic graph, and so also stay near ratio 1.0. The map therefore answers a benchmark-design question: the `data_free` regime is the only regime that meaningfully discriminates attack families, which justifies including it in the standard RQ1 protocol despite its much lower absolute fidelity.

Per-attack budget curves across all ten datasets. Figure 12 shows, for each of the twelve attacks, a small panel containing the surrogate fidelity vs. budget curve on every dataset (regime `both`). Three observations stand out. First, the strong data-driven attacks (`MEA0`, `MEA1`, `MEA3`, `MEA4`, `MEA5`,

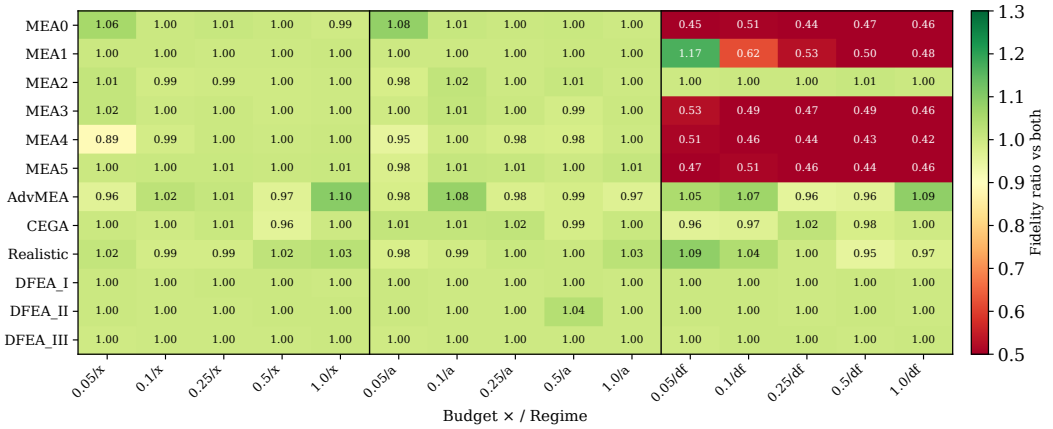


Figure 11: Regime sensitivity across budgets. Cells show the ratio between the average fidelity in a constrained regime and the average fidelity in the features-and-structure (`both`) regime for the same attack at the same budget; darker red indicates larger drops. The map aggregates over all ten datasets (seven homophilic plus OGBN-Arxiv, RomanEmpire, AmazonRatings) and separates dependence on features (`x`) and adjacency (`a`) from raw budget effects.

`Realistic`, `CEGA`) saturate by $0.25\times$ on the seven small homophilic graphs, with curves that are visually indistinguishable above this budget; this is the empirical justification for using $0.25\times$ as the medium budget in the joint evaluation of RQ5. Second, the OGBN-Arxiv curve is consistently $\sim$ 10–15 % below the homophilic graphs across all data-driven attacks at every budget, which is consistent with the larger label space (40 classes) and not with a budget ceiling. Third, the data-free variants (`DFEA_I`, `DFEA_II`, `DFEA_III`) and the noisy `MEA2` have curves that are largely flat across budgets and reach high fidelity on most datasets, with `DFEA_II` on the high-degree product graphs (*Computers* and *Photo*) as the main outlier; this confirms that data-free extraction is broadly robust under our protocol while showing dataset-specific sensitivity.

Regime sensitivity: per-attack fidelity loss when one input is removed. Figure 13a reports, per attack, the mean fidelity drop relative to the `both` regime when only features (`x_only`), only structure (`a_only`), or no real input (`data_free`) is provided to the extractor. The bars expose a clear separation: the data-driven attacks lose only a few percentage points when one modality is removed (because they still receive the target's labels for real-graph queries), but lose 30–70 pp in the `data_free` regime; `CEGA` loses the most in `a_only` (its centrality-based selection becomes ill-defined without the real graph), and `AdvMEA` is the most robust to removing structure. Figure 13b provides the absolute view that complements these drops: it shows the absolute mean fidelity in each regime per attack, with error bars that aggregate across datasets, budgets, and seeds. The two views together motivate the four-regime protocol used in RQ1.

Runtime and resource distribution across attacks. Figure 14 shows the distribution of per-run wall-clock attack time in minutes, on a log scale, aggregated across all (dataset, regime, budget, seed) combinations. Three groups separate cleanly: (i) the lightweight `MEA0/MEA1/MEA3/MEA4/MEA5/CEGA` family, with median runtime under one minute and tail below ten minutes, (ii) the adaptive `AdvMEA` and `DFEA_I/II/III` family in the one-to-twenty-minute band, and (iii) the heavyweight `Realistic` pipeline, whose tail extends two orders of magnitude above the rest because it trains an auxiliary edge-prediction model. This distributional view supplements the per-dataset time tables in the main text (Tables 4–5): the overall ordering between groups is preserved on every dataset, but the absolute magnitude scales with graph size.

Inter-attack similarity across (dataset, budget) profiles. Figure 15 reports the pairwise Pearson correlation of attacks, where each attack is represented by its fifty-dimensional fidelity vector (ten datasets $\times$ five budgets, regime `both`). Three structural blocks emerge. The first is the strong-MEA cluster (`MEA0`, `MEA1`, `MEA3`, `MEA4`, `MEA5`, `Realistic`, and `CEGA`), with pairwise correlations above 0.9 and a single shared profile across datasets. The second is the data-free cluster (`DFEA_I`, `DFEA_II`,

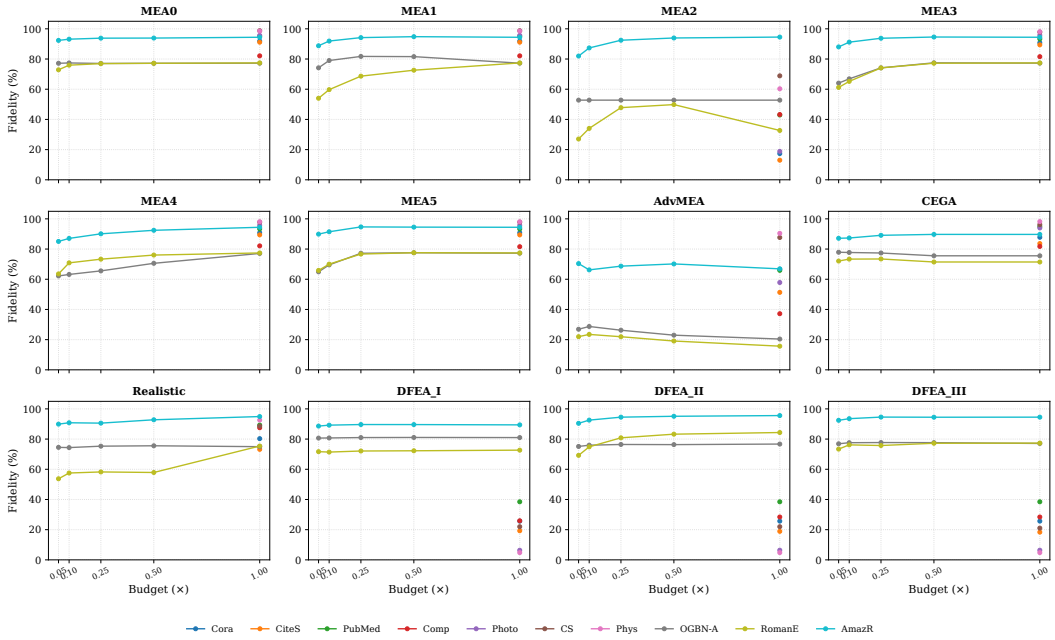
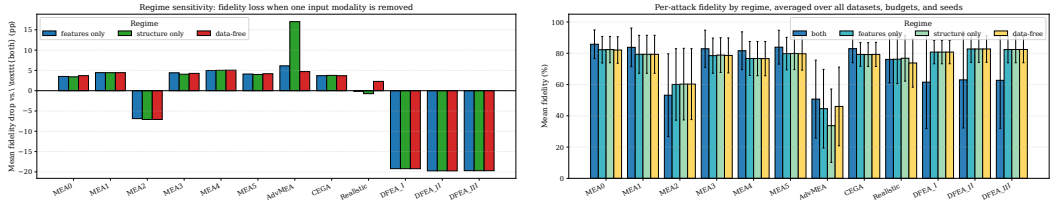


Figure 12: Per-attack surrogate-fidelity curves on all ten datasets in the `both` regime. Each panel is one attack; lines are mean over three seeds at five budgets ($0.05, 0.10, 0.25, 0.50, 1.00$). The strong data-driven attacks (top two rows) saturate near $0.25\times$ on the homophilic graphs; the data-free attacks (`DFEA_I/II/III`, bottom row) are competitive across most datasets and only degrade noticeably on the high-degree product graphs (*Computers* and *Photo*) for `DFEA_II`, indicating that data-free extraction is largely robust under our protocol but sensitive to specific graph structures.



(a) Mean fidelity drop relative to the `both` regime, per attack and per restricted regime.

(b) Absolute mean fidelity per attack, grouped by regime; error bars are ± std over (dataset, budget, seed).

Figure 13: Regime sensitivity from two complementary views: differential (left) and absolute (right). Both panels aggregate over all ten datasets, five budgets, and three seeds.

`DFEA_III`, plus `MEA2`), with correlations near 0.95 within the cluster and below 0.5 with the strong-MEA cluster. The third is `AdvMEA`, which sits between the two clusters and correlates only weakly with both, consistent with its hybrid adaptive-query design. The block structure suggests that, for benchmarking purposes, a representative subset that contains one element from each block (for example `MEA0`, `DFEA_I`, and `AdvMEA`) would already capture the qualitative behaviour of the full twelve-attack set, which we leave to future work as a benchmark-design recommendation.

Per-dataset utility cost of information-limiting defenses. Figure 16 reports the per-dataset utility loss of each of the seven information-limiting and query-detection defenses, computed as undefended GCN baseline accuracy minus the defended-model accuracy reported in Tables 41–42. The figure exposes three patterns that the per-row tables hide. *First, the four output-perturbation/rounding defenses (`OP_low`, `OP_high`, `PR_2bit`, `PR_top1`) cost essentially nothing on the seven homophilic graphs* (bars within ± 3 pp of zero), which is consistent with the design intent of these defenses: they perturb the returned scores at inference time without retraining, so the underlying classifier is unchanged. *Second, query-detection defenses split into two cost regimes.* `GradRedir` stays close

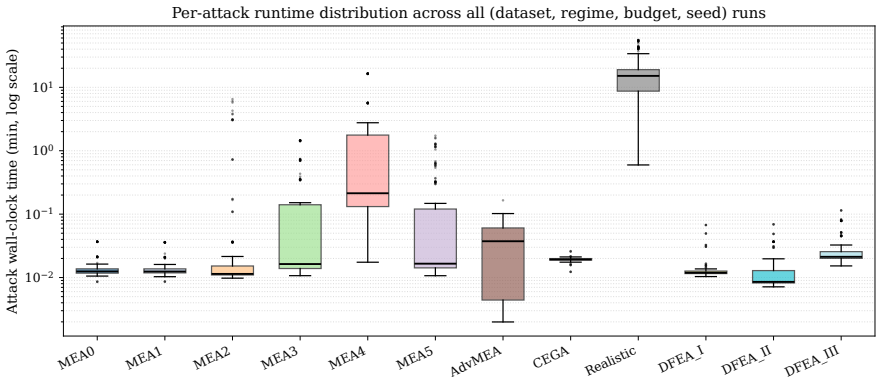


Figure 14: Distribution of per-run attack wall-clock time (log scale, in minutes) across all (dataset, regime, budget, seed) runs. Boxes show the inter-quartile range, whiskers extend to $1.5\times$ IQR, and dots show outlier runs. The `Realistic` pipeline has the longest tail because it includes an auxiliary edge predictor.

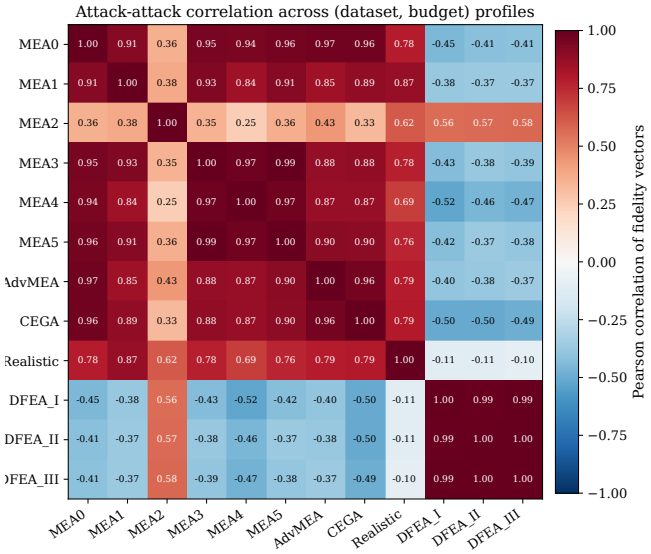


Figure 15: Pairwise Pearson correlation between the twelve attacks, where each attack is represented by its fifty-dimensional vector of mean fidelity over (ten datasets $\times$ five budgets) in the `both` regime. Two strong blocks (data-driven and data-free) and one outlier (`AdvMEA`) emerge.

to the no-defense baseline on most datasets (it perturbs only flagged queries), but on *Photo* it costs about 23 pp because the defense's gradient-redirection threshold flags many benign queries on the high-degree product graph; on *Computers* the loss is even larger ($\sim$ 45 pp). *Third, `AdaptMisinfo` consistently costs* 30–45 *pp across every dataset*, which is the highest among all seven and reflects the fact that the defense actively returns wrong labels on a large fraction of queries; users of the GraphIPBench API should treat `AdaptMisinfo` as a high-cost defense even when its verification proxy reaches $100\,\%$. The plot also surfaces a useful negative finding: `PRADA` on *RomanEmpire* loses 23 pp because the heterophilic structure makes random-query rejection blunt, suggesting that PRADA's distance-based query filter needs adaptation for graphs with low edge homophily.

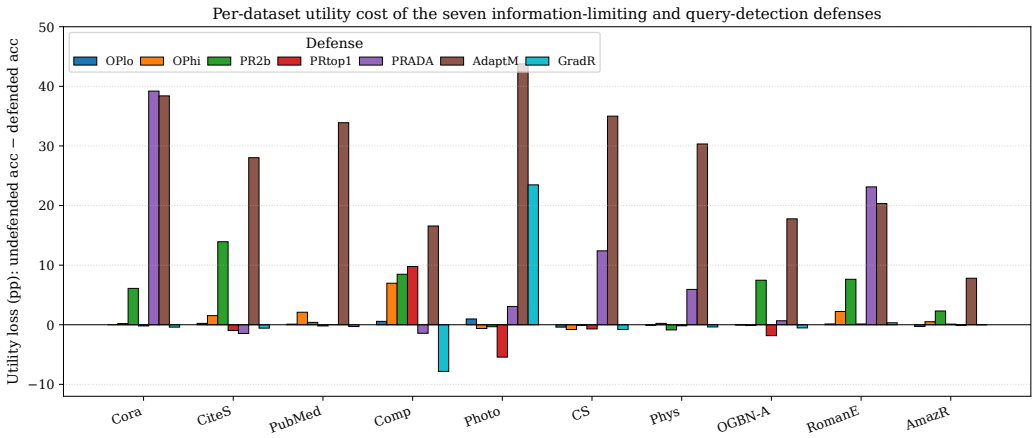
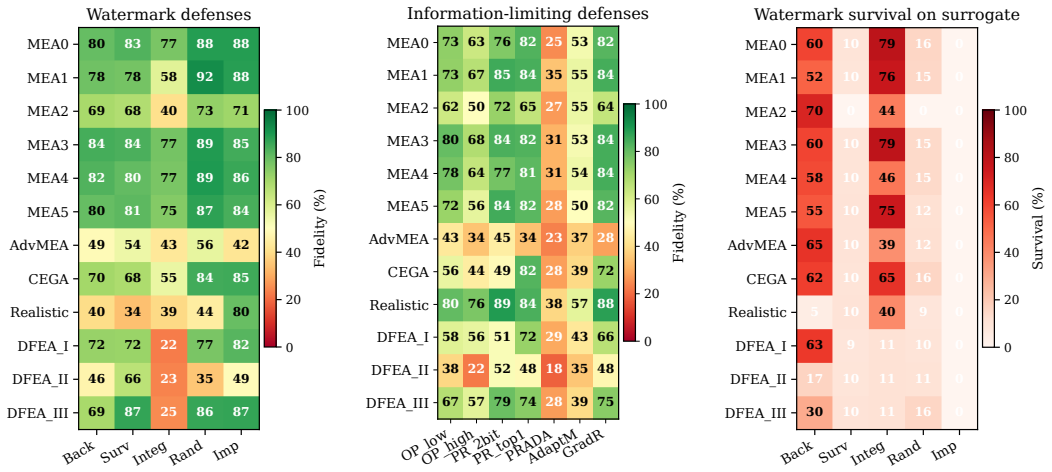


Figure 16: Per-dataset utility loss of the seven information-limiting and query-detection defenses (undefended GCN accuracy − defended accuracy, in percentage points; mean over three seeds). Output-perturbation and prediction-rounding defenses (`OP_low`, `OP_high`, `PR_2bit`, `PR_top1`) sit close to zero on the homophilic graphs, while `AdaptMisinfo` consistently loses 30–45 pp on every dataset because it actively returns wrong labels.



(a) Joint fidelity vs. watermarking defenses.

(b) Joint fidelity vs. information-limiting defenses.

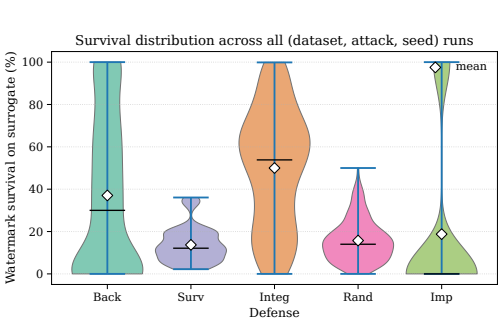
(c) Watermark survival on the surrogate.

Figure 17: RQ5 joint evaluation on *Computers* at $0.25\times$ (mean over three seeds; ten for Integrity). (a) Surrogate fidelity (%) against the five watermarks. (b) Surrogate fidelity (%) against the seven information-limiting defenses; `PRADA` and `AdaptMisinfo` reduce the strongest attacks from 80–92% to 25–55%. (c) Watermark verification rate (%) on the extracted surrogate. Query-based verification for `Integrity` is distinct from inherited watermark survival.

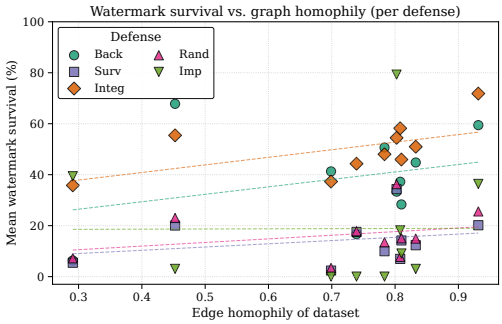
E.8 Joint evaluation and watermark survival per dataset

For `Integrity`, Computers and Photo use ten seeds at $0.25\times$. The remaining eight graphs use three seeds; some Integrity runs there use a $1.00\times$ budget or a different attack implementation and do not support matched comparisons with other defenses.

This subsection provides the full numerical record together with the analyses which anchor the cross-dataset claims of RQ5. We first show the consolidated Computers heatmap (Figure 17) which is referenced from the main text, and then the per-dataset tables. The tables report means and standard deviations across seeds.



(a) Violin: distribution of watermark survival per defense across all (dataset, attack, seed) runs.



(b) Scatter: edge homophily of the dataset vs. mean watermark survival on the surrogate (one point for each graph and defense pair).

Figure 18: Distribution and structural correlates of watermark survival.

Group 1 (joint surrogate fidelity, watermarking defenses). Tables 43–47 cover all ten datasets for the five watermarking and integrity defenses (`BackdoorWM`, `SurviveWM`, `Integrity`, `RandomWM`, `ImperceptibleWM`). On Computers, for example, MEA1 reaches 57.6% fidelity against Integrity and 92.0% against RandomWM (Table 45).

Group 2 (joint surrogate fidelity, information-limiting defenses). Tables 43–50 cover all ten datasets for the seven information-limiting and query-detection defenses (`OP_low`, `OP_high`, `PR_2bit`, `PR_top1`, `PRADA`, `AdaptMisinfo`, `GradRedir`). Two cross-dataset patterns hold. *First*, the relative ordering between defenses is highly stable: `PRADA` and `AdaptMisinfo` consistently produce the largest fidelity drop relative to the undefended baseline on every dataset and every attack, while the four output-perturbation and rounding variants (`OP_low`, `OP_high`, `PR_top1`, `GradRedir`) leave fidelity within ~ 5 pp of the undefended baseline. *Second*, prediction rounding to two bits (`PR_2bit`) is the only output-perturbation defense whose effect depends sharply on the attack: it has near-zero impact on the strong data-driven attacks (which already operate on label-like signal) but reduces `MEA2` and the `DFEA` family by an additional 5–15 pp on most datasets, which is consistent with the link-prediction behaviour reported in Appendix E.10.

Group 3 (watermark survival on the surrogate). Tables 43–52 report the available per-attack verification rates on the extracted surrogate. The four embedded watermarks and the query verifier are interpreted separately. The corrected mean surrogate fingerprint agreement for `Integrity` is 48.0% on *Computers* and 51.0% on *Photo*. The in-model marker `BackdoorWM` is more heterogeneous: it collapses for several data-driven attacks on *Cora*, but partially survives on the larger graphs (*Computers*, *Photo*, *CoauthorCS*) and for some `DFEA` variants; `SurviveWM` produces a stable but small ($\sim$ 10–15 %) survival rate that does not exceed the random-guess marker on most datasets; `RandomWM` yields 10–20 % survival across the board, again essentially indistinguishable from random; and `ImperceptibleWM` drops to zero on Cora, CiteSeer, PubMed, Computers, Photo, and on every data-free attack across all datasets, with sporadic non-zero survival appearing only on the heterophilic graphs. Across these schemes, verification on the protected model alone does not establish ownership after extraction.

The figures at the end of this subsection (Figures 18a–20) provide complementary statistical views: a violin plot of survival distributions per defense, a scatter that links survival to graph-level structural properties, an empirical CDF of surrogate fidelity stratified by defense family, and a per-dataset heatmap grid for joint fidelity.

Statistical views on the joint evaluation. The distribution panels summarize surrogate verification by defense and compare it with graph homophily. Comparisons across defenses require the same attack implementation and query budget.

Figure 19a shows the empirical distribution of surrogate fidelity by defense. Figure 19b compares surrogate accuracy on ground-truth labels with fidelity to the defended target. The diagonal marks equality between the two measures.

Table 43: RQ5 joint evaluation on *Cora* at budget $0.25\times$. (a) Surrogate fidelity (%) on defended targets for the five ownership methods. (b) Surrogate fidelity (%) on defended targets for the seven information-limiting and query-detection defenses. (c) Watermark verification rate (%) on the surrogate. Mean $\pm$ standard deviation over three seeds.

(a) Joint fidelity on *Cora*, watermarking defenses

Attack	BackdoorWM	SurviveWM	Integrity	RandomWM	ImperceptibleWM
MEA0	92.5 ± 0.7	92.3 ± 0.7	87.5 ± 1.2	91.7 ± 3.4	**92.9** ± 2.2
MEA1	91.5 ± 1.3	**93.7** ± 1.1	87.5 ± 1.2	90.9 ± 3.7	92.9 ± 2.3
MEA2	83.9 ± 1.3	83.8 ± 0.5	19.2 ± 5.6	84.1 ± 1.2	87.5 ± 0.3
MEA3	91.2 ± 1.7	**91.9** ± 0.6	86.7 ± 2.2	90.2 ± 3.2	91.9 ± 3.9
MEA4	91.4 ± 0.6	91.4 ± 0.9	86.7 ± 2.2	89.9 ± 2.6	91.9 ± 3.9
MEA5	91.4 ± 1.6	**92.2** ± 0.9	86.7 ± 2.2	91.9 ± 1.7	91.9 ± 3.9
AdvMEA	75.6 ± 2.6	76.8 ± 5.0	67.6 ± 1.9	**77.6** ± 3.7	76.4 ± 2.5
CEGA	87.4 ± 2.3	85.2 ± 2.7	85.5 ± 2.5	79.9 ± 5.6	**88.5** ± 2.4
Realistic	**91.5** ± 1.1	90.1 ± 1.4	87.5 ± 3.0	91.2 ± 1.7	91.0 ± 1.0
DFEA_I	89.4 ± 0.5	88.3 ± 3.2	21.2 ± 5.7	82.7 ± 1.2	89.2 ± 1.8
DFEA_II	88.6 ± 1.1	88.9 ± 0.5	21.2 ± 5.7	90.0 ± 0.1	91.3 ± 0.5
DFEA_III	90.3 ± 0.7	89.9 ± 0.8	21.2 ± 5.7	92.0 ± 1.3	91.2 ± 1.2

(b) Joint fidelity on *Cora*, information-limiting and query-detection defenses

Attack	OP_low	OP_high	PR_2bit	PR_top1	PRADA	AdaptMisinfo	GradRedir
MEA0	92.3 ± 0.4	89.7 ± 0.5	86.8 ± 0.1	**92.9** ± 0.3	42.4 ± 1.4	59.2 ± 0.2	92.9 ± 0.3
MEA1	92.0 ± 0.5	88.9 ± 1.0	86.2 ± 0.7	**92.4** ± 0.6	41.4 ± 0.8	57.7 ± 2.3	92.4 ± 0.6
MEA2	83.5 ± 1.3	81.5 ± 0.5	80.9 ± 0.8	84.6 ± 1.2	30.1 ± 1.7	57.6 ± 1.4	85.6 ± 1.2
MEA3	**91.4** ± 0.3	89.3 ± 0.7	84.0 ± 2.4	91.4 ± 0.7	44.1 ± 2.1	56.1 ± 0.6	91.4 ± 0.7
MEA4	91.0 ± 0.7	89.3 ± 0.8	86.5 ± 0.6	**92.4** ± 0.6	43.2 ± 1.2	58.5 ± 1.2	92.4 ± 0.6
MEA5	89.9 ± 2.5	88.6 ± 2.1	83.2 ± 1.8	**90.3** ± 2.9	43.3 ± 1.1	57.4 ± 0.5	90.3 ± 2.9
AdvMEA	**78.4** ± 1.5	76.4 ± 1.9	70.4 ± 0.5	72.4 ± 3.5	40.4 ± 1.3	43.7 ± 1.3	77.4 ± 1.9
CEGA	87.7 ± 1.0	86.4 ± 0.5	81.3 ± 2.7	**91.9** ± 1.0	40.3 ± 2.1	55.2 ± 0.9	89.4 ± 0.9
Realistic	90.9 ± 1.4	89.4 ± 1.4	83.6 ± 9.9	83.8 ± 2.6	54.5 ± 0.9	58.2 ± 1.0	**91.7** ± 1.0
DFEA_I	88.8 ± 0.3	87.2 ± 0.1	79.5 ± 2.3	89.2 ± 2.6	42.4 ± 0.6	53.8 ± 2.1	87.1 ± 0.8
DFEA_II	87.9 ± 0.8	85.2 ± 0.4	85.9 ± 0.7	88.4 ± 0.2	32.4 ± 2.2	62.0 ± 2.3	88.4 ± 0.2
DFEA_III	88.1 ± 2.0	86.4 ± 0.6	84.5 ± 1.4	90.0 ± 2.1	39.0 ± 1.8	57.2 ± 0.6	90.0 ± 2.1

(c) Watermark survival on the surrogate, *Cora*

Attack	BackdoorWM	SurviveWM	Integrity	RandomWM	ImperceptibleWM
MEA0	0.0 ± 0.0	14.9 ± 2.4	65.6 ± 3.5	12.0 ± 2.8	0.0 ± 0.0
MEA1	0.0 ± 0.0	14.6 ± 1.8	65.6 ± 3.5	18.7 ± 2.1	0.0 ± 0.0
MEA2	33.3 ± 57.7	0.0 ± 0.0	18.1 ± 3.2	0.0 ± 0.0	0.0 ± 0.0
MEA3	16.7 ± 40.8	14.2 ± 1.5	60.4 ± 4.0	15.3 ± 3.3	0.0 ± 0.0
MEA4	**16.7** ± 40.8	14.2 ± 1.3	60.4 ± 4.0	13.7 ± 2.3	0.0 ± 0.0
MEA5	**50.0** ± 54.8	13.6 ± 1.4	60.4 ± 4.0	13.7 ± 3.4	0.0 ± 0.0
AdvMEA	50.0 ± 54.8	15.0 ± 1.4	38.9 ± 5.1	13.7 ± 5.9	**66.7** ± 57.7
CEGA	**16.7** ± 40.8	13.7 ± 1.8	57.9 ± 3.2	15.7 ± 6.1	0.0 ± 0.0
Realistic	16.7 ± 40.8	13.6 ± 1.8	59.5 ± 7.3	17.7 ± 8.4	**33.3** ± 57.7
DFEA_I	66.7 ± 57.7	14.1 ± 2.3	21.6 ± 5.2	14.0 ± 3.5	0.0 ± 0.0
DFEA_II	**100.0** ± 0.0	13.8 ± 1.9	21.6 ± 5.2	13.3 ± 8.3	0.0 ± 0.0
DFEA_III	33.3 ± 57.7	14.0 ± 3.2	21.6 ± 5.2	18.0 ± 3.5	0.0 ± 0.0

Finally, Figure 20 renders the joint surrogate fidelity as a per-dataset heatmap grid, one 12×5 panel per dataset.

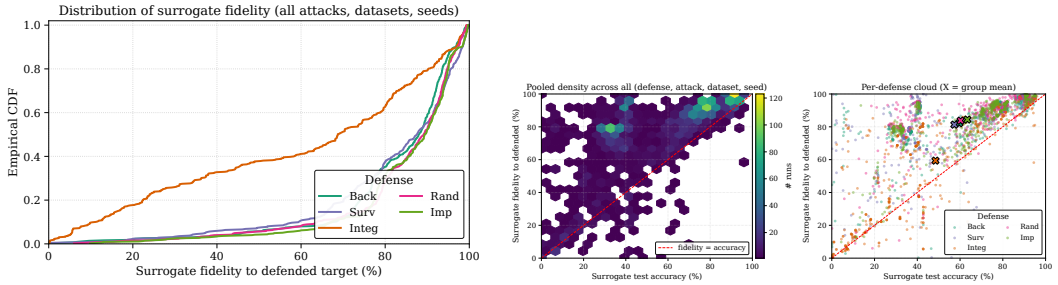
Table 44: Surrogate fidelity (%) on defended targets (5 watermarking defenses) for *CiteSeer* and *PubMed*. Mean ± standard deviation over three seeds.

(a) *CiteSeer*

Attack	BackdoorWM	SurviveWM	Integrity	RandomWM	ImperceptibleWM
MEA0	91.1 ± 1.0	87.3 ± 2.4	83.7 ± 2.1	92.3 ± 3.8	90.9 ± 0.3
MEA1	90.1 ± 2.8	87.6 ± 2.9	83.7 ± 2.1	91.3 ± 3.0	91.0 ± 0.4
MEA2	74.6 ± 0.6	75.2 ± 1.2	20.0 ± 4.9	74.7 ± 0.8	78.6 ± 0.9
MEA3	88.2 ± 1.0	85.6 ± 1.8	80.0 ± 2.9	88.6 ± 2.2	89.1 ± 1.5
MEA4	86.8 ± 2.4	82.1 ± 6.7	80.0 ± 2.9	88.8 ± 1.8	89.5 ± 1.4
MEA5	86.6 ± 0.5	85.0 ± 1.8	80.0 ± 2.9	88.5 ± 1.9	89.2 ± 1.2
AdvMEA	60.2 ± 5.6	61.2 ± 6.0	45.7 ± 4.6	62.4 ± 1.9	61.8 ± 4.8
CEGA	84.7 ± 1.1	62.8 ± 2.9	80.2 ± 2.1	73.9 ± 5.0	86.7 ± 1.0
DFEA_I	85.6 ± 1.7	67.0 ± 5.0	24.1 ± 2.3	73.7 ± 8.0	84.9 ± 1.7
DFEA_II	85.8 ± 0.5	85.4 ± 0.2	24.1 ± 2.3	88.2 ± 0.7	90.0 ± 0.6
DFEA_III	88.0 ± 0.9	86.2 ± 0.8	24.1 ± 2.3	88.5 ± 0.9	88.2 ± 0.7
Realistic	86.7 ± 1.1	84.2 ± 0.9	81.8 ± 2.0	88.7 ± 3.4	86.3 ± 0.7

(b) *PubMed*

Attack	BackdoorWM	SurviveWM	Integrity	RandomWM	ImperceptibleWM
MEA0	95.0 ± 0.8	95.2 ± 4.9	93.1 ± 0.9	94.5 ± 0.3	95.1 ± 0.5
MEA1	94.8 ± 0.4	94.9 ± 5.4	93.1 ± 0.9	95.3 ± 1.1	95.0 ± 0.4
MEA2	92.2 ± 1.1	91.7 ± 3.5	32.1 ± 9.6	91.1 ± 1.5	93.8 ± 0.6
MEA3	93.3 ± 1.4	89.7 ± 8.6	91.8 ± 1.7	93.9 ± 0.6	94.7 ± 0.4
MEA4	92.9 ± 1.8	89.8 ± 8.2	91.8 ± 1.8	93.8 ± 0.3	94.7 ± 0.4
MEA5	93.3 ± 0.8	90.7 ± 5.4	91.8 ± 1.8	93.5 ± 0.8	94.7 ± 0.4
AdvMEA	68.0 ± 2.4	43.4 ± 42.1	64.4 ± 4.9	62.5 ± 5.4	60.8 ± 2.7
CEGA	94.9 ± 0.3	98.7 ± 1.2	92.5 ± 1.1	93.5 ± 0.3	95.9 ± 0.3
DFEA_I	94.6 ± 0.7	98.4 ± 1.0	39.9 ± 3.9	94.1 ± 0.4	95.9 ± 0.3
DFEA_II	92.9 ± 0.9	85.3 ± 9.1	39.9 ± 3.9	94.2 ± 0.1	94.3 ± 0.2
DFEA_III	94.6 ± 0.6	94.4 ± 4.2	39.9 ± 3.9	94.1 ± 0.2	94.6 ± 0.1
Realistic	93.2 ± 1.3	35.5 ± 9.2	90.0 ± 3.3	91.7 ± 1.4	93.9 ± 0.7



(a) Empirical CDF of surrogate fidelity per defense.

(b) Surrogate accuracy vs. fidelity to defended target, pooled (left) and per defense (right).

Figure 19: Surrogate fidelity by defense. (a) Empirical cumulative distributions. (b) Surrogate accuracy versus fidelity to the defended target.

Table 45: Surrogate fidelity (%) on defended targets (5 watermarking defenses) for *Computers* and *Photo*. Mean ± standard deviation over three seeds (ten for Integrity on Computers and Photo).

(a) *Computers*

Attack	BackdoorWM	SurviveWM	Integrity	RandomWM	ImperceptibleWM
MEA0	80.0 ± 6.6	82.6 ± 8.4	76.9 ± 8.4	88.4 ± 5.5	88.4 ± 5.1
MEA1	78.3 ± 15.8	77.7 ± 12.4	57.6 ± 12.7	92.0 ± 1.7	87.9 ± 7.7
MEA2	69.3 ± 8.4	67.6 ± 2.2	40.4 ± 19.1	73.0 ± 3.8	70.8 ± 5.1
MEA3	84.2 ± 4.7	83.5 ± 10.1	77.4 ± 7.0	88.7 ± 6.2	84.7 ± 12.5
MEA4	82.5 ± 3.7	80.2 ± 8.6	76.6 ± 6.9	89.1 ± 3.4	85.9 ± 10.6
MEA5	80.0 ± 15.5	81.0 ± 12.2	75.3 ± 10.0	87.4 ± 2.8	83.9 ± 10.1
AdvMEA	48.7 ± 22.8	54.5 ± 16.9	42.8 ± 18.7	56.0 ± 11.5	42.1 ± 17.0
CEGA	70.3 ± 16.4	68.4 ± 27.4	55.4 ± 24.3	84.5 ± 10.7	85.1 ± 8.1
DFEA_I	71.9 ± 7.7	71.6 ± 10.4	22.3 ± 14.3	76.8 ± 9.3	81.7 ± 9.3
DFEA_II	46.5 ± 19.9	65.7 ± 15.8	23.5 ± 13.9	34.8 ± 8.1	49.0 ± 14.2
DFEA_III	69.3 ± 19.4	86.7 ± 5.5	25.0 ± 14.1	86.1 ± 5.3	86.7 ± 2.4
Realistic	39.6 ± 30.8	33.9 ± 31.3	38.8 ± 19.6	44.2 ± 17.6	79.6 ± 6.0

(b) *Photo*

Attack	BackdoorWM	SurviveWM	Integrity	RandomWM	ImperceptibleWM
MEA0	92.0 ± 4.0	94.8 ± 1.7	87.3 ± 16.5	98.1 ± 0.5	98.9 ± 0.5
MEA1	91.4 ± 2.4	96.5 ± 2.5	85.1 ± 15.3	93.6 ± 5.6	98.3 ± 1.5
MEA2	91.1 ± 1.4	94.8 ± 1.0	35.3 ± 26.6	94.4 ± 0.6	95.6 ± 0.5
MEA3	90.0 ± 6.1	96.1 ± 2.7	91.8 ± 6.7	96.8 ± 1.5	97.8 ± 1.5
MEA4	94.2 ± 1.3	97.6 ± 0.3	93.6 ± 5.3	96.2 ± 3.9	69.3 ± 48.8
MEA5	94.0 ± 0.9	96.9 ± 1.1	93.2 ± 5.8	97.8 ± 0.8	97.8 ± 2.2
AdvMEA	79.1 ± 7.0	42.9 ± 27.4	68.7 ± 20.8	67.2 ± 10.7	75.4 ± 13.4
CEGA	92.1 ± 3.2	96.2 ± 1.3	73.5 ± 30.8	93.2 ± 1.6	95.7 ± 5.4
DFEA_I	88.5 ± 7.3	76.3 ± 27.6	5.2 ± 5.0	95.4 ± 0.4	96.7 ± 1.4
DFEA_II	42.1 ± 31.1	22.1 ± 13.6	6.9 ± 6.6	23.1 ± 8.3	65.3 ± 31.4
DFEA_III	93.7 ± 1.9	96.8 ± 1.1	5.4 ± 5.9	94.2 ± 1.3	97.2 ± 1.0
Realistic	88.5 ± 7.6	95.0 ± 3.2	77.9 ± 27.8	63.4 ± 50.0	91.7 ± 6.2

Table 46: Surrogate fidelity (%) on defended targets (5 watermarking defenses) for *CoauthorCS* and *CoauthorPhysics*. Mean ± standard deviation over three seeds.

(a) *CoauthorCS*

Attack	BackdoorWM	SurviveWM	Integrity	RandomWM	ImperceptibleWM
MEA0	98.7 ± 0.2	99.5 ± 0.4	98.4 ± 0.2	98.5 ± 1.2	99.6 ± 0.1
MEA1	98.4 ± 0.4	99.5 ± 0.4	98.4 ± 0.2	98.9 ± 0.8	99.6 ± 0.1
MEA2	73.5 ± 0.8	77.9 ± 1.8	56.2 ± 7.9	77.9 ± 3.4	78.9 ± 0.4
MEA3	97.4 ± 0.5	99.0 ± 0.4	97.6 ± 0.1	98.5 ± 0.3	98.9 ± 0.3
MEA4	97.5 ± 0.5	98.8 ± 0.2	97.6 ± 0.1	97.7 ± 1.4	98.9 ± 0.3
MEA5	97.6 ± 0.4	98.7 ± 0.2	97.6 ± 0.1	98.3 ± 0.8	98.9 ± 0.3
AdvMEA	86.9 ± 0.8	91.6 ± 0.5	87.3 ± 0.5	91.1 ± 1.6	91.4 ± 1.6
CEGA	96.2 ± 0.7	97.2 ± 0.8	97.1 ± 0.3	96.4 ± 1.1	98.6 ± 0.3
DFEA_I	94.2 ± 0.7	96.1 ± 0.2	18.3 ± 4.9	96.8 ± 0.7	96.8 ± 0.3
DFEA_II	92.4 ± 0.7	94.5 ± 0.4	15.0 ± 10.0	94.5 ± 1.9	95.4 ± 0.6
DFEA_III	94.1 ± 0.4	95.6 ± 0.4	15.0 ± 10.0	96.2 ± 0.4	97.1 ± 0.5
Realistic	92.5 ± 0.4	94.6 ± 0.2	92.8 ± 1.0	91.7 ± 1.1	93.5 ± 0.5

(b) *CoauthorPhysics*

Attack	BackdoorWM	SurviveWM	Integrity	RandomWM	ImperceptibleWM
MEA0	99.1 ± 0.3	99.2 ± 0.5	99.2 ± 0.2	98.0 ± 1.1	99.6 ± 0.2
MEA1	99.2 ± 0.4	99.3 ± 0.4	99.2 ± 0.2	99.2 ± 0.1	99.6 ± 0.2
MEA2	68.4 ± 1.9	69.2 ± 2.0	31.6 ± 39.5	48.5 ± 14.3	64.7 ± 1.0
MEA3	98.7 ± 0.2	98.8 ± 0.1	99.2 ± 0.1	97.2 ± 1.4	99.4 ± 0.2
MEA4	98.6 ± 0.2	98.9 ± 0.3	99.2 ± 0.1	98.6 ± 0.7	99.4 ± 0.2
MEA5	98.7 ± 0.3	99.0 ± 0.3	99.2 ± 0.1	98.0 ± 0.9	99.4 ± 0.2
AdvMEA	89.4 ± 0.3	91.9 ± 1.3	92.6 ± 1.6	89.0 ± 2.9	93.2 ± 1.0
CEGA	98.3 ± 0.3	98.4 ± 0.5	98.9 ± 0.1	98.2 ± 0.1	99.4 ± 0.2
DFEA_I	97.6 ± 0.4	98.2 ± 0.4	5.7 ± 0.1	97.0 ± 0.4	98.3 ± 0.8
DFEA_II	96.8 ± 0.6	97.1 ± 0.3	5.7 ± 0.1	95.2 ± 2.0	97.9 ± 1.0
DFEA_III	97.0 ± 0.1	98.1 ± 0.2	5.7 ± 0.1	97.2 ± 0.7	98.0 ± 0.6
Realistic	94.8 ± 1.2	95.3 ± 0.8	94.4 ± 2.2	85.8 ± 2.0	95.0 ± 0.6

Table 47: Surrogate fidelity (%) on defended targets (5 watermarking defenses) for *OGBN-Arxiv*, *RomanEmpire*, and *AmazonRatings*. Mean ± standard deviation over three seeds.

(a) *OGBN-Arxiv*

Attack	BackdoorWM	SurviveWM	Integrity	RandomWM	ImperceptibleWM
MEA0	76.2 ± 3.9	67.8 ± 2.0	72.3 ± 3.1	80.1 ± 1.9	78.5 ± 1.1
MEA1	75.7 ± 3.2	67.8 ± 2.0	72.3 ± 3.1	81.9 ± 2.5	78.2 ± 0.8
MEA2	52.8 ± 1.8	25.8 ± 6.8	24.1 ± 21.1	48.4 ± 12.4	55.8 ± 1.9
MEA3	76.4 ± 3.6	67.7 ± 2.1	72.3 ± 3.1	80.1 ± 3.4	79.9 ± 0.8
MEA4	76.1 ± 3.3	67.9 ± 1.6	72.3 ± 3.1	81.9 ± 3.1	78.3 ± 0.9
MEA5	76.0 ± 3.5	66.9 ± 3.2	72.3 ± 3.1	79.8 ± 1.5	79.7 ± 0.8
AdvMEA	8.2 ± 1.1	25.8 ± 9.5	23.8 ± 3.2	49.0 ± 9.2	30.7 ± 8.0
CEGA	76.2 ± 2.5	63.1 ± 3.1	70.5 ± 3.2	76.8 ± 3.9	75.4 ± 1.4
DFEA_I	79.5 ± 0.9	65.6 ± 5.2	31.5 ± 20.7	82.5 ± 1.4	82.3 ± 1.4
DFEA_II	74.0 ± 2.4	82.6 ± 0.5	34.2 ± 21.6	79.4 ± 1.8	76.2 ± 0.1
DFEA_III	76.4 ± 3.4	67.7 ± 2.0	34.7 ± 22.1	82.6 ± 1.9	78.2 ± 1.1
Realistic	74.4 ± 1.6	54.2 ± 4.1	67.6 ± 3.9	60.7 ± 14.9	77.8 ± 3.3

(b) *RomanEmpire*

Attack	BackdoorWM	SurviveWM	Integrity	RandomWM	ImperceptibleWM
MEA0	76.8 ± 0.5	78.7 ± 0.9	69.0 ± 1.2	79.4 ± 2.2	78.6 ± 1.1
MEA1	76.9 ± 0.9	78.7 ± 1.1	69.0 ± 1.2	79.6 ± 0.7	78.7 ± 1.6
MEA2	46.0 ± 0.7	48.9 ± 1.6	12.6 ± 0.7	51.4 ± 1.6	49.8 ± 1.6
MEA3	76.9 ± 0.5	78.6 ± 1.1	69.0 ± 1.2	80.0 ± 0.7	78.6 ± 0.9
MEA4	77.0 ± 0.8	78.6 ± 1.1	69.0 ± 1.2	80.1 ± 2.3	78.5 ± 1.3
MEA5	77.0 ± 0.2	78.6 ± 1.1	69.0 ± 1.2	79.6 ± 0.7	78.7 ± 1.2
AdvMEA	18.0 ± 4.1	37.9 ± 3.7	18.7 ± 3.4	18.4 ± 11.2	18.6 ± 7.5
CEGA	70.8 ± 1.5	70.7 ± 2.6	63.7 ± 2.4	78.3 ± 1.3	76.8 ± 1.2
DFEA_I	70.7 ± 1.3	72.3 ± 2.4	15.4 ± 2.4	78.8 ± 1.2	76.7 ± 0.9
DFEA_II	80.3 ± 0.5	80.7 ± 0.5	17.5 ± 4.9	84.0 ± 0.4	81.6 ± 0.8
DFEA_III	76.4 ± 0.6	78.4 ± 0.6	14.2 ± 2.4	80.4 ± 1.1	78.2 ± 1.6
Realistic	74.1 ± 0.9	73.4 ± 0.6	63.7 ± 1.9	70.7 ± 4.0	67.3 ± 1.6

(c) *AmazonRatings*

Attack	BackdoorWM	SurviveWM	Integrity	RandomWM	ImperceptibleWM
MEA0	91.4 ± 1.0	94.1 ± 1.4	80.5 ± 1.3	92.7 ± 2.1	92.6 ± 1.5
MEA1	91.8 ± 1.2	94.2 ± 1.1	80.6 ± 1.2	93.5 ± 2.1	92.0 ± 1.1
MEA2	86.3 ± 2.3	91.6 ± 0.8	49.3 ± 14.3	91.6 ± 2.8	87.6 ± 1.6
MEA3	91.3 ± 1.3	93.8 ± 1.4	80.5 ± 1.3	93.0 ± 3.1	93.7 ± 1.1
MEA4	91.8 ± 0.5	93.8 ± 1.9	80.5 ± 1.1	93.6 ± 1.4	92.8 ± 0.4
MEA5	91.4 ± 0.6	94.2 ± 1.3	80.5 ± 1.1	93.6 ± 1.9	92.9 ± 0.9
AdvMEA	41.2 ± 15.8	47.1 ± 19.6	38.2 ± 5.2	47.9 ± 34.6	58.7 ± 17.6
CEGA	89.3 ± 1.3	88.3 ± 2.0	73.9 ± 4.4	94.7 ± 4.0	91.5 ± 1.3
DFEA_I	88.8 ± 0.6	87.2 ± 1.5	44.3 ± 16.3	88.0 ± 4.2	92.9 ± 1.6
DFEA_II	92.8 ± 0.5	94.0 ± 0.8	44.5 ± 16.1	95.1 ± 0.2	94.9 ± 0.2
DFEA_III	91.7 ± 0.4	94.0 ± 0.7	44.7 ± 15.9	93.6 ± 2.0	92.6 ± 1.0
Realistic	88.8 ± 0.7	94.3 ± 0.9	78.1 ± 2.1	76.2 ± 19.0	93.2 ± 1.8

Table 48: Surrogate fidelity (%) on defended targets (7 information-limiting and query-detection defenses) for *CiteSeer*, *PubMed*, and *Computers*. Mean ± standard deviation over three seeds.

(a) *CiteSeer*

Attack	OP_low	OP_high	PR_2bit	PR_top1	PRADA	AdaptMisinfo	GradRedir
MEA0	90.3±0.7	86.2±1.3	83.2±2.0	91.6±1.0	33.5±2.8	60.3±0.5	91.6±1.0
MEA1	90.3±0.7	86.2±1.3	83.2±2.0	91.6±1.0	33.5±2.8	60.3±0.5	91.6±1.0
MEA2	73.9±1.0	70.3±1.4	69.3±0.2	75.5±1.3	23.5±1.8	54.9±1.4	75.1±1.2
MEA3	87.6±0.8	84.0±0.9	72.5±9.1	88.5±1.6	33.6±1.3	56.2±1.3	88.5±1.6
MEA4	87.6±0.8	84.0±0.9	72.5±9.1	88.5±1.6	33.6±1.3	56.2±1.3	88.5±1.6
MEA5	87.6±0.8	84.0±0.9	72.5±9.1	88.5±1.6	33.6±1.3	56.2±1.3	88.5±1.6
AdvMEA	60.3±7.4	64.0±8.3	39.0±4.2	59.7±0.7	32.4±1.5	35.9±3.1	60.5±3.1
CEGA	83.6±0.5	81.1±1.1	65.4±0.2	90.9±2.0	34.4±1.8	52.1±2.0	81.2±2.2
DFEA_I	83.5±3.5	80.8±4.0	64.5±0.9	87.7±0.5	33.3±2.6	50.4±0.8	81.2±1.2
DFEA_II	85.0±1.1	79.2±1.5	78.4±1.0	86.1±1.9	26.1±0.9	61.1±2.0	86.1±1.9
DFEA_III	87.8±0.3	84.2±0.3	79.1±0.4	87.8±1.2	30.5±1.7	56.8±1.9	87.8±1.2
Realistic	88.1±2.0	85.3±1.3	97.6±1.4	79.6±4.7	45.5±1.8	57.5±1.7	91.2±2.7

(b) *PubMed*

Attack	OP_low	OP_high	PR_2bit	PR_top1	PRADA	AdaptMisinfo	GradRedir
MEA0	94.9±0.9	92.9±0.9	94.3±1.0	94.9±0.7	59.9±1.0	62.1±0.4	94.9±0.7
MEA1	94.9±0.9	92.9±0.9	94.3±1.0	94.9±0.7	59.9±1.0	62.1±0.4	94.9±0.7
MEA2	91.2±0.7	89.1±1.5	91.4±0.3	91.3±1.1	53.0±0.6	62.4±1.6	91.2±0.8
MEA3	92.9±1.1	91.0±1.1	93.3±1.0	93.0±0.8	59.8±1.3	61.1±0.7	93.0±0.8
MEA4	92.9±1.1	91.0±1.1	93.3±1.0	93.0±0.8	59.8±1.2	61.1±0.7	93.0±0.8
MEA5	92.9±1.1	91.0±1.1	93.3±1.0	93.0±0.8	59.8±1.3	61.1±0.7	93.0±0.8
AdvMEA	67.3±12.9	64.1±5.2	70.5±5.4	67.1±6.1	48.8±3.8	45.4±4.3	72.4±10.3
CEGA	94.8±0.6	92.9±1.0	92.6±0.7	94.8±0.7	59.5±1.1	60.1±0.8	94.5±0.6
DFEA_I	94.0±0.4	92.4±0.4	93.0±0.3	94.3±0.6	58.1±1.9	60.0±0.7	94.3±0.2
DFEA_II	92.8±0.8	90.4±1.2	93.2±1.4	92.7±1.2	55.5±1.1	67.9±1.2	92.7±1.2
DFEA_III	94.0±0.1	92.5±0.4	94.2±1.5	94.7±0.7	59.5±0.8	61.9±0.4	94.7±0.7
Realistic	95.2±0.6	94.1±0.5	89.5±0.6	92.7±0.8	70.7±2.5	63.0±1.4	94.3±0.2

(c) *Computers*

Attack	OP_low	OP_high	PR_2bit	PR_top1	PRADA	AdaptMisinfo	GradRedir
MEA0	73.4±11.3	62.6±25.0	75.7±13.3	82.5±3.1	24.9±9.1	52.9±9.2	82.0±3.1
MEA1	72.9±25.7	66.6±26.1	84.8±5.3	83.7±6.2	34.6±16.9	55.4±5.8	84.3±6.0
MEA2	62.5±6.1	49.7±16.7	71.9±5.5	64.8±2.3	27.2±9.5	54.8±0.9	64.2±1.9
MEA3	79.7±12.3	67.9±27.5	83.5±2.4	82.5±5.6	31.4±16.9	52.6±9.3	84.3±3.0
MEA4	77.5±11.6	64.4±25.5	77.4±12.4	80.9±4.9	31.3±17.3	54.2±6.1	84.0±3.2
MEA5	71.8±9.7	56.3±32.3	84.4±0.9	81.6±2.1	27.5±17.3	50.1±8.1	82.0±2.5
AdvMEA	43.3±13.4	34.4±13.4	44.7±21.6	34.3±27.8	23.1±7.3	37.1±10.2	28.5±26.1
CEGA	55.8±39.6	44.3±32.8	48.7±29.4	82.2±4.5	27.8±14.1	38.7±7.8	71.7±15.2
DFEA_I	58.1±12.3	56.1±15.7	51.2±22.2	72.0±5.7	29.4±8.7	42.8±8.1	66.4±8.6
DFEA_II	38.3±22.6	21.9±8.5	51.5±26.1	48.1±25.7	18.2±4.9	35.1±8.9	47.6±26.6
DFEA_III	66.8±10.1	57.3±18.4	79.2±6.9	74.5±8.5	27.6±10.7	39.2±6.0	74.6±8.7
Realistic	80.1±6.7	76.4±7.0	88.7±11.8	83.5±10.7	38.5±21.5	56.9±7.2	87.7±4.1

Table 49: Surrogate fidelity (%) on defended targets (7 information-limiting and query-detection defenses) for *Photo*, *CoauthorCS*, and *CoauthorPhysics*. Mean ± standard deviation over three seeds.

(a) *Photo*

Attack	OP_low	OP_high	PR_2bit	PR_top1	PRADA	AdaptMisinfo	GradRedir
MEA0	93.9±3.8	77.3±29.6	93.3±5.1	94.9±3.2	64.5±25.7	50.0±8.6	94.8±3.3
MEA1	93.9±3.8	77.3±29.6	93.3±5.1	94.9±3.2	64.5±25.7	50.0±8.6	94.8±3.3
MEA2	92.7±2.2	90.4±3.4	92.5±2.1	92.8±2.0	71.9±7.5	59.1±1.0	92.2±2.8
MEA3	93.9±3.9	77.4±29.7	93.3±5.2	94.8±3.4	64.6±25.8	50.2±8.7	94.8±3.4
MEA4	93.9±3.9	77.4±29.7	93.3±5.2	94.8±3.4	64.6±25.8	50.2±8.7	94.8±3.4
MEA5	93.9±3.9	77.4±29.7	93.3±5.2	94.8±3.4	64.6±25.8	50.2±8.7	94.8±3.4
AdvMEA	68.9±11.7	48.6±32.2	73.9±6.8	78.4±3.3	51.5±24.9	42.1±1.6	77.3±3.4
CEGA	93.9±1.0	93.3±2.7	92.8±1.3	93.2±2.9	76.6±7.9	52.8±5.0	78.2±28.2
DFEA_I	80.5±17.7	78.3±13.5	86.0±2.9	89.7±3.6	74.2±7.2	49.6±4.0	67.0±13.3
DFEA_II	12.1±6.0	12.0±6.0	18.7±4.6	13.2±5.2	24.0±22.5	35.6±9.5	13.2±5.2
DFEA_III	92.5±4.5	93.3±2.6	93.2±2.6	93.4±3.4	74.4±7.5	50.6±3.0	93.4±3.4
Realistic	96.9±0.7	96.3±1.5	94.1±6.6	96.1±6.8	86.7±8.7	47.6±0.6	75.6±27.2

(b) *CoauthorCS*

Attack	OP_low	OP_high	PR_2bit	PR_top1	PRADA	AdaptMisinfo	GradRedir
MEA0	98.8±0.2	97.8±0.4	98.8±0.2	99.0±0.0	79.8±1.4	75.1±1.4	99.0±0.0
MEA1	98.8±0.2	97.8±0.4	98.8±0.2	99.0±0.0	79.9±1.4	75.2±1.4	99.0±0.0
MEA2	74.3±1.0	75.8±0.8	75.4±0.8	76.1±1.2	63.1±0.2	51.7±1.8	76.3±0.4
MEA3	97.7±0.2	97.0±0.2	97.9±0.2	97.9±0.1	79.7±1.4	73.0±0.2	97.9±0.1
MEA4	97.6±0.2	97.0±0.2	97.9±0.2	97.9±0.1	79.8±1.4	73.1±0.1	97.9±0.1
MEA5	97.7±0.2	97.0±0.2	97.9±0.2	97.9±0.1	79.8±1.4	73.0±0.1	97.9±0.1
AdvMEA	88.2±0.9	88.5±0.8	87.7±1.4	88.3±0.6	75.4±2.0	52.9±0.6	88.2±0.7
CEGA	96.5±1.0	96.2±0.7	95.9±0.7	98.8±0.1	81.3±1.1	73.5±0.7	97.8±0.5
DFEA_I	95.1±0.8	95.1±0.5	94.0±0.4	94.4±0.2	79.0±0.4	63.6±0.3	94.0±0.3
DFEA_II	93.1±0.4	93.1±0.2	93.7±0.9	93.9±0.9	75.8±0.3	73.2±1.8	93.9±0.9
DFEA_III	94.6±0.2	94.2±0.6	95.1±0.6	94.9±1.1	76.8±0.4	64.6±1.4	94.9±1.1
Realistic	95.3±0.6	95.0±1.0	100.0±0.0	90.8±5.3	88.4±1.5	71.6±1.2	96.5±0.7

(c) *CoauthorPhysics*

Attack	OP_low	OP_high	PR_2bit	PR_top1	PRADA	AdaptMisinfo	GradRedir
MEA0	98.4±0.9	98.4±0.5	98.9±0.4	98.6±0.5	89.1±0.4	61.3±1.4	98.5±0.5
MEA1	98.4±0.9	98.4±0.5	98.9±0.4	98.6±0.5	89.1±0.4	61.6±1.8	98.5±0.5
MEA2	70.2±0.2	69.4±1.3	70.9±3.1	68.8±3.9	64.8±0.9	43.0±1.7	69.7±1.1
MEA3	98.0±0.7	98.2±0.6	98.6±0.3	98.2±0.6	89.0±0.7	63.1±2.2	98.2±0.6
MEA4	98.0±0.7	98.2±0.6	98.6±0.3	98.2±0.6	89.0±0.7	63.0±2.5	98.2±0.6
MEA5	98.0±0.7	98.2±0.6	98.6±0.3	98.2±0.6	89.0±0.7	63.9±1.6	98.2±0.6
AdvMEA	90.9±0.4	91.3±0.5	91.4±0.6	91.1±1.0	85.7±0.8	58.7±0.9	91.1±1.0
CEGA	98.1±0.9	98.1±0.6	98.1±0.6	98.5±0.6	88.6±0.8	60.6±2.3	98.0±0.6
DFEA_I	97.1±0.4	96.9±0.4	97.4±0.4	96.5±0.7	86.8±0.6	58.5±0.5	96.7±0.8
DFEA_II	95.8±1.0	95.5±0.5	96.7±0.1	95.9±0.5	85.4±0.6	76.7±0.4	95.9±0.5
DFEA_III	96.8±0.6	96.7±0.6	97.0±0.2	96.7±0.6	87.5±0.7	58.6±0.8	96.7±0.6
Realistic	96.8±0.3	96.2±0.1	100.0±0.0	95.4±2.6	93.1±0.6	60.8±2.0	97.1±0.2

Table 50: Surrogate fidelity (%) on defended targets (7 information-limiting and query-detection defenses) for *OGBN-Arxiv*, *RomanEmpire*, and *AmazonRatings*. Mean ± standard deviation over three seeds.

(a) *OGBN-Arxiv*

Attack	OP_low	OP_high	PR_2bit	PR_top1	PRADA	AdaptMisinfo	GradRedir
MEA0	77.3±4.5	71.9±3.5	73.7±5.2	77.8±4.7	16.1±1.0	44.1±1.7	77.9±4.8
MEA1	77.3±4.5	72.0±3.6	73.8±5.3	77.9±4.8	16.1±1.0	44.1±1.8	77.9±4.8
MEA2	52.4±2.9	48.1±2.4	41.9±1.9	52.8±2.9	8.9±0.1	28.9±1.5	52.8±2.9
MEA3	77.3±4.5	72.0±3.6	73.8±5.3	77.9±4.8	16.1±1.0	44.1±1.7	77.9±4.8
MEA4	77.3±3.7	71.9±2.9	73.8±4.3	77.9±3.9	16.1±0.8	44.1±1.4	77.9±3.9
MEA5	77.3±4.5	71.9±3.6	73.7±5.2	77.9±4.8	16.1±1.0	44.1±1.7	77.9±4.8
AdvMEA	31.6±3.7	36.5±5.8	33.8±2.8	34.2±2.5	9.8±0.6	17.1±1.6	28.8±1.6
CEGA	76.2±3.9	69.5±2.7	52.6±2.2	73.5±5.4	15.7±0.8	34.8±1.1	72.0±2.5
DFEA_I	81.5±3.0	73.6±1.8	54.4±2.0	77.3±2.5	16.0±0.6	37.0±0.5	76.5±1.9
DFEA_II	75.7±0.9	69.3±0.3	71.1±1.4	76.2±1.2	15.4±0.9	57.3±1.4	76.2±1.2
DFEA_III	77.7±4.1	71.8±2.7	73.5±4.8	77.7±3.8	16.1±0.8	44.7±1.8	77.8±3.7
Realistic	74.1±2.5	70.0±2.6	99.8±0.1	70.4±9.6	24.7±0.9	41.4±0.6	79.9±2.2

(b) *RomanEmpire*

Attack	OP_low	OP_high	PR_2bit	PR_top1	PRADA	AdaptMisinfo	GradRedir
MEA0	76.8±0.6	71.8±0.7	74.3±0.3	77.7±0.3	24.3±0.8	49.6±0.5	77.7±0.3
MEA1	76.6±0.5	71.3±0.8	74.4±0.3	77.5±0.3	24.5±0.7	49.6±0.5	77.5±0.3
MEA2	46.6±0.1	41.6±0.5	51.2±1.3	47.4±0.6	15.9±0.4	39.7±0.4	47.6±0.8
MEA3	76.9±0.8	71.6±0.6	74.5±0.4	77.8±0.4	24.6±0.7	49.5±0.4	77.8±0.4
MEA4	77.0±1.0	71.8±0.6	74.3±0.3	77.8±0.4	24.6±0.7	49.2±0.7	77.8±0.4
MEA5	76.6±0.6	71.5±0.7	74.0±0.7	77.4±0.6	24.6±0.7	49.2±0.7	77.4±0.6
AdvMEA	17.1±3.9	19.5±5.8	41.0±1.0	16.5±3.5	13.6±3.2	11.4±3.3	18.0±4.6
CEGA	72.1±1.8	67.5±2.0	57.1±1.2	78.2±0.8	25.6±0.1	43.8±0.2	65.2±0.3
DFEA_I	73.6±1.1	68.7±1.1	57.0±2.0	77.3±0.7	25.2±0.4	43.1±0.3	64.7±0.9
DFEA_II	79.5±0.3	72.3±0.1	78.7±0.6	81.0±0.5	21.4±0.3	65.5±0.5	81.0±0.5
DFEA_III	76.4±0.8	70.9±0.8	74.7±0.5	77.0±0.5	24.7±0.6	48.8±0.7	77.0±0.5
Realistic	73.3±0.7	68.5±0.7	94.9±4.5	75.2±6.9	33.6±0.5	55.3±0.3	78.0±0.5

(c) *AmazonRatings*

Attack	OP_low	OP_high	PR_2bit	PR_top1	PRADA	AdaptMisinfo	GradRedir
MEA0	91.9±0.7	78.3±0.7	90.0±0.5	94.0±1.1	33.6±0.3	63.7±0.8	94.1±1.1
MEA1	91.8±0.8	78.3±0.7	89.9±0.5	94.1±1.1	33.6±0.3	63.7±0.8	94.1±1.1
MEA2	88.7±0.5	71.1±4.5	90.4±0.8	91.3±1.9	31.0±0.9	62.0±0.9	90.4±0.8
MEA3	91.8±0.8	78.3±0.7	90.0±0.5	94.0±1.1	33.6±0.3	63.7±0.8	94.1±1.1
MEA4	91.9±0.7	78.3±0.7	90.0±0.5	94.1±1.0	33.6±0.3	63.7±0.8	94.1±1.0
MEA5	91.8±0.7	78.3±0.7	90.0±0.5	94.0±1.1	33.6±0.4	63.7±0.8	94.0±1.1
AdvMEA	42.9±24.3	40.5±21.6	55.9±1.1	44.5±23.3	29.6±3.6	27.3±10.7	47.8±21.8
CEGA	87.6±2.0	76.8±1.0	69.2±3.7	94.1±1.0	34.3±0.9	52.8±1.5	93.3±0.9
DFEA_I	88.4±2.2	76.7±1.2	73.4±2.2	93.7±0.5	32.9±0.4	51.7±0.7	92.9±0.8
DFEA_II	91.9±0.7	77.9±1.4	88.7±0.4	94.1±0.5	29.1±0.6	77.2±1.4	94.1±0.5
DFEA_III	91.4±1.7	78.4±1.6	90.0±0.4	93.2±1.2	33.1±0.2	63.5±0.5	93.2±1.2
Realistic	92.0±0.8	79.3±0.6	100.0±0.0	65.2±15.3	43.0±0.6	64.3±0.6	94.5±0.4

Table 51: Watermark verification rate (%) on the surrogate produced by each attack against each watermarking defense, on *CiteSeer*, *PubMed*, *Computers*, and *Photo*. Higher is better. Mean ± standard deviation over three seeds (ten for Integrity on Computers and Photo).

(a) *CiteSeer*

Attack	BackdoorWM	SurviveWM	Integrity	RandomWM	Impercept.
MEA0	0.0±0.0	17.5±1.4	62.2±5.5	17.3±7.6	0.0±0.0
MEA1	33.3±57.7	17.7±1.9	62.2±5.5	22.0±4.0	0.0±0.0
MEA2	33.3±47.1	0.0±0.0	24.5±2.8	0.0±0.0	0.0±0.0
MEA3	0.0±0.0	18.8±3.0	55.2±5.5	20.7±2.3	0.0±0.0
MEA4	33.3±57.7	15.9±1.3	55.2±5.5	17.3±2.3	0.0±0.0
MEA5	33.3±57.7	17.5±0.8	55.2±5.5	16.7±3.1	0.0±0.0
AdvMEA	0.0±0.0	15.1±0.5	28.9±3.3	17.3±6.1	0.0±0.0
CEGA	33.3±57.7	19.0±1.4	51.5±6.2	17.3±1.2	0.0±0.0
DFEA_I	0.0±0.0	17.9±2.0	28.7±4.7	14.0±4.9	0.0±0.0
DFEA_II	33.3±47.1	19.1±0.9	28.7±4.7	18.0±2.8	0.0±0.0
DFEA_III	0.0±0.0	18.3±2.8	28.7±4.7	20.0±8.6	0.0±0.0
Realistic	0.0±0.0	16.4±1.8	50.6±4.9	15.3±1.2	0.0±0.0

(b) *PubMed*

Attack	BackdoorWM	SurviveWM	Integrity	RandomWM	Impercept.
MEA0	33.3±57.7	33.9±0.6	67.2±1.3	36.0±6.0	66.7±57.7
MEA1	33.3±57.7	34.1±0.6	67.2±1.3	36.7±1.2	66.7±57.7
MEA2	0.0±0.0	0.0±0.0	30.6±5.8	0.0±0.0	0.0±0.0
MEA3	0.0±0.0	34.6±0.6	65.9±0.7	42.7±6.4	100.0±0.0
MEA4	33.3±57.7	34.7±0.4	65.9±0.7	34.7±6.4	100.0±0.0
MEA5	33.3±57.7	34.7±0.2	65.9±0.7	30.7±9.2	100.0±0.0
AdvMEA	66.7±57.7	34.4±0.3	49.4±6.3	30.7±2.3	38.9±53.6
CEGA	66.7±57.7	35.1±0.9	66.9±2.0	37.3±5.0	66.7±57.7
DFEA_I	33.3±47.1	34.6±0.2	36.9±5.2	38.7±5.0	66.7±47.1
DFEA_II	66.7±47.1	34.4±1.3	36.9±5.2	36.7±3.4	100.0±0.0
DFEA_III	0.0±0.0	34.1±0.2	36.9±5.2	42.7±4.1	66.7±47.1
Realistic	33.3±57.7	33.0±1.4	63.8±4.3	32.7±5.0	100.0±0.0

(c) *Computers*

Attack	BackdoorWM	SurviveWM	Integrity	RandomWM	Impercept.
MEA0	60.0±20.0	9.9±0.6	79.4±15.2	15.7±5.6	0.0±0.0
MEA1	51.7±35.4	9.6±0.8	75.6±18.3	15.3±5.3	0.0±0.0
MEA2	70.0±24.5	0.0±0.0	43.9±33.8	0.0±0.0	0.0±0.0
MEA3	60.0±21.9	10.0±0.7	79.1±16.6	14.7±7.8	0.0±0.0
MEA4	58.3±30.6	10.1±0.6	45.7±27.7	14.7±3.7	0.0±0.0
MEA5	55.0±27.4	10.2±0.9	74.9±20.8	12.0±2.5	0.0±0.0
AdvMEA	65.0±26.6	10.4±0.6	38.5±25.8	12.3±6.1	0.0±0.0
CEGA	61.7±33.1	9.8±0.7	65.4±28.4	16.0±5.4	0.0±0.0
DFEA_I	63.3±12.5	9.2±0.8	11.2±11.3	10.0±0.0	0.0±0.0
DFEA_II	16.7±23.6	9.7±0.1	11.1±11.3	10.7±2.5	0.0±0.0
DFEA_III	30.0±35.6	10.5±0.4	11.2±11.2	16.0±2.8	0.0±0.0
Realistic	5.0±8.4	10.2±0.9	40.1±16.3	9.0±3.9	0.0±0.0

(d) *Photo*

Attack	BackdoorWM	SurviveWM	Integrity	RandomWM	Impercept.
MEA0	33.3±7.2	12.3±0.3	76.7±11.1	17.3±4.2	0.0±0.0
MEA1	54.2±19.1	12.7±1.1	74.1±12.3	10.0±4.0	0.0±0.0
MEA2	66.7±11.8	0.0±0.0	29.0±32.5	0.0±0.0	0.0±0.0
MEA3	29.2±7.2	12.4±0.9	78.7±10.7	14.0±2.0	0.0±0.0
MEA4	50.0±25.0	12.3±0.8	49.3±21.1	12.7±4.2	0.0±0.0
MEA5	58.3±7.2	12.3±0.8	82.2±8.8	14.7±2.3	33.3±57.7
AdvMEA	62.5±33.1	12.2±0.6	53.9±20.5	18.0±2.0	0.0±0.0
CEGA	50.0±21.7	12.1±0.3	72.7±22.9	16.0±2.0	0.0±0.0
DFEA_I	25.0±20.4	12.1±0.3	11.8±7.3	17.3±1.9	0.0±0.0
DFEA_II	45.8±41.2	12.5±0.6	11.7±7.2	19.3±2.5	0.0±0.0
DFEA_III	45.8±21.2	12.2±0.3	10.3±6.3	12.0±3.3	0.0±0.0
Realistic	16.7±7.2	12.6±0.7	61.2±16.8	12.7±3.1	0.0±0.0

Table 52: Watermark verification rate (%) on the surrogate produced by each attack against each watermarking defense, on *CoauthorCS*, *CoauthorPhysics*, *RomanEmpire*, and *AmazonRatings*. Higher is better. Mean ± standard deviation over three seeds.

(a) *CoauthorCS*

Attack	BackdoorWM	SurviveWM	Integrity	RandomWM	Impercept.
MEA0	42.2±20.4	7.2±0.2	84.2±0.1	9.3±1.2	33.3±57.7
MEA1	55.6±10.2	7.0±0.3	84.2±0.1	10.0±4.0	33.3±57.7
MEA2	35.6±8.3	0.0±0.0	34.8±1.9	0.0±0.0	0.0±0.0
MEA3	48.9±16.8	7.1±0.4	82.0±0.3	7.3±4.2	33.3±57.7
MEA4	44.4±13.9	7.1±0.3	82.0±0.3	6.0±2.0	33.3±57.7
MEA5	53.3±20.0	6.9±0.4	82.0±0.3	4.7±5.0	33.3±57.7
AdvMEA	11.1±10.2	7.3±0.8	58.3±0.9	4.7±2.3	0.0±0.0
CEGA	37.8±20.4	7.0±0.4	78.3±0.3	9.3±6.1	33.3±57.7
DFEA_I	40.0±9.4	6.9±0.3	16.4±6.1	12.0±3.3	0.0±0.0
DFEA_II	33.3±5.4	6.5±0.3	14.7±3.1	6.7±2.5	0.0±0.0
DFEA_III	42.2±11.3	6.8±0.3	14.7±3.1	9.3±0.9	0.0±0.0
Realistic	2.2±3.8	6.7±0.3	67.0±0.2	6.0±3.5	0.0±0.0

(b) *CoauthorPhysics*

Attack	BackdoorWM	SurviveWM	Integrity	RandomWM	Impercept.
MEA0	80.0±20.0	20.5±0.6	93.7±0.2	26.7±3.1	33.3±57.7
MEA1	53.3±11.5	20.5±0.6	93.7±0.2	25.3±4.6	33.3±57.7
MEA2	26.7±18.9	0.0±0.0	31.8±25.6	0.0±0.0	0.0±0.0
MEA3	53.3±11.5	20.3±0.7	92.6±0.1	25.3±2.3	33.3±57.7
MEA4	66.7±30.6	20.4±0.6	92.6±0.1	23.3±4.2	33.3±57.7
MEA5	80.0±0.0	20.3±0.7	92.6±0.1	22.0±3.5	33.3±57.7
AdvMEA	26.7±30.6	19.4±1.0	68.7±1.0	19.3±10.3	33.3±57.7
CEGA	86.7±11.5	20.1±0.7	92.6±0.1	34.7±4.2	33.3±57.7
DFEA_I	80.0±16.3	20.4±0.2	41.9±0.7	29.3±2.5	33.3±47.1
DFEA_II	73.3±9.4	19.6±0.7	41.9±0.7	22.7±1.9	66.7±47.1
DFEA_III	73.3±18.9	20.4±0.5	41.9±0.7	26.0±6.5	33.3±47.1
Realistic	13.3±11.5	20.2±0.8	77.7±1.0	26.7±7.0	33.3±57.7

(c) *RomanEmpire*

Attack	BackdoorWM	SurviveWM	Integrity	RandomWM	Impercept.
MEA0	5.8±2.1	5.5±0.1	49.3±1.5	6.8±3.0	100.0±0.0
MEA1	4.8±2.8	5.5±0.1	49.3±1.5	4.4±3.8	66.7±57.7
MEA2	0.9±0.7	0.0±0.0	10.9±1.2	0.0±0.0	0.0±0.0
MEA3	5.8±2.8	5.5±0.1	49.3±1.5	8.4±2.6	66.7±57.7
MEA4	8.3±2.9	5.5±0.1	49.3±1.5	8.8±5.4	33.3±57.7
MEA5	7.1±3.9	5.5±0.1	49.3±1.5	5.6±2.6	66.7±57.7
AdvMEA	26.3±22.8	5.5±0.2	26.5±3.7	10.0±2.0	0.0±0.0
CEGA	1.0±1.4	5.4±0.2	37.8±0.6	8.7±4.4	66.7±57.7
DFEA_I	0.9±0.7	5.4±0.1	18.2±5.6	4.0±1.6	0.0±0.0
DFEA_II	31.9±5.9	5.4±0.1	22.7±6.1	6.0±1.6	0.0±0.0
DFEA_III	4.7±1.1	5.4±0.1	23.0±6.4	6.0±1.6	33.3±47.1
Realistic	0.5±1.0	5.4±0.1	44.6±2.9	8.0±4.2	0.0±0.0

(d) *AmazonRatings*

Attack	BackdoorWM	SurviveWM	Integrity	RandomWM	Impercept.
MEA0	70.8±10.2	20.0±1.0	67.5±4.5	22.7±6.4	0.0±0.0
MEA1	68.0±12.8	20.0±1.2	67.9±4.6	32.7±4.2	0.0±0.0
MEA2	15.0±2.7	0.0±0.0	35.9±36.3	0.0±0.0	0.0±0.0
MEA3	69.1±8.7	20.1±1.2	67.5±4.5	26.0±3.5	0.0±0.0
MEA4	73.2±6.0	20.3±1.1	67.9±4.6	20.7±1.2	0.0±0.0
MEA5	74.3±8.2	20.0±1.1	67.6±4.6	22.7±4.6	0.0±0.0
AdvMEA	94.0±7.0	20.0±0.7	42.7±37.7	20.7±7.6	33.3±57.7
CEGA	66.1±1.7	20.0±0.7	53.2±6.1	23.3±4.2	0.0±0.0
DFEA_I	68.3±4.5	20.0±0.6	41.9±36.8	18.7±4.1	0.0±0.0
DFEA_II	99.2±0.7	19.7±0.9	42.8±37.4	26.7±4.7	0.0±0.0
DFEA_III	71.9±4.8	20.0±0.9	43.2±37.8	21.3±3.4	0.0±0.0
Realistic	43.7±6.2	20.4±0.9	67.5±11.5	18.0±6.0	0.0±0.0



Figure 20: Per-dataset heatmap grid of joint surrogate fidelity (%). Each panel is a 12×5 matrix on one dataset (rows: attacks; columns: watermarking defenses); a single shared colormap (RdYlGn, 0–100 %) supports cross-panel comparison.

E.8.1 Post-extraction verification beyond embedded watermarks

We evaluated GrOVe and CREDIT on extracted surrogates using their released implementations, with the protected model as the reference. Table 53 gives the results in each verifier's native metric; neither AUC nor true positive rate is interchangeable with trigger accuracy.

Table 53: Ownership verification on extracted surrogates.

Verifier	Evaluation	Result
GrOVe	Node classification	TPR 0.740, FPR 0.004
CREDIT	ENZYMES	AUC 0.778
CREDIT	PROTEINS	AUC 0.750

Under the corrected Integrity protocol, no extracted surrogate reached perfect fidelity in the 120 runs on either product graph (Table 54). The target and surrogate verification rates use the same owner-side query procedure.

Table 54: Corrected Integrity results (%). Target verification denotes fingerprint self-agreement; surrogate verification is mean fingerprint agreement over 120 runs.

Dataset	Target acc.	Target collapse	Target verif.	Median fidelity	Surrogate verif.	Perfect fidelity
Computers	44.5	0/10	100.0	49.1	48.0	0/120
Photo	86.4	0/10	100.0	75.7	51.0	0/120

Table 55: Fidelity to the undefended target (%) at the smallest and largest budgets. The last column gives the largest difference between endpoints at a fixed budget (percentage points).

Dataset	$0.05\times$	$1.00\times$	Largest endpoint difference
Cora	83.2	92.7	1.7
Computers	69.0	81.4	21.0
RomanEmpire	73.0	79.3	12.1

Table 56: Surrogate verification (%): minimum and maximum over three budgets and three endpoints. The last row uses a query verifier; the other rows measure inherited marks.

Defense	Cora	RomanEmpire
BackdoorWM	0–33	0–5.9
RandomWM	9–15	9–12
SurviveWM	12–15	5.3–5.5
Integrity	52–57	38–51

E.9 RQ5 watermark survival under each paper's original setup

The headline RQ5 finding is that two graph watermarks (`SurviveWM` and `BackdoorWM`) appear to survive extraction in their source papers but reach much lower surrogate-side verification under our 12-attack joint protocol. Two reasonable rebuttals must be ruled out: (a) the gap is an artefact of our broader protocol diverging from the original setups, and (b) our re-implementations fail to embed the watermark on the protected target in the first place. This appendix runs each watermark under *the original paper's own* protocol and shows that the gap survives both rebuttals.

Setup mismatch with prior watermark papers. Table 57 compares our main-text RQ5 protocol against each watermark paper's reported setup. Both papers evaluate against a single, narrowly defined extraction attack and a different task or dataset family, while our protocol evaluates against twelve attacks on the same node-classification graphs. Any direct numerical comparison must therefore be made under either protocol's setup, not across them.

Table 57: Protocol mismatch between the two graph-watermark papers most directly affected by RQ5 and the GraphIP-Bench joint protocol.

Axis	SurviveWM [28]	BackdoorWM [33]	GraphIP-Bench RQ5
Task	Graph classification	Node + graph classification	Node classification
Datasets	MSRC-9, ENZYMES	Cora, CiteSeer, NCI1, COLLAB, REDDIT-BINARY	10 datasets, incl. *Computers*
Attack family	Same-arch hard-label MEA	Same-arch knowledge distillation	12 black-box attacks (MEA0–5, AdvMEA, CEGA, Realistic, DFEA_I/II/III)
Verification metric	$\bar{E}$ binary effective rate	WM accuracy on trigger nodes	Surrogate-side verification rate

SurviveWM under the paper-faithful graph-classification protocol. We re-implement `SurviveWM` on the original three graph-classification datasets (MSRC-9, ENZYMES, PROTEINS) with the paper's hyperparameters (SAGE host, L=4, hidden 160, dropout 0.05, 200 clean + 200 watermark epochs, SNNL coefficient α=0.1, key-input ratio a=0.1, T_{opt}=20) and the paper's effective-watermark metric E_{ave}, defined as the fraction of trials in which $E_{\text{sin}}(M) > E_{\text{sin}}(M_{\text{clean}})$ *and* $E_{\text{sin}}(M) > E_{\text{sin}}(M_{\text{random}})$. We use $80/20$ stratified splits with ten seeds per dataset, and we evaluate the watermark against the same twelve attacks as in the main RQ5 (rather than only the same-architecture hard-label MEA the original paper considered). Headline aggregates and per-attack numbers on the paper's own MSRC-9 dataset are in Table 58 and Table 59.

Table 58: `SurviveWM` under its paper-faithful protocol on the three graph-classification datasets it was originally evaluated on. medFid / medTgtWM / medSurWM are medians over 10 seeds $\times$ 12 attacks (120 rows per dataset). $E_{\text{ave},T}$ is the binary effective rate of the watermark on the protected target; $E_{\text{ave},S}$ is the same metric on the extracted surrogate. "Random floor" is $1/C$ for a task with C classes.

Dataset	medFid (%)	medTgtWM (%)	medSurWM (%)	$E_{\text{ave},T}$	$E_{\text{ave},S}$	Random floor
MSRC-9 (paper's own)	88.9	88.2	5.9	**1.00**	**0.42**	12.5 % (1/8)
ENZYMES	37.5	57.3	16.7	**1.00**	**0.51**	16.7 % (1/6)
PROTEINS	80.7	83.1	65.2	**1.00**	**0.67**	50.0 % (1/2)

Table 59: `SurviveWM` on *MSRC-9* (the paper's own dataset) under twelve attacks. TgtWM is the verification rate on the protected target (paper's E_{sin}); SurWM is the verification rate on the extracted surrogate; $E_{\text{ave},S}$ is the paper's binary effective rate on the surrogate, averaged over 10 seeds. Bold rows mark $E_{\text{ave},S}$=1.00 (every seed effective).

Attack	Family	TgtWM (%)	SurWM (%)	$E_{\text{ave},S}$
`MEA0`	Same-arch hard label	88.2	0.0	0.00
`MEA1`	Shuffled-order hard label	88.2	14.7	0.60
`MEA2`	Soft label, T=3	88.2	2.9	0.30
`MEA3`	Soft label, T=1	88.2	0.0	0.20
`MEA4`	Cross-arch SAGE, hard	88.2	0.0	0.10
`MEA5`	Cross-arch SAGE, soft	88.2	5.9	0.30
`AdvMEA`	10 % adversarial flip	88.2	0.0	0.20
`CEGA`	Centrality / entropy, soft	88.2	5.9	0.30
`Realistic`	Edge-graph reconstruction (0.3$\times$)	88.2	0.0	0.00
`DFEA_I`	Data-free, GCN	88.2	47.1	**1.00**
`DFEA_II`	Data-free, SAGE	88.2	41.2	**1.00**
`DFEA_III`	Data-free, GIN	88.2	47.1	**1.00**

Three findings follow. *First, SurviveWM's target embedding is fully reproducible.* Under the paper-faithful protocol the watermark embeds on the protected target with $E_{\text{ave},T}$=1.00 on every dataset and every attack, and the protected target's watermark accuracy reaches 88.2% on MSRC-9 (vs. a random-classifier floor of 12.9%); the embedding step is therefore not the source of the gap. *Second, surrogate survival on the same dataset is highly attack-dependent and median surrogate $E_{ave,S}$ never reaches the paper's reported* > 0.9. On MSRC-9, the same-architecture hard-label attacks (`MEA0`, `MEA3`, `MEA4`) and the structure-aware `Realistic` attack reach $E_{\text{ave},S}$=0.00–0.20, i.e. the watermark is completely washed out, even though the original paper's setup is closest to `MEA0`. *Third, an attack-regime asymmetry exists.* Data-free attacks (`DFEA_I/II/III`) reach $E_{\text{ave},S}$=1.00 on MSRC-9 because the SNNL training step pulls the watermark distribution into a region that off-manifold synthetic queries also activate; this is the unique attack regime in which SurviveWM's watermark survives, and it is the inverse of the data-driven setting that the paper reports. The headline finding of

RQ5 — that SurviveWM's extracted surrogate does not preserve the watermark under a broad attack panel — therefore holds even on the paper's own dataset and under the paper's own metric, and the gap to the paper's > 0.9 reflects the fact that the paper's effective-rate result is reported only on the protected target M_1 rather than on the extracted surrogate M_2.

BackdoorWM under the paper-faithful KD protocol. Xu et al. (2023) evaluate watermark transferability under same-architecture knowledge distillation: a freshly initialised GCN student is trained on the teacher's softened logits over half of the held-out test mask. We replay this exact setup on the protocol's default `BackdoorWM` configuration (trigger rate 0.01, ℓ=20 trigger feature dimensions at value 0.99, α=0.3, 100 pretrain + 200 defense epochs) with KL distillation at T=4.0 for 200 epochs, on five node-classification datasets (*Computers*, *Photo*, *PubMed*, *CiteSeer*, *RomanEmpire*) and five seeds each. Results in Table 60.

Table 60: `BackdoorWM` under its paper-faithful same-architecture knowledge-distillation extraction. TeachAcc / StuAcc are protected-target / surrogate test accuracy; Fid is fidelity to the teacher; TgtWM / SurWM are watermark verification on the teacher / on the KD student; RandFloor is the verification rate of a freshly initialised GCN; $E_{\text{ave},S}$ is the surrogate-side effective rate (per-seed binary SurWM $> \max(\text{RandFloor}, \text{TgtWM}/2)$, averaged over 5 seeds). ‡ flags two seeds on *Computers* where joint training collapsed (TeacherAcc<10%); their high SurWM is not genuine watermark transfer (see caveat below).

Dataset	TeachAcc (%)	StuAcc (%)	Fid (%)	TgtWM (%)	SurWM (%)	RandFloor (%)	$E_{\text{ave},T}$	$E_{\text{ave},S}$
Computers ‡	55.8	45.4	78.4	90.0	**70.0**	2.0	1.00	**1.00**
Photo	87.2	86.6	88.2	87.5	37.5	10.0	1.00	0.60
PubMed	77.8	77.2	94.0	100.0	**100.0**	20.0	0.80	0.60
CiteSeer	69.2	68.6	83.0	100.0	**0.0**	20.0	1.00	0.00
RomanEmpire	43.2	31.6	59.8	100.0	**0.0**	7.3	1.00	0.00

Two findings follow. *First, the paper's KD-transfer claim replicates where teacher training is stable.* On *Computers*, the median KD student reaches surrogate watermark 70% versus a random-classifier floor of 2% (all five seeds rated effective); on *PubMed* the median is 100% versus a 20% floor. This neutralises the rebuttal that our re-implementation is unfaithful to the paper's setup — the watermark genuinely transfers under same-architecture KD on the dataset GraphIP-Bench reports its main RQ5 result on. *Second, even under the paper's own setup, KD-style transferability is dataset-sensitive.* On *CiteSeer* and *RomanEmpire* the surrogate watermark drops to 0.0% across all five seeds, even though target embedding still reaches 100%. The headline RQ5 number on *Computers* (55% surrogate verification) and the paper-faithful KD number on *Computers* (70%) are consistent: the KD recipe is the most favourable extraction setting BackdoorWM was ever evaluated against, and even there the surrogate watermark is below the protected-target 90%. The broader 12-attack benchmark therefore reports the gap rather than contradicting the paper.

‡ *Caveat.* Two of the five *Computers* seeds had the watermark joint loss (α=0.3) collapse the teacher to a constant-label predictor (TeacherAcc $< 10\%$). Their high SurWM reflects the student trivially mimicking the constant teacher rather than genuine watermark transfer. Excluding the two collapsed seeds the *Computers* surrogate-watermark median is still 70% (seeds 1, 2, 4: 80, 70, 30), so the aggregate finding is unchanged.

Combined statement. The two paper-faithful replays close the most credible rebuttals to the RQ5 finding. `SurviveWM`'s embedding step is reproducible ($E_{\text{ave},T}$=1.00 on every dataset including the paper's own MSRC-9), but the surrogate-side $E_{\text{ave},S}$ is 0.42–0.67 in median across the three datasets and reaches 0.00–0.20 on the same-architecture attacks the original paper most closely matches; the watermark survival the paper claims is therefore a target-side claim, not a surrogate-side one. `BackdoorWM`'s KD-transfer claim replicates on the GraphIP-Bench RQ5 dataset (*Computers*: surrogate WM 70% vs. 2% random floor), but is dataset-sensitive (0% on *CiteSeer*/*RomanEmpire*) even within the paper's own setup; the broader 12-attack benchmark reports a 55% surrogate verification on *Computers*, which is consistent with the KD ceiling and not in tension with it. Together these results sharpen the load-bearing finding of the paper: a watermark's reported transferability under one narrow extraction setting (same-arch hard-label MEA, or same-arch KD) does not generalise to a broader black-box extraction protocol, and ownership-tracing designs should be evaluated on the surrogate as the primary metric across attack families.

E.10 Generalisation across structure, architecture, and tasks

This subsection contains the generalisation analysis which complements the five main-text research questions. We collect four complementary studies, each of which varies one dimension of the protocol at a time: graph structural properties, which separate the role of the underlying graph from the role of attack or defense design; the GNN backbone, which separates the role of model architecture from the role of attack design; the prediction task, which checks whether the same protocol transfers from node classification to link prediction and graph classification; and the query-budget grid, which checks whether the standard five-budget grid omits a relevant inflection point. Across the four studies the qualitative conclusions of the main-text experiments transfer: extraction effectiveness correlates positively with edge homophily, a backbone mismatch reduces but does not prevent successful extraction, the relative ordering of attacks is preserved across tasks, and only label-quantising or query-detection defenses substantively change surrogate fidelity on the additional tasks.

Structural properties. For every dataset we compute the number of nodes and edges, the average degree, the edge density, and the edge homophily [20]; Table 64 reports all five quantities. The structural numbers connect to RQ1 and RQ5 in three concrete ways. First, fidelity at the medium budget is positively associated with edge homophily: on *RomanEmpire* and *AmazonRatings* (homophily 0.291 and 0.452), the strongest data-driven attacks reach lower fidelity than on the homophilic graphs at the same budget, which is consistent with the hypothesis that homophilic neighbourhoods make it easier to learn the target's local decision rule from a small set of queries. Second, average degree drives the variance of `CEGA`: its high variance on *Computers* coincides with the highest average degree (36.8) in the benchmark, which supports the explanation that centrality-based selection is unstable when the degree distribution is dominated by a small number of hubs. Third, scale alone does not block extraction: on *OGBN-Arxiv* ($169{,}343$ nodes, 40 classes) the strongest data-driven and data-free attacks reach 75–82% fidelity at $0.25\times$, with `AdvMEA`'s adversarial pipeline as the only attack that drops to $\sim 26\%$ on the long-tailed 40-class label space (Table 40).

Cross-architecture extraction (undefended targets). We vary the target backbone and the surrogate backbone independently across GCN, GAT, and GraphSAGE on four representative datasets and run `MEA0` at the medium budget. Table 61 reports the 3×3 fidelity matrix on *Computers*, and Table 65 extends the matrix to *Cora*, *OGBN-Arxiv*, and *RomanEmpire*. The diagonal cells are typically the highest, but the off-diagonal cells remain practical: on *Cora* the worst off-diagonal fidelity is 83.3%, only 4 pp below the matched case, so an adversary who does not know the target backbone still extracts a useful surrogate. The matrix is also asymmetric and dataset-specific: on *Computers* some off-diagonal cells drop by more than 30 pp, while on *Cora* the loss is small. The defended-target extension in Tables 66–68 is consistent with RQ5: existing defenses do not reduce surrogate fidelity in a substantive way once we control for the target backbone.

Table 61: Cross-architecture extraction on *Computers*. Surrogate fidelity (%); rows are the target backbone, columns are the surrogate backbone (mean $\pm$ std over three seeds). Results for *Cora*, *OGBN-Arxiv*, and *RomanEmpire* are reported in Table 65.

Target \ Surrogate	GCN	GAT	GraphSAGE
GCN	75.8 ± 13.6	60.5 ± 27.4	45.9 ± 27.8
GAT	76.1 ± 3.0	89.8 ± 0.4	77.0 ± 3.8
GraphSAGE	60.7 ± 16.3	81.2 ± 3.7	72.9 ± 8.9

Transfer to link prediction and graph classification. We adapt the same protocol to two further tasks. For link prediction we use *Cora* with eleven attacks and four perturbation defenses plus a no-defense baseline; the results are in Table 62. For graph classification we use the ENZYMES and PROTEINS datasets from TUDataset [17] with six attacks and six defenses; the results are in Table 63. Two observations follow. First, the relative ordering of attacks transfers across tasks while the absolute scale changes. On link prediction the strongest attacks reach fidelity in the 90–98% range when no defense is applied, which matches the node-classification results, while `MEA3` alone is markedly weaker. On graph classification the high baseline accuracy of the target on PROTEINS (67.5%) is reproduced by surrogate models with fidelity above 95% for most attacks, while ENZYMES (target accuracy 24.8%) shows a wider range. Second, prediction rounding to two bits is the only defense which yields a consistent fidelity drop across these two additional tasks. On

link prediction PR_2bit reduces MEA2 and the data-free variants to about 28.9%, which equals the marginal probability of a positive edge in the test split; on ENZYMES it reduces MEA0 from 92.2% to 16.7%. Other defenses largely preserve fidelity at levels comparable to the undefended baseline. The conclusion is that the joint pattern observed on node classification, in which only label-quantisation or query-detection defenses change surrogate fidelity in a substantive way, also transfers to link prediction and graph classification.

Table 62: Link prediction on *Cora* at $0.25\times$. Surrogate fidelity (%), mean over three seeds; standard deviations are zero or near-zero because Cora link prediction uses a fixed positive/negative split.

Defense	MEA0	MEA1	MEA2	MEA3	MEA4	MEA5	AdvMEA	CEGA	DFEA_I	DFEA_II	DFEA_III
None	95.3	94.8	95.6	73.1	85.3	93.8	97.9	92.1	94.4	94.0	94.4
OP_low	96.1	93.7	92.8	71.0	84.4	92.4	96.0	92.0	94.4	92.1	92.9
OP_high	94.2	92.8	90.4	70.2	81.6	89.3	93.1	92.8	89.9	91.3	91.1
PR_2bit	84.9	87.2	28.9	68.8	28.9	81.9	82.4	87.8	28.9	28.9	28.9
GradRedir	70.9	71.9	94.3	70.4	79.2	71.1	80.7	71.0	92.6	93.4	28.9

Table 63: Graph classification on ENZYMES (target accuracy 24.8 ± 1.3) and PROTEINS (target accuracy 67.5 ± 1.5) at budget $0.25\times$. Surrogate fidelity (%), mean $\pm$ std over three seeds.

	ENZYMES						PROTEINS					
Attack	None	OPlo	OPhi	PR2b	PRt1	GR	None	OPlo	OPhi	PR2b	PRt1	GR
MEA0	92.2±1.7	88.9±3.9	86.9±5.0	16.7±2.9	91.1±2.9	90.9±0.8	95.5±2.9	90.9±3.5	96.2±2.7	83.8±2.6	96.2±1.0	94.9±1.6
MEA1	29.4±3.8	28.1±5.2	24.4±8.6	3.1±5.5	32.4±6.1	29.6±4.2	63.4±2.1	61.9±3.0	63.3±2.7	62.4±2.5	65.1±4.8	63.2±2.3
AdvMEA	84.6±3.3	85.6±0.6	83.0±4.2	16.5±3.2	86.1±2.0	85.6±2.4	90.2±1.2	88.7±0.5	89.9±2.7	85.0±6.7	91.6±0.8	92.5±2.2
CEGA	88.7±3.1	92.2±0.6	90.2±4.5	59.1±6.4	90.9±1.4	85.0±2.4	97.1±1.2	96.8±2.0	97.5±0.2	94.7±1.6	97.8±0.3	97.1±0.9
DFEA_I	93.0±0.3	91.3±0.3	91.1±1.5	60.0±4.9	91.3±0.8	83.0±1.2	97.5±0.7	97.4±0.7	97.9±0.6	95.0±2.4	97.7±0.2	96.6±0.5
DFEA_II	90.6±3.8	90.2±2.1	84.1±3.9	16.7±4.5	91.3±1.2	91.7±1.5	96.3±0.6	94.7±1.2	94.2±2.8	84.9±0.3	95.9±1.4	95.5±1.4

Figure 21 reports the same numbers as Tables 62–63 as a three-panel heatmap: link prediction on *Cora* and graph classification on *ENZYMES* and *PROTEINS*. The heatmap view exposes two regularities which the per-task tables show only column by column. *First, the column for PR_2bit is the only column which is uniformly dark across the three tasks*: it cuts MEA2 and the DFEA family to about 28.9% on link prediction (the marginal probability of a positive edge) and to about 17% on *ENZYMES*, while the four sibling output-perturbation defenses (OP_low, OP_high, PR_top1, GradRedir) leave fidelity within 5 pp of the undefended baseline on every cell. This is the same label-quantisation effect identified in Appendix E.8 on node classification, and it transfers across tasks because all three target outputs are categorical. *Second, the row for MEA1 is uniformly faint on ENZYMES* (fidelity around 30% regardless of defense), which means the weakness is intrinsic to the attack on the small ENZYMES task rather than caused by any defense; the same attack reaches above 95% on link prediction and around 63% on PROTEINS, so the row is task-bound rather than defense-bound. The cross-task panel therefore confirms the conclusion of RQ5 in a setting where neither the protocol nor the dataset matches the original: the only defense that meaningfully reduces surrogate fidelity is the one which constrains the information content of every query, regardless of the underlying task.

Budget grid. To verify that the standard five-budget grid does not omit a relevant inflection point, we run MEA0 at three additional budgets (0.02, 0.75, 2.00) on four representative datasets; the full table is Table 69. These additional budgets do not change the qualitative conclusions of RQ1: the very small budget at $0.02\times$ already reaches a fidelity which is close to the value at $0.05\times$, the medium budget at $0.75\times$ reaches a fidelity which is close to the value at $1.00\times$, and the large budget at $2.00\times$ yields a small further gain on *Cora* only. On *RomanEmpire* the curve flattens at about 64%, well below the homophilic baselines and consistent with the structural-property analysis above. The five-budget grid therefore covers the small, medium, and saturation ranges and does not omit a relevant inflection point.

Defended-target tables. Tables 66–68 below report the cross-architecture experiment with the same three backbones but on every defended target across the ten datasets, where the surrogate is fixed to GCN.

Table 64: Structural properties of the ten graphs used in our benchmark. Edge homophily is the fraction of edges whose endpoints share the same label.

Dataset	**# Nodes**	**# Edges**	**# Classes**	**Avg. degree**	**Density**	**Edge homophily**
Cora	2,708	5,278	7	3.9	0.00144	0.810
CiteSeer	3,327	4,614	6	2.8	0.00083	0.739
PubMed	19,717	44,325	3	4.5	0.00023	0.802
Computers	13,752	252,737	10	36.8	0.00267	0.783
Photo	7,650	122,906	8	32.1	0.00420	0.833
CoauthorCS	18,333	81,894	15	8.9	0.00049	0.808
CoauthorPhysics	34,493	247,962	5	14.4	0.00042	0.931
OGBN-Arxiv	169,343	667,793	40	7.9	0.00005	0.699
RomanEmpire	22,662	44,258	18	3.9	0.00017	0.291
AmazonRatings	24,492	105,296	5	8.6	0.00035	0.452

Table 65: Cross-architecture extraction (undefended targets) on the three datasets not shown above. Surrogate fidelity (%); rows are the target backbone, columns are the surrogate backbone. Mean $\pm$ std over three seeds. The *Computers* matrix is in the main text (Table 61).

(a) *Cora*

Target \ Surrogate	GCN	GAT	GraphSAGE
GCN	87.5 ± 1.4	89.4 ± 1.1	88.5 ± 0.1
GAT	83.3 ± 4.5	90.6 ± 2.0	87.0 ± 2.6
GraphSAGE	84.0 ± 1.1	86.0 ± 0.6	96.0 ± 0.7

(b) *OGBN-Arxiv*

Target \ Surrogate	GCN	GAT	GraphSAGE
GCN	83.1 ± 5.0	62.4 ± 0.7	63.0 ± 1.4
GAT	44.9 ± 0.4	80.7 ± 0.2	90.9 ± 0.3
GraphSAGE	41.9 ± 0.8	71.4 ± 0.1	90.3 ± 1.5

(c) *RomanEmpire*

Target \ Surrogate	GCN	GAT	GraphSAGE
GCN	63.1 ± 3.1	74.4 ± 0.2	82.7 ± 0.4
GAT	53.9 ± 1.3	76.7 ± 1.5	78.3 ± 0.5
GraphSAGE	38.5 ± 0.6	47.9 ± 0.9	92.3 ± 0.3

Table 66: Surrogate fidelity (%) when `MEA0` extracts a defended target with three victim backbones across *Cora*, *CiteSeer*, *PubMed*, and *Computers*. The surrogate is fixed to GCN. Mean $\pm$ standard deviation over three seeds.

(a) *Cora*

Victim	`None`	`OP_low`	`OP_high`	`PR_top1`	`GradRedir`
GCN	87.5±1.4	85.1±3.9	85.2±3.5	87.4±0.2	87.7±0.4
GAT	82.8±3.9	82.8±4.5	82.9±4.4	85.3±2.1	83.0±3.4
GraphSAGE	84.0±1.2	83.3±2.0	83.5±1.7	84.1±1.0	81.0±3.2

(b) *CiteSeer*

Victim	`None`	`OP_low`	`OP_high`	`PR_top1`	`GradRedir`
GCN	79.7±4.9	81.7±2.3	81.5±2.9	87.6±0.3	79.7±1.7
GAT	76.7±1.7	76.1±2.5	76.6±3.3	83.0±1.8	73.2±2.1
GraphSAGE	80.8±0.5	81.1±0.7	80.9±1.2	83.6±0.9	78.1±0.4

(c) *PubMed*

Victim	`None`	`OP_low`	`OP_high`	`PR_top1`	`GradRedir`
GCN	94.9±0.3	95.0±0.5	95.0±0.5	94.6±1.4	94.3±0.3
GAT	92.1±1.1	92.2±0.8	92.2±0.8	92.7±0.6	91.6±1.0
GraphSAGE	88.9±0.5	88.8±0.7	88.8±0.8	88.8±0.7	88.3±0.3

(d) *Computers*

Victim	`None`	`OP_low`	`OP_high`	`PR_top1`	`GradRedir`
GCN	75.9±13.8	71.6±11.7	73.0±9.8	69.4±6.7	56.7±4.0
GAT	73.1±5.5	76.0±3.3	77.1±5.1	82.7±1.5	69.1±3.2
GraphSAGE	66.0±20.2	74.8±3.4	75.6±4.9	79.2±3.5	75.2±4.1

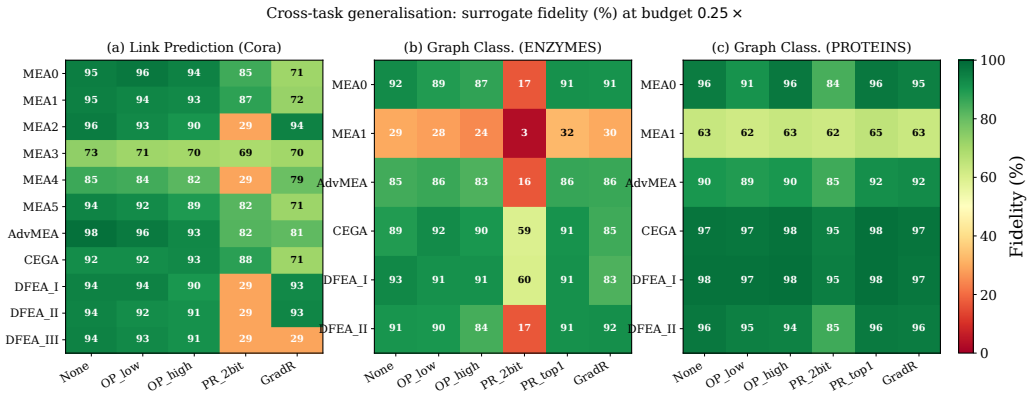


Figure 21: Cross-task heatmap of surrogate fidelity (%) on three task settings: link prediction on *Cora* (left, attacks × five defenses) and graph classification on *ENZYMES* (centre) and *PROTEINS* (right). Colour saturation encodes fidelity (darker = lower fidelity, higher protection). Numbers are taken from Tables 62–63. The `PR_2bit` column is the only column which is uniformly dark across the three tasks; the `MEA1` row on *ENZYMES* is uniformly faint, which is intrinsic to the attack rather than caused by any defense.

Table 67: Surrogate fidelity (%) when `MEA0` extracts a defended target with three victim backbones across *Photo*, *CoauthorCS*, *CoauthorPhysics*, and *OGBN-Arxiv*. The surrogate is fixed to GCN. Mean ± standard deviation over three seeds.

(a) *Photo*

Victim	None	OP_low	OP_high	PR_top1	GradRedir
GCN	95.3±2.0	95.2±1.7	95.5±1.7	93.2±3.9	92.0±4.7
GAT	96.5±0.6	96.5±0.3	96.2±0.9	95.7±1.3	96.1±0.5
GraphSAGE	94.7±1.3	92.7±3.7	94.8±1.1	94.3±1.2	94.0±1.5

(b) *CoauthorCS*

Victim	None	OP_low	OP_high	PR_top1	GradRedir
GCN	94.9±1.1	94.9±1.5	94.9±1.4	93.9±0.7	93.7±1.5
GAT	95.5±1.0	95.4±0.9	95.8±0.5	95.0±0.5	95.0±0.7
GraphSAGE	94.1±0.7	94.1±0.7	94.1±0.9	94.4±0.3	93.5±0.8

(c) *CoauthorPhysics*

Victim	None	OP_low	OP_high	PR_top1	GradRedir
GCN	97.1±1.0	97.0±1.0	97.1±1.1	96.2±1.2	96.2±1.2
GAT	96.6±1.1	97.0±0.8	96.1±1.2	95.9±0.3	96.2±1.1
GraphSAGE	97.6±0.6	97.6±0.6	97.5±0.5	97.2±0.6	97.3±0.5

(d) *OGBN-Arxiv*

Victim	None	OP_low	OP_high	PR_top1	GradRedir
GCN	83.6±4.2	83.6±3.9	83.6±3.9	78.7±6.8	75.6±2.8
GAT	45.3±0.8	45.1±0.8	45.2±0.8	50.4±2.0	37.5±1.5
GraphSAGE	41.7±1.0	42.0±0.8	41.6±0.3	47.6±1.9	38.8±1.7

Table 68: Surrogate fidelity (%) when `MEA0` extracts a defended target with three victim backbones across *Cora*, *Computers*, *RomanEmpire*, and *AmazonRatings*. The surrogate is fixed to GCN. Mean ± standard deviation over three seeds. (*Cora* and *Computers* cells are duplicated from Tables 66 for a self-contained 2×2 layout.)

(a) *Cora*

Victim	None	OP_low	OP_high	PR_top1	GradRedir
GCN	87.5±1.4	85.1±3.9	85.2±3.5	87.4±0.2	87.7±0.4
GAT	82.8±3.9	82.8±4.5	82.9±4.4	85.3±2.1	83.0±3.4
GraphSAGE	84.0±1.2	83.3±2.0	83.5±1.7	84.1±1.0	81.0±3.2

(b) *Computers*

Victim	None	OP_low	OP_high	PR_top1	GradRedir
GCN	75.9±13.8	71.6±11.7	73.0±9.8	69.4±6.7	56.7±4.0
GAT	73.1±5.5	76.0±3.3	77.1±5.1	82.7±1.5	69.1±3.2
GraphSAGE	66.0±20.2	74.8±3.4	75.6±4.9	79.2±3.5	75.2±4.1

(c) *RomanEmpire*

Victim	None	OP_low	OP_high	PR_top1	GradRedir
GCN	63.1±3.0	63.2±3.0	63.2±3.1	71.6±1.0	57.5±1.2
GAT	54.8±1.5	54.5±1.4	54.5±1.5	63.3±0.1	48.1±0.9
GraphSAGE	38.6±0.4	38.6±0.4	38.5±0.4	43.1±0.4	36.0±0.6

(d) *AmazonRatings*

Victim	None	OP_low	OP_high	PR_top1	GradRedir
GCN	87.5±2.3	87.6±1.3	87.9±1.8	91.8±1.2	92.8±0.8
GAT	85.3±1.4	85.2±1.4	85.1±1.4	89.8±1.0	90.2±0.7
GraphSAGE	64.0±0.8	56.1±1.3	61.9±3.0	64.5±2.9	62.3±2.0

The cross-architecture-on-defended-target tables (Tables 66–68) yield four deep observations that complement the cross-architecture analysis above. *First, on the homophilic citation, coauthor, and product graphs the fidelity numbers are nearly identical across the five defenses (`None`, `OP_low`, `OP_high`, `PR_top1`, `GradRedir`).* The within-row variation across defenses is typically ≤ 3 pp

on Cora, CiteSeer, PubMed, and Photo, which means that the perturbation defenses do not reduce surrogate fidelity beyond the variation that the backbone itself introduces. The implication is that, on these datasets, the value of an information-limiting defense as a fidelity-reducing mechanism is essentially zero once we control for the target backbone. *Second, the diagonal of every* 3×3 *within-defense block is the highest cell on the homophilic graphs but flips to non-diagonal on OGBN-Arxiv and RomanEmpire.* On *OGBN-Arxiv* the $\langle$GAT victim, GraphSAGE surrogate$\rangle$ cell reaches $90.9\,\%$, exceeding the matched $\langle \mathrm{GAT}, \mathrm{GAT}\rangle$ cell at $80.7\,\%$ by ten percentage points; on *RomanEmpire* the $\langle$GCN victim, GraphSAGE surrogate$\rangle$ cell reaches $82.7\,\%$, also above the matched $\langle \mathrm{GCN}, \mathrm{GCN}\rangle$ cell at $63.1\,\%$. This means that on large or heterophilic graphs, an attacker who guesses the wrong surrogate backbone may actually do *better* than one who matches the target — a counterintuitive finding that overturns the intuition that backbone matching always helps. *Third,* `GradRedir` *is the only defense that consistently reduces fidelity below the no-defense baseline*, and only on graphs where the GCN target is itself fragile (*Computers* and *OGBN-Arxiv*); on the heterophilic graphs and on the high-utility graphs it leaves fidelity unchanged or slightly increases it, which suggests that gradient-redirection's filter triggers more often when the target's confidence is already volatile. *Fourth,* `PR_top1` *(top-1 label-only output) shows the largest defense-induced gain on RomanEmpire*, where $\langle \mathrm{GCN}, \mathrm{GCN}\rangle$ rises from $63.1\,\%$ undefended to $71.6\,\%$ with PR_top1; this is consistent with our finding in RQ5 that on heterophilic graphs the noise in the soft scores of an undefended GCN actually hurts the surrogate, so quantizing them helps the attacker. Together, these four observations imply that practitioners cannot treat "defense" as a single axis: the protection effect of each information-limiting defense flips sign as a function of (i) the target backbone, (ii) the graph homophily, and (iii) the surrogate's choice of backbone.

Table 69: Budget-grid sensitivity for the `MEAO` attack on four representative datasets at three additional budget multipliers (0.02, 0.75, 2.00). Each row reports the number of query nodes induced by the budget multiplier, the surrogate fidelity, the surrogate accuracy, and the victim test accuracy. All values are mean $\pm$ standard deviation over three seeds.

Dataset	Budget	# Query nodes	Fidelity (%)	Accuracy (%)	Victim acc. (%)
Cora	0.02	54	68.5 ± 3.7	67.1 ± 3.0	79.4 ± 0.5
Cora	0.75	2,031	87.5 ± 2.1	77.7 ± 1.6	79.4 ± 0.5
Cora	2.00	2,708	88.7 ± 1.9	78.9 ± 0.7	79.4 ± 0.5
CiteSeer	0.02	66	60.7 ± 5.9	56.4 ± 6.7	67.8 ± 1.1
CiteSeer	0.75	2,495	82.6 ± 2.3	68.4 ± 1.9	67.8 ± 1.1
CiteSeer	2.00	3,327	81.9 ± 5.6	69.0 ± 2.0	67.8 ± 1.1
Computers	0.02	275	50.6 ± 33.2	37.8 ± 28.8	44.6 ± 22.4
Computers	0.75	10,314	82.6 ± 4.5	41.2 ± 25.3	44.6 ± 22.4
Computers	2.00	13,752	73.6 ± 8.0	42.0 ± 18.8	44.6 ± 22.4
RomanEmpire	0.02	453	61.6 ± 1.6	31.5 ± 0.7	42.8 ± 0.3
RomanEmpire	0.75	16,996	61.9 ± 1.5	31.3 ± 1.0	42.8 ± 0.3
RomanEmpire	2.00	22,662	64.7 ± 1.8	32.4 ± 0.6	42.8 ± 0.3

The budget-grid table exposes three deep findings that the standard five-budget grid in the main text does not surface. *First, the marginal value of doubling the budget collapses near* $0.75\times$. On *Cora*, fidelity grows by ~ 19 pp from $0.02\times$ to $0.75\times$ ($68.5 \rightarrow 87.5$) but only by 1.2 pp from $0.75\times$ to $2.00\times$ ($87.5 \rightarrow 88.7$); the same flattening appears on *CiteSeer* (where $2.00\times$ even underperforms $0.75\times$ within one standard deviation). This is direct empirical evidence that no realistic operator should query beyond ~ 0.5–$0.75\times$ on this grid — the cost-per-pp curve becomes essentially flat. *Second, the very small budget of* $0.02\times$ *already extracts a non-trivial surrogate.* With only 54 Cora queries the surrogate reaches $68.5\,\%$ fidelity, which is approximately $77\,\%$ of the maximum fidelity at $2.00\times$; this is consistent with the homophily-driven local-decision-rule hypothesis of the structural-properties analysis and quantifies an extraction floor that no current API rate-limiter is likely to defeat. *Third, on RomanEmpire the curve is essentially flat across all four orders of magnitude of the budget multiplier* ($61.6 \rightarrow 61.9 \rightarrow 64.7$), which is the strongest single piece of evidence that the heterophilic ceiling of $\sim 64\,\%$ is structural and not budget-driven. The observation also tightens the budget-grid recommendation: the five-budget grid does not omit a relevant inflection point, and extending beyond $1.00\times$ does not change qualitative conclusions on any of the four datasets.

E.11 Defense hyperparameter ablation

To complement the protection-utility analysis in the main text, we sweep the key hyperparameter of each defense and report the protected-model accuracy together with the verification proxy on

Cora and *Computers*. The sweep covers `BackdoorWM` (trigger rate), `OutputPerturbation` (noise scale σ), `PredictionRounding` (precision in bits), `RandomWM` (number of watermark nodes), and `SurviveWM` (defense ratio). Tables 70–71 report the results.

Table 70: Defense hyperparameter ablation on *Cora*. Each row reports protected-model accuracy and the verification proxy as mean ± standard deviation over multiple seeds.

Defense	Hyperparameter	Acc (%)	WM Acc (%)
`BackdoorWM`	trigger_rate=0.005	78.7±2.0	100.0±0.0
`BackdoorWM`	trigger_rate=0.01	78.6±2.1	100.0±0.0
`BackdoorWM`	trigger_rate=0.05	78.8±1.2	100.0±0.0
`BackdoorWM`	trigger_rate=0.1	77.4±0.4	100.0±0.0
`OutputPerturbation`	sigma=0.01	79.4±0.4	99.8±0.2
`OutputPerturbation`	sigma=0.05	80.0±0.7	98.6±0.5
`OutputPerturbation`	sigma=0.1	79.5±0.4	97.2±0.2
`OutputPerturbation`	sigma=0.2	78.8±0.4	94.4±0.4
`OutputPerturbation`	sigma=0.5	72.9±1.3	84.3±1.5
`PredictionRounding`	precision_bits=1	77.5±0.2	90.6±1.6
`PredictionRounding`	precision_bits=2	72.8±0.4	82.2±1.1
`PredictionRounding`	precision_bits=4	80.1±0.0	96.8±0.4
`PredictionRounding`	precision_bits=8	79.9±0.8	99.7±0.2
`RandomWM`	wm_node=10	77.5±3.0	95.0±7.1
`RandomWM`	wm_node=50	78.8±0.4	67.0±21.2
`RandomWM`	wm_node=100	78.8±0.8	53.5±10.6
`RandomWM`	wm_node=200	78.3±0.6	34.2±1.1
`SurviveWM`	defense_ratio=0.05	81.0±1.3	79.3±3.1
`SurviveWM`	defense_ratio=0.1	80.0±0.4	39.4±2.9
`SurviveWM`	defense_ratio=0.2	78.4±1.1	20.2±0.1
`SurviveWM`	defense_ratio=0.3	77.0±2.5	17.9±0.8

Table 71: Defense hyperparameter ablation on *Computers*. Each row reports protected-model accuracy and the verification proxy as mean ± standard deviation over multiple seeds. Single-value entries indicate runs with one seed.

Defense	Hyperparameter	Acc (%)	WM Acc (%)
`BackdoorWM`	trigger_rate=0.005	33.1±43.4	100.0±0.0
`BackdoorWM`	trigger_rate=0.01	2.7±2.4	95.0±7.1
`BackdoorWM`	trigger_rate=0.05	16.4±21.1	82.0±17.0
`BackdoorWM`	trigger_rate=0.1	27.4±0.7	55.0±0.0
`OutputPerturbation`	sigma=0.01	48.2	99.6
`OutputPerturbation`	sigma=0.05	38.6	77.0
`OutputPerturbation`	sigma=0.1	67.6	97.3
`OutputPerturbation`	sigma=0.2	37.4	61.1
`OutputPerturbation`	sigma=0.5	18.5	21.4
`RandomWM`	wm_node=10	44.8±9.7	100.0±0.0
`RandomWM`	wm_node=50	67.2±4.1	100.0±0.0
`RandomWM`	wm_node=100	68.8±0.1	71.5±3.5
`RandomWM`	wm_node=200	70.2±2.2	30.5±7.1
`SurviveWM`	defense_ratio=0.05	13.6±15.0	10.9±0.0
`SurviveWM`	defense_ratio=0.1	32.2±24.0	11.1±0.8
`SurviveWM`	defense_ratio=0.2	43.7±32.9	10.5±0.9
`SurviveWM`	defense_ratio=0.3	55.0±24.2	10.1±0.6

On Cora, BackdoorWM maintains 100% verification across the tested trigger rates, with protected accuracy between 77% and 79%. On Computers, both measures vary with the trigger rate and seed. Increasing the RandomWM watermark size from 10 to 200 nodes reduces verification from 95.0% to 34.2% on Cora and from 100.0% to 30.5% on Computers. The same configuration can therefore give substantially different utility and verification across graphs.